Qualitative analysis of a three-tiered food-web in a chemostat with multiple substrate inflow

By Szymon Sobieszek,

A Thesis Submitted to the School of Graduate Studies in the Partial Fulfillment of the Requirements for the Degree MSc thesis

McMaster University
MSc thesis (2019)
Hamilton, Ontario (Department of Math and Stats)

TITLE: Qualitative analysis of a three-tiered food-web in a chemostat with multiple substrate inflow
AUTHOR: Szymon Sobieszek (McMaster University)
SUPERVISOR: Prof Gail S. K. Wolkowicz
NUMBER OF PAGES: ix, 87

Acknowledgements

I would like to thank my supervisor, Dr. Gail Wolkowicz, for her guidance through each stage of the process of writing this thesis, and for her devotion towards this work. Without her insightful notes and comments, this thesis would have not been possible.

I would also like to thank Dr. Matthew Wade for his very thorough explanations of all the intricacies of the biological phenomena studied in this work. His practical point of view helped me to not only see the bigger picture behind this work, but also was immensely helpful in choosing the direction of the research.

Contents

List of Figures

List of Tables

Declaration of Authorship

I, Szymon Sobieszek, declare that this thesis titled, "Qualitative analysis of a three-tiered food-web in a chemostat with multiple substrate inflow" and the work presented in it are my own.

Chapter 1

Introduction and the model

We analyze a simplified mathematical model of the complete degradation of monochlorophenol. This is a biological process in which chlorophenol is reduced to more simple compounds by populations of microorganisms. In our case we will focus on hydrogen, since we assume that all the other products do not affect the dynamics of the process. The process is anaerobic, which means it occurs without the presence of oxygen. It is also one of the subprocesses of the complete anaerobic digestion process, which describes the degradation of organic matter in the absence of oxygen. Conventional anaerobic digestion processes (i.e., those converting organic material from typical sources such as agriculture and post-wastewater treatment solids) have been modelled with the highly structured Anaerobic Digestion Model No. 1 [1], which contains a large number of parameters, state variables, and algebraic expressions. These complications make its deep theoretical analysis extremely limited, although numerical investigations have been conducted (see for example [2]). For this reason, we study a simplified model. We try to maintain as much generality as possible so that the results can be applied to other phenomena, such as benzene degradation, which naturally occurs in crude oil. Understanding this process is especially important from the applications point of view. For example, chlorophenol is an extremely toxic compound, used extensively in the agricultural industry. Chlorophenols are not typically included in the ADM1 for standard anaerobic digestion studies, however, the model's inherent flexibility allows for their inclusion and an adapted model has previously highlighted the inhibitory effect of chlorophenol on the methanogenesis step of the process [13]. Therefore, the use of a reduced and simplified model based on ADM1 for studying the ecological interactions in a three-tiered food-web describing cholorophenol mineralisation is valid.

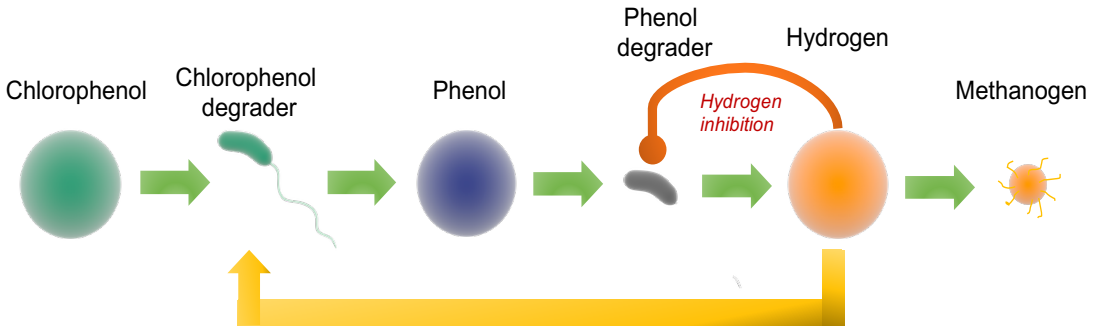

FIGURE 1.1: Schematic representation of the three-tier chlorophenol degradation. Reproduced with permission from the authors of [14].

In our work, a population of microorganisms is introduced that breaks down chlorophenol into phenol. The question of existence of such an microorganism is currently a focus of many biologists, see [6], or [8]. Another population of microorganisms then degrades phenol into hydrogen (for specific species, see [12]). Actually, phenol degrades to many other chemical compounds, however in our case we consider only hydrogen, as it is a resource for the chlorophenol degrader, which also inhibits growth of the phenol degrader. Finally, hydrogen is a resource for a population of methanogens. The entire process is presented in the Figure 1.1. This form of the interaction between microorganisms is called a food web, that is, an interconnection of food chains. The entire process is assumed to happen in a laboratory controlled environment, in a bioreactor (a chemostat) supplied by a steady flow of nutrients, from which the liquid containing the mixture of microorganisms and chemical compounds is removed at the same rate, to keep the volume constant. Although anaerobic digestion occurs freely in nature, the laboratory settings allow us to manipulate the parameters and guarantee a better control over the process. The model developed in [16] consists of six differential equations (three biomass and three substrates variables). Using the same notation as in [16], it has the following

form:

$$\frac{dX_{\mathrm{ch}}}{d\tau} = -DX_{\mathrm{ch}} + Y_{\mathrm{ch}} f_0\left(S_{\mathrm{ch}}, S_{\mathrm{H_2}}\right) X_{\mathrm{ch}} - k_{\mathrm{dec,ch}} X_{\mathrm{ch}}, \tag{1.1}$$

$$\frac{dX_{\mathrm{ph}}}{d\tau} = -DX_{\mathrm{ph}} + Y_{\mathrm{ph}} f_1\left(S_{\mathrm{ph}}, S_{\mathrm{H_2}}\right) X_{\mathrm{ph}} - k_{\mathrm{dec,ph}} X_{\mathrm{ph}}, \tag{1.2}$$

$$\frac{dX_{\mathrm{H_2}}}{d\tau} = -DX_{\mathrm{H_2}} + Y_{\mathrm{H_2}} f_2\left(S_{\mathrm{H_2}}\right) X_{\mathrm{H_2}} - k_{\mathrm{dec,H_2}} X_{\mathrm{H_2}}, \tag{1.3}$$

$$\frac{dS_{\mathrm{ch}}}{d\tau} = D\left(S_{\mathrm{ch,in}} - S_{\mathrm{ch}}\right) - f_0\left(S_{\mathrm{ch}}, S_{\mathrm{H_2}}\right) X_{\mathrm{ch}}, \tag{1.4}$$

$$\frac{dS_{\mathrm{ph}}}{d\tau} = D\left(S_{\mathrm{ph,in}} - S_{\mathrm{ph}}\right) + \frac{224}{208}\left(1 - Y_{\mathrm{ch}}\right) f_0\left(S_{\mathrm{ch}}, S_{\mathrm{H_2}}\right) X_{\mathrm{ch}} - f_1\left(S_{\mathrm{ph}}, S_{\mathrm{H_2}}\right) X_{\mathrm{ph}}, \tag{1.5}$$

$$\begin{aligned}\frac{dS_{\mathrm{H_2}}}{d\tau} &= D\left(S_{\mathrm{H_2,\,in}} - S_{\mathrm{H_2}}\right) + \frac{32}{224}\left(1 - Y_{\mathrm{ph}}\right) f_1\left(S_{\mathrm{ph}}, S_{\mathrm{H_2}}\right) X_{\mathrm{ch}} - f_2\left(S_{\mathrm{H_2}}\right) X_{\mathrm{H_2}} \\ &\quad - \frac{16}{208} f_0\left(S_{\mathrm{ch}}, S_{\mathrm{H_2}}\right) X_{\mathrm{ch}},\end{aligned} \tag{1.6}$$

where X_{ch}, X_{ph}, and $X_{\mathrm{H_2}}$ denote concentrations of chlorophenol (S_{ch}), phenol (S_{ph}), and hydrogen ($S_{\mathrm{H_2}}$) degraders respectively, $S_{\mathrm{ch,in}}$, $S_{\mathrm{ph,in}}$, and $S_{\mathrm{H_2,in}}$ are concentrations of the substrates inflow (chlorophenol, phenol, and hydrogen respectively), Y_{ch}, Y_{ph}, and $Y_{\mathrm{H_2}}$ are the corresponding yield coefficients, $k_{\mathrm{dec,ch}}$, $k_{\mathrm{dec,ph}}$, $k_{\mathrm{dec,H_2}}$ represent the corresponding death rates, and D is the dilution rate. The quantity $\frac{224}{208}\left(1 - Y_{\mathrm{ch}}\right)$ represents the part of chlorophenol degraded to phenol, $\frac{32}{224}\left(1 - Y_{\mathrm{ph}}\right)$ represents the part of phenol degraded to hydrogen, and $\frac{16}{208}$ is the fraction of phenol consumed as hydrogen by X_{ch}. The functions f_0, f_1, and f_2 are the growth functions, usually taking Monod forms [11]. For the purpose of numerical simulations, we choose the test functions to be given as

$$f_0\left(S_{\mathrm{ch}}, S_{\mathrm{H_2}}\right) = \frac{k_{\mathrm{m,ch}} S_{\mathrm{H_2}}}{K_{\mathrm{S,H_2,c}} + S_{\mathrm{H_2}}} \frac{S_{\mathrm{ch}}}{K_{\mathrm{S,ch}} + S_{\mathrm{ch}}}, \tag{1.7}$$

$$f_1\left(S_{\mathrm{ph}}, S_{\mathrm{H_2}}\right) = \frac{k_{\mathrm{m,ph}} S_{\mathrm{ph}}}{K_{\mathrm{S,ph}} + S_{\mathrm{ph}}} I_2, \tag{1.8}$$

$$f_2\left(S_{\mathrm{H_2}}\right) = \frac{k_{\mathrm{m,H_2}} S_{\mathrm{H_2}}}{K_{\mathrm{S,H_2}} + S_{\mathrm{H_2}}}, \tag{1.9}$$

where $k_{\mathrm{m,ch}}$, $k_{\mathrm{m,ph}}$, $k_{\mathrm{m,H_2}}$ are the maximum specific growth rates pertaining to the chlorophenol, phenol, and hydrogen degraders respectively, and $K_{\mathrm{S,H_2,c}}$, $K_{\mathrm{S,ch}}$, $K_{\mathrm{S,ph}}$, $K_{\mathrm{S,H_2}}$ are the half saturation coefficients, respectively, for each species.

Following the approach in [16] we introduce the dimensionless scaling

$$t = k_{\mathrm{m,ch}} Y_{\mathrm{ch}} \tau, \tag{1.10}$$

$$s_0 = \frac{S_{\mathrm{ch}}}{K_{\mathrm{S,ch}}}, \quad s_1 = \frac{S_{\mathrm{ph}}}{K_{\mathrm{S,ph}}}, \quad \frac{S_{\mathrm{H_2}}}{K_{\mathrm{S,H_2}}}, \tag{1.11}$$

$$x_0 = \frac{X_{\mathrm{ch}}}{K_{\mathrm{S,ch}} Y_{\mathrm{ch}}}, \quad x_1 = \frac{X_{\mathrm{ph}}}{K_{\mathrm{S,ph}} Y_{\mathrm{ph}}}, \quad x_2 = \frac{X_{\mathrm{H_2}}}{K_{\mathrm{S,H_2}} Y_{\mathrm{H_2}}}, \tag{1.12}$$

which transforms the system into the following form:

$$\begin{cases} x_0' &= -\alpha x_0 + \mu_0\left(s_0, s_2\right) x_0 - k_{_A} x_0, \\ x_1' &= -\alpha x_1 + \mu_1\left(s_1, s_2\right) x_1 - k_{_B} x_1, \\ x_2' &= -\alpha x_2 + \mu_2\left(s_2\right) x_2 - k_{_C} x_2, \\ s_0' &= \alpha\left(u_f - s_0\right) - \mu_0\left(s_0, s_2\right) x_0, \\ s_1' &= \alpha(u_g - s_1) + \omega_0 \mu_0\left(s_0, s_2\right) x_0 - \mu_1\left(s_1, s_2\right) x_1, \\ s_2' &= \alpha(u_h - s_2) - \omega_2 \mu_0\left(s_0, s_2\right) x_0 + \omega_1 \mu_1\left(s_1, s_2\right) x_1 - \mu_2\left(s_2\right) x_2, \end{cases} \tag{1.13}$$

where

$$\alpha = \frac{D}{k_{\mathrm{m,ch}} Y_{\mathrm{ch}}}, \tag{1.14}$$

$$u_f = \frac{S_{\mathrm{ch,in}}}{K_{\mathrm{S,ch}}}, \quad u_g = \frac{S_{\mathrm{ph,in}}}{K_{\mathrm{S,ph}}}, \quad u_h = \frac{S_{\mathrm{H_2,in}}}{K_{\mathrm{S,H_2}}}, \tag{1.15}$$

$$\omega_0 = \frac{K_{\mathrm{S,ch}}}{K_{\mathrm{S,ph}}} \frac{224}{208}\left(1 - Y_{\mathrm{ch}}\right), \quad \omega_1 = \frac{K_{\mathrm{S,ph}}}{K_{\mathrm{S,H_2}}} \frac{32}{224}\left(1 - Y_{\mathrm{ph}}\right), \quad \omega_2 = \frac{16}{208} \frac{K_{\mathrm{S,ch}}}{K_{\mathrm{S,H_2}}}, \tag{1.16}$$

$$\phi_1 = \frac{k_{\mathrm{m,ph}} Y_{\mathrm{ph}}}{k_{\mathrm{m,ch}} Y_{\mathrm{ch}}}, \quad \phi_2 = \frac{k_{\mathrm{m,H_2}} Y_{\mathrm{H_2}}}{k_{\mathrm{m,ch}} Y_{\mathrm{ch}}}, \tag{1.17}$$

$$K_P = \frac{K_{\mathrm{S,H_2,c}}}{K_{\mathrm{S,H_2}}}, \quad K_I = \frac{K_{\mathrm{S,H_2}}}{K_{I,\mathrm{H_2}}}, \tag{1.18}$$

$$k_{_A} = \frac{k_{\mathrm{dec,ch}}}{k_{\mathrm{m,ch}} Y_{\mathrm{ch}}}, \quad k_{_B} = \frac{k_{\mathrm{dec,ph}}}{k_{\mathrm{m,ch}} Y_{\mathrm{ch}}}, \quad k_{_C} = \frac{k_{\mathrm{dec,H_2}}}{k_{\mathrm{m,ch}} Y_{\mathrm{ch}}}, \tag{1.19}$$

$$\mu_0\left(s_0, s_2\right) = \frac{s_0}{1 + s_0} \frac{s_2}{K_P + s_2}, \quad \mu_1\left(s_1, s_2\right) = \frac{\phi_1 s_1}{1 + s_1} \frac{1}{1 + K_I s_2}, \quad \mu_2\left(s_2\right) = \frac{\phi_2 s_2}{1 + s_2}. \tag{1.20}$$

For the purpose of numerical simulations, we assume that the dimensionless parameters have the values given in the Table 1.1, (the full derivation of these values is presented in [16]). Notice that we do not list α, u_f, u_g, and u_h, since we treat them as bifurcation parameters and thus their values will change.

In the previous work [14], it was assumed that $u_g = u_h = 0$. Here we study the qualitative behaviour of the system without this limiting assumption. We will show that this leads to much more complex dynamics (for example, new equilibria appear). In our analysis we also assume that

$$k_{_A} = k_{_B} = k_{_C} = 0. \tag{1.21}$$

Parameters	Value
ω_0	0.1854
ω_1	1656.69
ω_2	163.08
ϕ_1	1.8875
ϕ_2	3.8113
K_P	0.04
K_I	7.1429

Table 1.1: Parameter regimes for the system (1.13).

This is not a very limiting assumption, since usually the death rates are insignificant compared to the dilution rate. We will see that this allows us to find conservation laws and consequently reduce the system to a simpler form.

In the next chapters we begin by listing all the possible equilibria of the system, followed by conditions for their existence and uniqueness. We then analyze the system on the parts of the invariant set for which one of the variables x_0, x_1, or x_2 is zero. This helps us derive alternative conditions for existence and uniqueness of the equilibria (which sometimes might be more useful than the more general, implicit ones). We conclude our work by discussing possible bifurcations that occur in the system, focusing mainly on the Hopf bifurcation, followed by finding conditions that guarantee uniform persistence, i.e., conditions that guarantee that all of the microbial populations survive. We illustrate the theoretical results obtained with numerical examples. We conclude with a discussion of the ramifications of our results for applications and discuss future directions.

Chapter 2

Reduction of the model

We are able to obtain many theoretical results assuming general forms of the growth functions provided we assume the death rates of the microbial populations are insignificant compared to the dilution rate. We thus consider the following system that is identical to system (1.13), except that we assume $k_i = 0$, $i \in \{A, B, C\}$:

$$\begin{cases} x_0' &= -\alpha x_0 + \mu_0(s_0, s_2)\, x_0, \\ x_1' &= -\alpha x_1 + \mu_1(s_1, s_2)\, x_1, \\ x_2' &= -\alpha x_2 + \mu_2(s_2)\, x_2, \\ s_0' &= \alpha(u_f - s_0) - \mu_0(s_0, s_2)\, x_0, \\ s_1' &= \alpha(u_g - s_1) + \omega_0 \mu_0(s_0, s_2)\, x_0 - \mu_1(s_1, s_2)\, x_1, \\ s_2' &= \alpha(u_h - s_2) - \omega_2 \mu_0(s_0, s_2)\, x_0 + \omega_1 \mu_1(s_1, s_2)\, x_1 - \mu_2(s_2)\, x_2, \end{cases} \tag{2.1}$$

$$x_i(0) \geq 0, \quad s_i(0) \geq 0, \quad i \in \{1, 2, 3\}.$$

We assume that $\mu_0(s_0, s_2)$, $\mu_1(s_1, s_2)$, $\mu_2(s_2)$ are $\mathcal{C}^1$ functions that satisfy the following general conditions:

- For all $s_0 \geq 0$ and $s_2 \geq 0$, $\mu_0(0, s_2) = 0$, $\mu_0(s_0, 0) = 0$. As a consequence, $\partial_{s_0}\mu_0(s_0, 0) = 0$, $\partial_{s_2}\mu_0(0, s_2) = 0$. Thus we assume that the chlorophenol degrader cannot grow in the absence of either chlorophenol or hydrogen.
- For all $s_0 > 0$ and $s_2 > 0$, $\partial_{s_0}\mu_0(s_0, s_2) > 0$, $\partial_{s_2}\mu_0(s_0, s_2) > 0$. Thus we assume that the chlorophenol degrader grows on both chlorophenol and hydrogen.
- For all $s_2 \geq 0$ and $s_1 \geq 0$, $\mu_1(0, s_2) = 0$, $\partial_{s_2}\mu_1(0, s_2) = 0$. Thus we assume that the phenol degrader cannot grow in the absence of phenol.
- For all $s_1 > 0$ and $s_2 > 0$, $\partial_{s_1}\mu_1(s_1, s_2) > 0$, $\partial_{s_2}\mu_1(s_1, s_2) < 0$. Thus we assume that the supply of phenol results in growth of the phenol degrader, and that hydrogen inhibits its growth.
- $\mu_2(0) = 0$ and $\mu_2'(s_2) > 0$ for all $s_2 > 0$. Thus we assume that the mathanogen cannot grow without the presence of hydrogen, and that increasing the supply of hydrogen results in faster growth of the methanogen.

We use the prototypes μ_0, μ_1, and μ_2 defined in (1.20), which satisfy these conditions, when we are able to prove results in general, and when providing numerical simulations or bifurcation diagrams. We now prove a lemma that we will use to show global well-posedness of system (2.1).

Lemma 2.0.1. *All solutions of system (2.1) with positive initial conditions remain positive and bounded for all positive times.*

If $x_i(0) = 0$, $i \in \{1,2,3\}$, then $x_i(t) = 0$ for all $t \geq 0$.

Proof. Consider any solution $\vec{\varphi}(t)$ with positive initial conditions. By existence and uniqueness theory, there cannot be a time $\bar{t} > 0$, such that $x_i(\bar{t}) = 0$ for some $i \in \{1,2,3\}$, since then $x_i(t) \equiv 0$ for all $t \in \mathbb{R}$, contradicting $x_i(0) > 0$. Hence $x_i(t) > 0$ for all $t \geq 0$. Also, if $x_i(0) = 0$ for some $i \in \{1,2,3\}$, then there is a solution of system (2.1) with $x_i(t) \equiv 0$ for all $t \in \mathbb{R}$. By existence and uniqueness theory, this is the only solution.

Now, consider $\vec{\varphi}(t)$, and suppose that there is some $\bar{t} > 0$, such that $s_0(t) > 0$ for $t \in [0, \bar{t})$, $s_0(\bar{t}) = 0$, and $s_1(t), s_2(t) \geq 0$ for $t \in [0, \bar{t}]$. Then $s_0'(\bar{t}) \leq 0$. However, from system (2.1), $s_0'(\bar{t}) = \alpha u_f$. If $u_f > 0$, then $s_0'(\bar{t}) > 0$, a contradiction. If $u_f = 0$, then there is a solution of system (2.1) with $s_0(t) \equiv 0$, which contradicts uniqueness of solutions. It follows that $s_0(t) > 0$ for all $t \geq 0$.

Next, consider $\vec{\varphi}(t)$, and suppose that there is some $\bar{t} > 0$, such that $s_2(t) > 0$ for $t \in [0, \bar{t})$, $s_2(\bar{t}) = 0$, and $s_1(t) \geq 0$ for $t \in [0, \bar{t}]$. Then $s_2'(\bar{t}) \leq 0$. However, from system (2.1), $s_2'(\bar{t}) = \alpha u_h + \omega_1 \mu_1(s_1(\bar{t}), 0) x_1$. If $u_h > 0$, or $s_1(\bar{t}) > 0$, then $s_2'(\bar{t}) > 0$, a contradiction. If both $u_h = 0$, and $s_1(\bar{t}) = 0$, then $s_2'(\bar{t}) = 0$, and there is another solution with $s_2(t) \equiv 0$, which contradicts uniqueness of solutions to initial value problems. It follows that $s_2(t) > 0$ for all $t \geq 0$.

Finally, consider $\vec{\varphi}(t)$, and suppose that there is some $\bar{t} > 0$, such that $s_1(t) > 0$ for $t \in [0, \bar{t})$, $s_1(\bar{t}) = 0$. Then $s_1'(\bar{t}) \leq 0$. However, from system (2.1), $s_1'(\bar{t}) = \alpha u_g + \omega_0 \mu_0(s_0(\bar{t}), s_2(\bar{t})) x_0$, so $s_1'(\bar{t}) > 0$, a contradiction. It follows that $s_1(t) > 0$ for all $t \geq 0$.

We have thus proved the positivity of solutions and move on to showing the boundedness of solutions.

By adding the first and the fourth equations of (2.1), we obtain

$$x_0' + s_0' = -\alpha(x_0 + s_0 - u_f),$$

hence

$$(x_0 + s_0 - u_f)' = -\alpha(x_0 + s_0 - u_f),$$

which implies that

$$x_0(t) + s_0(t) = u_f + (x_0(0) + s_0(0) - u_f) e^{-\alpha t}. \tag{2.2}$$

Similarly, we obtain

$$x_1(t)+\omega_0 s_0(t)+s_1(t)=\omega_0 u_f+u_g+\left(x_1(0)+\omega_0 s_0(0)+s_1(0)-\omega_0 u_f-u_g\right)e^{-\alpha t}, \quad (2.3)$$

and

$$\begin{aligned}\omega_2 x_0(t)+x_2(t)+\omega_0\omega_1 s_0(t)+\omega_1 s_1(t)+s_2(t)=\omega_0\omega_1 u_f+\omega_1 u_g+u_h+\\ \left(\omega_0 x_0(0)+x_2(0)+\omega_0\omega_1 s_0(0)+\omega_1 s_1(0)+s_2(0)-\omega_0\omega_1 u_f-\omega_1 u_g-u_h\right)e^{-\alpha t}. \quad (2.4)\end{aligned}$$

Since all terms of the sums in (2.2), (2.3) and (2.4) are positive for all positive initial conditions, the solutions of (2.1) are bounded. Also, taking the limit as $t\to\infty$ in equations (2.2), (2.3), and (2.4) we obtain that

$$\lim_{t\to\infty}\left(x_0(t)+s_0(t)\right)=u_f, \quad (2.5)$$

$$\lim_{t\to\infty}\left(x_1(t)+\omega_0 s_0(t)+s_1(t)\right)=\omega_0 u_f+u_g, \quad (2.6)$$

$$\lim_{t\to\infty}\left(\omega_2 x_0(t)+x_2(t)+\omega_0\omega_1 s_0(t)+\omega_1 s_1(t)+s_2(t)\right)=\omega_0\omega_1 u_f+\omega_1 u_g+u_h. \quad (2.7)$$

Starting with any positive initial conditions, the solutions of system (2.1) eventually satisfy

$$x_0+s_0=u_f, \quad (2.8)$$

$$x_1+\omega_0 s_0+s_1=\omega_0 u_f+u_g, \quad (2.9)$$

$$\omega_2 x_0+x_2+\omega_0\omega_1 s_0+\omega_1 s_1+s_2=\omega_0\omega_1 u_f+\omega_1 u_g+u_h. \quad (2.10)$$

□

We call relations (2.8)-(2.10) "conservation principles". In other words, system (2.1) admits a positively invariant attracting set $\Omega\subset\mathbb{R}^6$, such that

$$\begin{aligned}\Omega=\{(x_0,x_1,x_2,s_0,s_1,s_2)\in\mathbb{R}^6 : x_i,s_i\geq 0, i=0,1,2;\\ x_0+s_0=u_f,\\ x_1+\omega_0 s_0+s_1=\omega_0 u_f+u_g,\\ \omega_2 x_0+x_2+\omega_0\omega_1 s_0+\omega_1 s_1+s_2=\omega_0\omega_1 u_f+\omega_1 u_g+u_h\}.\end{aligned} \quad (2.11)$$

Using the conservation principles we can compute s_0, s_1, and s_2 as functions of x_0, x_1, x_2

$$\begin{aligned}s_0&=-x_0+u_f,\\ s_1&=\omega_0 x_0-x_1+u_g,\\ s_2&=-\omega_2 x_0+\omega_1 x_1-x_2+u_h.\end{aligned} \quad (2.12)$$

Now, we can reduce the analysis of the original system (2.1) to the analysis of the following equivalent three-dimensional system on the invariant set Ω

$$\begin{cases} x_0' = -\alpha x_0 + \mu_0\left(-x_0 + u_f, -\omega_2 x_0 + \omega_1 x_1 - x_2 + u_h\right) x_0, \\ x_1' = -\alpha x_1 + \mu_1\left(\omega_0 x_0 - x_1 + u_g, -\omega_2 x_0 + \omega_1 x_1 - x_2 + u_h\right) x_1, \\ x_2' = -\alpha x_2 + \mu_2\left(-\omega_2 x_0 + \omega_1 x_1 - x_2 + u_h\right) x_2. \end{cases} \tag{2.13}$$

From now on, we will study the reduced system (2.13). We begin by analyzing all the possible equilibria.

2.1 Equilibria of the reduced system and their local stability

The equilibria are found by setting the right hand sides of equations in (2.13) equal to zero. Below, we list all the possibilities obtained this way. Since equations (2.12) give a one-to-one correspondence of the equilibria of system (2.13) with the equilibria of system (2.1), we also list the corresponding steady states $(x_0, x_1, x_2, s_0, s_1, s_2)$ of the six-dimensional system in each case.

Types of equilibria of system (2.13):

- Zero equilibrium ${}_{(000)}\mathcal{E} = (0,0,0)$. The corresponding equilibrium ${}_{(000)}\mathbb{E}$ in the six-dimensional system:

$$ {}_{(000)}\mathbb{E} = (0,0,0,u_f,u_g,u_h)\,. \tag{2.14}$$

  In this case, all the populations die, hence the only source for the substrates comes from the inflow rates u_f, u_g, and u_h.

- Boundary equilibria:

  - ${}_{(100)}\mathcal{E} = \left({}_{(100)}x_0, 0, 0\right)$, where $x_0 = {}_{(100)}x_0 > 0$ is a solution (if it exists) of

$$\mu_0(-x_0 + u_f, -\omega_2 x_0 + u_h) = \alpha. \tag{2.15}$$

    The corresponding equilibrium ${}_{(100)}\mathbb{E}$ in the six-dimensional system:

$$ {}_{(100)}\mathbb{E} = \left({}_{(100)}x_0, 0, 0, -\,{}_{(100)}x_0 + u_f, \omega_0\,{}_{(100)}x_0 + u_g, -\omega_2\,{}_{(100)}x_0 + u_h\right). \tag{2.16}$$

    In this case, the only microorganism surviving is the chlorophenol degrader. It consumes the chlorophenol, hence the value of s_0 is given as the balance between this consumption, and the supply inflow u_f. Since x_0 produces phenol this value is added to u_g in the total phenol amount s_1. Since x_0 consumes

hydrogen as well, the value $\omega_{2\,(100)}x_0$ is subtracted from s_2 as well. This steady state is not desirable because of the phenol build-up in the system.

- ${}_{(010)}\mathcal{E} = \left(0, {}_{(010)}x_1, 0\right)$, where $x_1 = {}_{(010)}x_1 > 0$ is a solution (if it exists) of

$$\mu_1(-x_1 + u_g, \omega_1 x_1 + u_h) = \alpha. \tag{2.17}$$

The corresponding equilibrium ${}_{(010)}\mathbb{E}$ in the six-dimensional system:

$${}_{(010)}\mathbb{E} = \left(0, {}_{(010)}x_1, 0, u_f, -{}_{(010)}x_1 + u_g, \omega_{1\,(010)}x_1 + u_h\right). \tag{2.18}$$

In this case, only the phenol degrader survives, and hence the value of s_1 at the equilibrium is equal to the balance between its consumption and inflow u_g. Chlorophenol is not being consumed, hence its total amount equals the inflow u_f. Hydrogen is being produced by the phenol degrader, and also its value is increased by the inflow u_h.

- ${}_{(001)}\mathcal{E} = \left(0, 0, {}_{(001)}x_2\right)$, where $x_2 = {}_{(001)}x_2 > 0$ is a solution (if it exists) of

$$\mu_2(-x_2 + u_h) = \alpha. \tag{2.19}$$

The corresponding equilibrium ${}_{(001)}\mathbb{E}$ in the six-dimensional system:

$${}_{(001)}\mathbb{E} = \left(0, 0, {}_{(001)}x_2, u_f, u_g, -{}_{(001)}x_2 + u_h\right). \tag{2.20}$$

Here, only the methanogen is present, hence the values of chlotophenol and phenol are equal the inflow rates u_f and u_g respectively.

- ${}_{(101)}\mathcal{E} = \left({}_{(101)}x_0, 0, -\omega_{2\,(101)}x_0 + u_h - \mu_2^{-1}(\alpha)\right)$, where $x_0 = {}_{(101)}x_0 > 0$ is a solution (if it exists) of

$$\mu_0(-x_0 + u_f, \mu_2^{-1}(\alpha)) = \alpha. \tag{2.21}$$

The corresponding equilibrium ${}_{(101)}\mathbb{E}$ in the six-dimensional system:

$$\begin{aligned} {}_{(101)}\mathbb{E} = \Big({}_{(101)}x_0, 0, -\omega_{2\,(101)}x_0 + u_h - \mu_2^{-1}(\alpha), \\ -{}_{(101)}x_0 + u_f, \omega_{0\,(101)}x_0 + u_g, \mu_2^{(-1)}(\alpha) \Big). \end{aligned} \tag{2.22}$$

In this case, both chlorophenol degrader and methanogen are present. The lack of phenol degrader results in phenol build-up. We can also observe competition for hydrogen between the phenol degrader and methanogen.

- ${}_{(011)}\mathcal{E} = \left(0, {}_{(011)}x_1, \omega_1 {}_{(011)}x_1 + u_h - \mu_2^{-1}(\alpha)\right)$, where $x_1 = {}_{(011)}x_1 > 0$ is a solution (if it exists) of

$$\mu_1\left(-x_1 + u_g, \mu_2^{-1}(\alpha)\right) = \alpha. \tag{2.23}$$

The corresponding equilibrium ${}_{(011)}\mathbb{E}$ in the six-dimensional system:

$${}_{(011)}\mathbb{E} = \left(0, {}_{(011)}x_1, \omega_1 {}_{(011)}x_1 + u_h - \mu_2^{-1}(\alpha), u_f, -{}_{(011)}x_1 + u_g, \mu_2^{-1}(\alpha)\right). \tag{2.24}$$

This steady state represents a two-tiered food chain, with the phenol degrader and methanogen present. Hydrogen has an inhibiting effect on the phenol degrader.

- ${}_{(110)}\mathcal{E} = \left({}_{(110)}x_0, {}_{(110)}x_1, 0\right)$, where $x_0 = {}_{(110)}x_0 > 0$ and $x_1 = {}_{(110)}x_1 > 0$ are solutions of

$$\begin{aligned} \mu_0(-x_0 + u_f, -\omega_2 x_0 + \omega_1 x_1 + u_h) &= \alpha, \\ \mu_1(\omega_0 x_0 - x_1 + u_g, -\omega_2 x_0 + \omega_1 x_1 + u_h) &= \alpha. \end{aligned} \tag{2.25}$$

The corresponding equilibrium ${}_{(110)}\mathbb{E}$ in the six-dimensional system:

$$\begin{aligned} {}_{(110)}\mathbb{E} = \big({}_{(110)}x_0, {}_{(110)}x_1, 0, -{}_{(110)}x_0 + u_f, \\ \omega_0 {}_{(110)}x_0 - {}_{(110)}x_1 + u_g, -\omega_2 {}_{(110)}x_0 + \omega_1 {}_{(110)}x_1 + u_h\big). \end{aligned} \tag{2.26}$$

In this case, both the chlorophenol and phenol degraders are present, however the methanogen is washed out. Thus full mineralisation to methane is not possible, and hence the hydrogen amount might accumulate to some maximum value.

- Positive (interior) equilibrium ${}_{(111)}\mathcal{E} = \left(\overset{*}{x}_0, \overset{*}{x}_1, \overset{*}{x}_2\right)$, where $x_0 = \overset{*}{x}_0 > 0$, $x_1 = \overset{*}{x}_1 > 0$, and $x_2 = \overset{*}{x}_2 > 0$ are solutions of

$$\begin{aligned} \mu_0(-x_0 + u_f, -\omega_2 x_0 + \omega_1 x_1 - x_2 + u_h) &= \alpha, \\ \mu_1(\omega_0 x_0 - x_1 + u_g, -\omega_2 x_0 + \omega_1 x_1 - x_2 + u_h) &= \alpha, \\ \mu_2(-\omega_2 x_0 + \omega_1 x_1 - x_2 + u_h) &= \alpha. \end{aligned} \tag{2.27}$$

The corresponding equilibrium ${}_{(111)}\mathbb{E}$ in the six-dimensional system:

$${}_{(111)}\mathbb{E} = \left(\overset{*}{x}_0, \overset{*}{x}_1, \overset{*}{x}_2, -\overset{*}{x}_0 + u_f, \omega_0 \overset{*}{x}_0 - \overset{*}{x}_1 + u_g, \mu_2^{(-1)}(\alpha)\right). \tag{2.28}$$

Here, all species are present and thus we observe full chlorophenol mineralisation. For this reason, asymptotic stability of this equilibrium is the most desirable situation.

Since it is not clear whether the listed equations have solutions, and if the solutions are unique, we now derive conditions on the parameters that answer these questions.

2.1.1 Existence and uniqueness

Since there are many parameters in system (2.13), it was not possible to obtain explicit expressions for some of the equilibria. We did however simplify the computations by only looking for equilibria in the invariant set Ω. This assumption is reasonable, since the dynamics of the original system reduces to the dynamics on the set Ω.

- ${}_{(000)}\mathcal{E} = (0,0,0)$ equilibrium always exists.
- ${}_{(100)}\mathcal{E} = \left({}_{(100)}x_0, 0, 0\right)$. As we mentioned in the beginning of subsection 2.1.1, we are looking for the equilibria in feasible set Ω, i.e., where all of the components in corresponding six-dimensional equilibria are nonnegative. Thus, we want $x_0 = {}_{(100)}x_0$ to satisfy ${}_{(100)}x_0 \in (0, u_f]$, and ${}_{(100)}x_0 \leq \frac{u_h}{\omega_2}$; hence we consider only $x_0 \in \left(0, \min\left(u_f, \frac{u_h}{\omega_2}\right)\right]$. For such x_0 the differentiable mapping $x_0 \mapsto \mu_0\left(u_f - x_0, -\omega_2 x_0 + u_h\right)$ is decreasing, and thus ${}_{(100)}\mathcal{E}$ exists in Ω if and only if $\alpha \in [0, \mu_0(u_f, u_h))$, and when it exists, it is unique.
- ${}_{(010)}\mathcal{E} = \left(0, {}_{(010)}x_1, 0\right)$. By a similar argument, we consider $x_1 \in (0, u_g]$. The differentiable mapping $x_1 \mapsto \mu_1(u_g - x_1, \omega_1 x_1 + u_h)$ is decreasing, so ${}_{(010)}\mathcal{E}$ exists in Ω if and only if $\alpha \in [0, \mu_1(u_g, u_h))$, and when it exists, it is unique.
- ${}_{(001)}\mathcal{E} = \left(0, 0, {}_{(001)}x_2\right)$. Once again, we consider only $x_2 \in (0, u_h]$, for which the differentiable mapping $x_2 \mapsto \mu_2(-x_2 + u_h)$ is decreasing, so ${}_{(001)}\mathcal{E}$ exists in Ω if and only if $\alpha \in [0, \mu_2(u_h))$, and when it exists, it is unique (notice that if $\mu_2(s_2) = \frac{\phi_2 s_2}{1+s_2}$, we have ${}_{(001)}x_2 = u_h - \frac{\alpha}{\phi_2 - \alpha}$).
- ${}_{(101)}\mathcal{E} = \left({}_{(101)}x_0, 0, -\omega_2\,{}_{(101)}x_0 + u_h - \mu_2^{-1}(\alpha)\right)$. For ${}_{(101)}x_2 = -\omega_2\,{}_{(101)}x_0 + u_h - \mu_2^{-1}(\alpha)$, the restriction ${}_{(101)}x_2 > 0$ gives us the condition ${}_{(101)}x_0 < \frac{u_h - \mu_2^{-1}(\alpha)}{\omega_2}$ (notice that this already implies that ${}_{(101)}x_0 \leq \frac{u_h}{\omega_2}$ is satisfied), and thus the requirement ${}_{(101)}x_0 > 0$ results in the first condition on α, i.e., $\alpha < \mu_2(u_h)$. We also require that ${}_{(101)}x_0 \leq u_f$. We therefore only consider the mapping $x_0 \mapsto \mu_0(-x_0 + u_f, \mu_2^{-1}(\alpha))$ for $x_0 \in \left(0, \min\left(u_f, \frac{u_h - \mu_2^{-1}(\alpha)}{\omega_2}\right)\right)$. This differentiable mapping is decreasing, so ${}_{(101)}\mathcal{E}$ exists in Ω if and only if

$$\alpha \in \left(\mu_0\left(u_f - \min\left(u_f, \frac{u_h - \mu_2^{-1}(\alpha)}{\omega_2}\right), \mu_2^{-1}(\alpha)\right), \mu_0\left(u_f, \mu_2^{-1}(\alpha)\right)\right), \tag{2.29}$$

and $\alpha < \mu_2(u_h)$, and when it exists, it is unique.

By solving the equation

$$\mu_0(-x_0 + u_f, \mu_2^{-1}(\alpha)) = \alpha, \tag{2.30}$$

we obtain the following explicit formulas for ${}_{(101)}x_0$ and ${}_{(101)}x_2$ with our test prototypes μ_0, μ_1, and μ_2:

$${}_{(101)}x_0 = \frac{\alpha\left(1+u_f\right)\left(K_P+\mu_2^{-1}\left(\alpha\right)\right)-u_f\mu_2^{-1}\left(\alpha\right)}{\alpha\left(K_P+\mu_2^{-1}\left(\alpha\right)\right)-\mu_2^{-1}\left(\alpha\right)}, \tag{2.31}$$

$${}_{(101)}x_2 = \omega_2\frac{u_f\mu_2^{-1}\left(\alpha\right)-\alpha\left(1+u_f\right)\left(K_P+\mu_2^{-1}\left(\alpha\right)\right)}{\alpha\left(K_P+\mu_2^{-1}\left(\alpha\right)\right)-\mu_2^{-1}\left(\alpha\right)}+u_h-\mu_2^{-1}\left(\alpha\right). \tag{2.32}$$

- ${}_{(011)}\mathcal{E} = \left(0, {}_{(011)}x_1, \omega_1\,{}_{(011)}x_1 + u_h - \mu_2^{-1}\left(\alpha\right)\right)$. For $x_2 = \omega_1\,{}_{(011)}x_1 + u_h - \mu_2^{-1}(\alpha)$ the restriction ${}_{(011)}x_2 > 0$ gives the condition $x_1 > \frac{\mu_2^{-1}(\alpha)-u_h}{\omega_1}$, so the requirement ${}_{(011)}x_1 \leq u_g$ results in the first condition on α, i.e., $\alpha < \mu_2\left(\omega_1 u_g + u_h\right)$ (notice that this already implies that $\omega_1\,{}_{(011)}x_1 + u_h \geq 0$ is satisfied). We therefore only consider the mapping $x_1 \mapsto \mu_1\left(-x_1 + u_g, \mu_2^{-1}(\alpha)\right)$ for $\left(\max\left(0, \frac{\mu_2^{-1}(\alpha)-u_h}{\omega_1}\right), u_g\right]$. For such x_1, this differentiable mapping is decreasing, so ${}_{(011)}\mathcal{E}$ exists in Ω if and only if $\alpha \in \left[0, \mu_1\left(u_g - \max\left(0, \frac{\mu_2^{-1}(\alpha)-u_h}{\omega_1}\right), \mu_2^{-1}\left(\alpha\right)\right)\right)$ and $\alpha < \mu_2\left(\omega_1 u_g + u_h\right)$, and when it exists, it is unique. By solving the equation

$$\mu_1\left(-x_1 + u_g, \mu_2^{-1}\left(\alpha\right)\right) = \alpha, \tag{2.33}$$

for the prototypes given by (1.20), we obtain the following explicit formulas for ${}_{(011)}x_1$ and ${}_{(011)}x_2$

$${}_{(011)}x_1 = \frac{\alpha\left(1+u_g\right)\left(1+K_I\mu_2^{-1}\left(\alpha\right)\right)-u_g\phi_1}{\alpha\left(1+K_I\mu_2^{-1}\left(\alpha\right)\right)-\phi_1}, \tag{2.34}$$

$${}_{(011)}x_2 = \omega_1\frac{\alpha\left(1+u_g\right)\left(1+K_I\mu_2^{-1}\left(\alpha\right)\right)-u_g\phi_1}{\alpha\left(1+K_I\mu_2^{-1}\left(\alpha\right)\right)-\phi_1}+u_h-\mu_2^{-1}\left(\alpha\right). \tag{2.35}$$

- ${}_{(110)}\mathcal{E} = \left({}_{(110)}x_0, {}_{(110)}x_1, 0\right)$. This case is much more complicated since we cannot explicitly compute x_0 as a function of x_1, or x_1 as a function of x_0 in the same way as in the previous cases. In this case more than one equilibrium of the form ${}_{(110)}\mathcal{E}$ can exist. In the case of the growth functions defined in (1.20), it was proved in [14] that if $u_g = u_h = 0$, then there exist at most two equilibria of this form. By using the specific growth functions (1.20), the equilibria, given as positive solutions

of the following system of equations

$$\begin{aligned} \frac{-x_0+u_f}{1-x_0+u_f}\frac{-\omega_2 x_0+\omega_1 x_1+u_h}{K_P-\omega_2 x_0+\omega_1 x_1+u_h} &= \alpha, \\ \phi_1\frac{\omega_0 x_0-x_1+u_g}{1+\omega_0 x_0-x_1+u_g}\frac{1}{1+K_I\omega_0 x_0-x_1+u_g} &= \alpha, \end{aligned} \tag{2.36}$$

must also satisfy $x_0 < u_f$ and $\max\left(0, \frac{\omega_2 x_0 - u_h}{\omega_1}\right) < x_1 < u_g + \omega_0 x_0$. Notice that the first equation in (2.36) is linear in x_1, hence we can compute it as a function of x_0, and substitute this expression into the second equation of (2.36), obtaining a fourth order polynomial in x_0. Each zero of this polynomial, together with the corresponding value of x_1, which satisfies the aforementioned conditions, will constitute an equilibrium ${}_{(110)}\mathcal{E}$ of system (2.13). Since the polynomial in x_0 is of order four, and x_1 is given as a function of x_0, we can have at most four equilibria of the form ${}_{(110)}\mathcal{E}$.

- ${}_{(111)}\mathcal{E} = \left(\overset{*}{x}_0, \overset{*}{x}_1, \overset{*}{x}_2\right)$. For the interior equilibrium, we have to consider two cases, depending on the sign of $\omega_2 u_f - u_h$, since the bounds on the values of x_1 are different in each case. We are looking for solutions of system (2.27), for which x_0, x_1, and x_2 satisfy

$$\begin{aligned} x_0 &\in (0, u_f], \\ x_1 &\in \left(\max\left(0, \frac{\omega_2 x_0 - u_h}{\omega_1}\right), \omega_0 x_0 + u_g\right], \\ x_2 &\in (0, -\omega_2 x_0 + \omega_1 x_1 + u_h], \end{aligned} \tag{2.37}$$

if $\omega_2 u_f - u_h > 0$, and

$$\begin{aligned} x_0 &\in (0, u_f], \\ x_1 &\in (0, \omega_0 x_0 + u_g], \\ x_2 &\in (0, -\omega_2 x_0 + \omega_1 x_1 + u_h], \end{aligned} \tag{2.38}$$

if $\omega_2 u_f - u_h < 0$. In both cases, if we let $x_2 = -\omega_2 x_0 + \omega_1 x_1 + u_h - \mu_2^{-1}(\alpha)$ (which immediately gives us a necessary condition $\alpha < \sup_{s_2 \geq 0} \mu_2(\alpha)$), we obtain the following system for x_0 and x_1

$$\begin{aligned} \mu_0\left(-x_0 + u_f, \mu_2^{-1}(\alpha)\right) &= \alpha, \\ \mu_1\left(\omega_0 x_0 - x_1 + u_g, \mu_2^{-1}(\alpha)\right) &= \alpha. \end{aligned} \tag{2.39}$$

For $x_0 \in (0, u_f]$ the differentiable mapping $x_0 \mapsto \mu_0\left(-x_0 + u_f, \mu_2^{-1}(\alpha)\right)$ is decreasing, so $x_0 = \overset{*}{x}_0$ exists if and only if $\alpha \in \left[0, \mu_0\left(u_f, \mu_2^{-1}(\alpha)\right)\right)$ and when this value exists, it is unique. Now consider

$$\mu_1\left(\omega_0 \overset{*}{x}_0 - x_1 + u_g, \mu_2^{-1}(\alpha)\right) = \alpha. \tag{2.40}$$

We have two cases

- $\omega_2 u_f - u_h > 0$. For $x_1 \in \left(\max\left(0, \frac{\omega_2 \overset{*}{x}_0 - u_h}{\omega_1}\right), \omega_0 \overset{*}{x}_0 + u_g\right]$ the differentiable mapping $x_1 \mapsto \mu_1\left(\omega_0 \overset{*}{x}_0 - x_1 + u_g, \mu_2^{-1}(\alpha)\right)$ is decreasing, so $x_1 = \overset{*}{x}_1$ exists if and only if $\alpha \in \left[0, \mu_1\left(\omega_0 \overset{*}{x}_0 - \max\left(0, \frac{\omega_2 \overset{*}{x}_0 - u_h}{\omega_1}\right) + u_g, \mu_2^{-1}(\alpha)\right)\right)$ and when this value exists, it is unique.
- $\omega_2 u_f - u_h < 0$. Similarly, by considering $x_1 \in \left(0, \omega_0 \overset{*}{x}_0 + u_g\right]$ it follows that $x_1 = \overset{*}{x}_1$ exists if and only if $\alpha \in \left[0, \mu_1\left(\omega_0 \overset{*}{x}_0 + u_g, \mu_2^{-1}(\alpha)\right)\right)$.

Having $\overset{*}{x}_0$ and $\overset{*}{x}_1$ defined, we let $\overset{*}{x}_2 = -\omega_2 \overset{*}{x}_0 + \omega_1 \overset{*}{x}_1 + u_h - \mu_2^{-1}(\alpha)$. In order to have $\overset{*}{x}_2 > 0$ we need $\alpha < \mu_2\left(-\omega_2 \overset{*}{x}_0 + \omega_1 \overset{*}{x}_1 + u_h\right)$; hence ${}_{(111)}\mathcal{E}$ exists in Ω if and only if

$$\begin{aligned}\alpha \in \Bigg[0, \min\Bigg(&\mu_0\left(u_f, \mu_2^{-1}(\alpha)\right), \\ &\mu_1\left(\omega_0 \overset{*}{x}_0 - \max\left(0, \frac{\omega_2 \overset{*}{x}_0 - u_h}{\omega_1}\right) + u_g, \mu_2^{-1}(\alpha)\right), \\ &\mu_2\left(-\omega_2 \overset{*}{x}_0 + \omega_1 \overset{*}{x}_1 + u_h\right)\Bigg)\Bigg),\end{aligned} \tag{2.41}$$

in the $\omega_2 u_f - u_h > 0$ case, and

$$\begin{aligned}\alpha \in \Big[0, \min\Big(&\mu_0\left(u_f, \mu_2^{-1}(\alpha)\right), \mu_1\left(\omega_0 \overset{*}{x}_0 + u_g, \mu_2^{-1}(\alpha)\right), \\ &\mu_2\left(-\omega_2 \overset{*}{x}_0 + \omega_1 \overset{*}{x}_1 + u_h\right)\Big)\Big),\end{aligned} \tag{2.42}$$

in the $\omega_2 u_f - u_h < 0$ case. Although the conditions on α are implicit and very complicated, we now know that if ${}_{(111)}\mathcal{E}$ exists, it is unique. With the growth functions defined in (1.20), we can solve the equations (2.27) explicitly and obtain

the following formulas for the interior equilibrium

$$\overset{*}{x}_0 = 1 + u_f + \frac{1}{K_P(\phi_2 - \alpha) + \alpha - 1}, \tag{2.43}$$

$$\overset{*}{x}_1 = \omega_0 \overset{*}{x}_0 + u_g + 1 + \frac{\phi_1}{\alpha\left(1 + K_I \frac{\alpha}{\phi_2 - \alpha}\right) - \phi_1}, \tag{2.44}$$

$$\overset{*}{x}_2 = -\omega_2 \overset{*}{x}_0 + \omega_1 \overset{*}{x}_1 + u_h - \frac{\alpha}{\phi_2 - \alpha}. \tag{2.45}$$

2.1.2 Local stability results

We now study the local stability of the equilibria by considering the eigenvalues of the Jacobian evaluated at each equilibrium. These results will be summarized in section 2.2, table 2.1.

The Jacobian J for system (2.13) evaluated at (x_0, x_1, x_2) has the following form

$$J = \begin{bmatrix} \mu_0 - \alpha + x_0\left(-\frac{\partial \mu_0}{\partial s_0} - \omega_2 \frac{\partial \mu_0}{\partial s_2}\right) & \omega_1 x_0 \frac{\partial \mu_0}{\partial s_2} & -x_0 \frac{\partial \mu_0}{\partial s_2} \\ x_1\left(\omega_0 \frac{\partial \mu_1}{\partial s_1} - \omega_2 \frac{\partial \mu_1}{\partial s_2}\right) & \mu_1 - \alpha + x_1\left(-\frac{\partial \mu_1}{\partial s_1} + \omega_1 \frac{\partial \mu_1}{\partial s_2}\right) & -x_1 \frac{\partial \mu_1}{\partial s_2} \\ -\omega_2 x_2 \mu_2' & \omega_1 x_2 \mu_2' & \mu_2 - \alpha - x_2 \mu_2' \end{bmatrix}. \tag{2.46}$$

- For the zero equilibrium ${}_{(000)}\mathcal{E}$, the corresponding Jacobian ${}_{(000)}J$ has the following form

$${}_{(000)}J = \begin{bmatrix} \mu_0 - \alpha & 0 & 0 \\ 0 & \mu_1 - \alpha & 0 \\ 0 & 0 & \mu_2 - \alpha \end{bmatrix}, \tag{2.47}$$

  and its eigenvalues are $\lambda_1 = \mu_0(u_f, u_h) - \alpha$, $\lambda_2 = \mu_1(u_g, u_h) - \alpha$, $\lambda_3 = \mu_2(u_h) - \alpha$. This implies that if

  - $\alpha > \max(\mu_0(u_f, u_h), \mu_1(u_g, u_h), \mu_2(u_h))$, then ${}_{(000)}\mathcal{E}$ is a stable node,
  - $\min(\mu_0(u_f, u_h), \mu_1(u_g, u_h), \mu_2(u_h)) < \alpha < \max(\mu_0(u_f, u_h), \mu_1(u_g, u_h), \mu_2(u_h))$, then ${}_{(000)}\mathcal{E}$ is a saddle point,
  - $\alpha < \min(\mu_0(u_f, u_h), \mu_1(u_g, u_h), \mu_2(u_h))$, then ${}_{(000)}\mathcal{E}$ is an unstable node.

- For the boundary equilibrium ${}_{(100)}\mathcal{E}$, the corresponding Jacobian ${}_{(100)}J$ has the following form

$${}_{(100)}J = \begin{bmatrix} {}_{(100)}x_0\left(-\frac{\partial \mu_0}{\partial s_0} - \omega_2 \frac{\partial \mu_0}{\partial s_2}\right) & \omega_1 \, {}_{(100)}x_0 \frac{\partial \mu_0}{\partial s_2} & -{}_{(100)}x_0 \frac{\partial \mu_0}{\partial s_2} \\ 0 & \mu_1 - \alpha & 0 \\ 0 & 0 & \mu_2 - \alpha \end{bmatrix}, \tag{2.48}$$

and its eigenvalues are $\lambda_1 = {}_{(100)}x_0\left(-\frac{\partial\mu_0}{\partial s_0} - \omega_2\frac{\partial\mu_0}{\partial s_2}\right) < 0$, $\lambda_2 = \mu_1\left(\omega_0\,{}_{(100)}x_0 + u_g, -\omega_2\,{}_{(100)}x_0 + u_h\right) - \alpha$, and $\lambda_3 = \mu_2\left(-\omega_2\,{}_{(100)}x_0 + u_h\right) - \alpha$. Hence if

- $\alpha > \max\left(\mu_1\left(\omega_0\,{}_{(100)}x_0 + u_g, -\omega_2\,{}_{(100)}x_0 + u_h\right), \mu_2\left(-\omega_2\,{}_{(100)}x_0 + u_h\right)\right)$, then ${}_{(100)}\mathcal{E}$ is a stable node,
- $\alpha < \max\left(\mu_1\left(\omega_0\,{}_{(100)}x_0 + u_g, -\omega_2\,{}_{(100)}x_0 + u_h\right), \mu_2\left(-\omega_2\,{}_{(100)}x_0 + u_h\right)\right)$, then ${}_{(100)}\mathcal{E}$ is a saddle point.

- For the boundary equilibrium ${}_{(010)}\mathcal{E}$, the corresponding Jacobian ${}_{(010)}J$ has the following form

$$ {}_{(010)}J = \begin{bmatrix} \mu_0 - \alpha & 0 & 0 \\ {}_{(010)}x_1\left(\omega_0\frac{\partial\mu_1}{\partial s_1} - \omega_2\frac{\partial\mu_1}{\partial s_2}\right) & {}_{(010)}x_1\left(-\frac{\partial\mu_1}{\partial s_1} + \omega_1\frac{\partial\mu_1}{\partial s_2}\right) & -\,{}_{(010)}x_1\frac{\partial\mu_1}{\partial s_2} \\ 0 & 0 & \mu_2 - \alpha \end{bmatrix}, \tag{2.49} $$

and its eigenvalues are $\lambda_1 = \mu_0\left(u_f, \omega_1\,{}_{(010)}x_1 + u_h\right) - \alpha$, $\lambda_2 = {}_{(010)}x_1\left(-\frac{\partial\mu_1}{\partial s_1} + \omega_1\frac{\partial\mu_1}{\partial s_2}\right) < 0$, and $\lambda_3 = \mu_2\left(\omega_1\,{}_{(010)}x_1 + u_h\right) - \alpha$. Hence if

- $\alpha > \max\left(\mu_0\left(u_f, \omega_1\,{}_{(010)}x_1 + u_h\right), \mu_2\left(\omega_1\,{}_{(010)}x_1 + u_h\right)\right)$, then ${}_{(010)}\mathcal{E}$ is a stable node,
- $\alpha < \max\left(\mu_0\left(u_f, \omega_1\,{}_{(010)}x_1 + u_h\right), \mu_2\left(\omega_1\,{}_{(010)}x_1 + u_h\right)\right)$, then ${}_{(010)}\mathcal{E}$ is a saddle point.

- For the boundary equilibrium ${}_{(001)}\mathcal{E}$, the corresponding Jacobian ${}_{(001)}J$ has the following form

$$ {}_{(001)}J = \begin{bmatrix} \mu_0 - \alpha & 0 & 0 \\ 0 & \mu_1 - \alpha & 0 \\ -\omega_2\,{}_{(001)}x_2\mu_2' & \omega_1\,{}_{(001)}x_2\mu_2' & \mu_2 - \alpha - {}_{(001)}x_2\mu_2' \end{bmatrix}, \tag{2.50} $$

and its eigenvalues are $\lambda_1 = \mu_0\left(u_f, -\,{}_{(001)}x_2 + u_h\right) - \alpha$, $\lambda_2 = \mu_1\left(u_g, -\,{}_{(001)}x_2 + u_h\right) - \alpha$, and $\lambda_3 = -\,{}_{(001)}x_2\mu_2'\left(-\,{}_{(001)}x_2 + u_h\right) < 0$. Hence if

- $\alpha > \max\left(\mu_0\left(u_f, -\,{}_{(001)}x_2 + u_h\right), \mu_1\left(u_g, -\,{}_{(001)}x_2 + u_h\right)\right)$, then ${}_{(001)}\mathcal{E}$ is a stable node,
- $\alpha < \max\left(\mu_0\left(u_f, -\,{}_{(001)}x_2 + u_h\right), \mu_1\left(u_g, -\,{}_{(001)}x_2 + u_h\right)\right)$, then ${}_{(001)}\mathcal{E}$ is a saddle point.

- For the boundary equilibrium ${}_{(101)}\mathcal{E}$, the corresponding Jacobian ${}_{(101)}J$ has the following form

$$ {}_{(101)}J = \begin{bmatrix} {}_{(101)}x_0 \left(-\frac{\partial \mu_0}{\partial s_0} - \omega_2 \frac{\partial \mu_0}{\partial s_2}\right) & \omega_1 \, {}_{(101)}x_0 \frac{\partial \mu_0}{\partial s_2} & - {}_{(101)}x_0 \frac{\partial \mu_0}{\partial s_2} \\ 0 & \mu_1 - \alpha & 0 \\ -\omega_2 \, {}_{(101)}x_2 \mu_2' & \omega_1 \, {}_{(101)}x_2 \mu_2' & - {}_{(101)}x_2 \mu_2' \end{bmatrix}, \tag{2.51} $$

where ${}_{(101)}x_2 = -\omega_2 \, {}_{(101)}x_0 + u_h - \mu_2^{-1}(\alpha)$. We immediately obtain one of the eigenvalues $\lambda_1 = \mu_1 \left(\omega_0 \, {}_{(101)}x_0 + u_g, \mu_2^{-1}(\alpha)\right) - \alpha$. The other two eigenvalues are given as the solutions of the following quadratic equation

$$ \lambda^2 + a_1 \lambda + a_0 = 0, \tag{2.52} $$

where

$$ a_1 = {}_{(101)}x_0 \left(\frac{\partial \mu_0}{\partial s_0} + \omega_2 \frac{\partial \mu_0}{\partial s_2}\right) + {}_{(101)}x_2 \mu_2' \tag{2.53} $$

$$ a_0 = {}_{(101)}x_0 \, {}_{(101)}x_2 \frac{\partial \mu_0}{\partial s_0} \mu_2'. \tag{2.54} $$

Since both $a_1 > 0$, and $a_0 > 0$, by the Routh-Hurwitz criterion, all roots of the equation (2.52) have negative real parts. Hence if

  - $\alpha > \mu_1 \left(\omega_0 \, {}_{(101)}x_0 + u_g, \mu_2^{-1}(\alpha)\right)$, then ${}_{(101)}\mathcal{E}$ is asymptotically stable,
  - $\alpha < \mu_1 \left(\omega_0 \, {}_{(101)}x_0 + u_g, \mu_2^{-1}(\alpha)\right)$, then ${}_{(101)}\mathcal{E}$ is a saddle point.

- For the boundary equilibrium ${}_{(011)}\mathcal{E}$, the corresponding Jacobian ${}_{(011)}J$ has the following form

$$ {}_{(011)}J = \begin{bmatrix} \mu_0 - \alpha & 0 & 0 \\ {}_{(011)}x_1 \left(\omega_0 \frac{\partial \mu_1}{\partial s_1} - \omega_2 \frac{\partial \mu_1}{\partial s_2}\right) & {}_{(011)}x_1 \left(-\frac{\partial \mu_1}{\partial s_1} + \omega_1 \frac{\partial \mu_1}{\partial s_2}\right) & - {}_{(011)}x_1 \frac{\partial \mu_1}{\partial s_2} \\ -\omega_2 \, {}_{(011)}x_2 \mu_2' & \omega_1 \, {}_{(011)}x_2 \mu_2' & - {}_{(011)}x_2 \mu_2' \end{bmatrix}, \tag{2.55} $$

where ${}_{(011)}x_2 = \omega_1 \, {}_{(011)}x_1 + u_h - \mu_2^{-1}(\alpha)$. We immediately obtain one of the eigenvalues $\lambda_1 = \mu_0 \left(u_f, \mu_2^{-1}(\alpha)\right) - \alpha$. The other two eigenvalues are given as the solutions of the following quadratic equation

$$ \lambda^2 + a_1 \lambda + a_0 = 0, \tag{2.56} $$

where

$$a_1 = {}_{(011)}x_1 \left(\frac{\partial \mu_1}{\partial s_1} - \omega_1 \frac{\partial \mu_1}{\partial s_2} \right) + {}_{(011)}x_2 \mu_2', \tag{2.57}$$

$$a_0 = {}_{(011)}x_1 \, {}_{(011)}x_2 \frac{\partial \mu_1}{\partial s_1} \mu_2'. \tag{2.58}$$

Since both $a_1 > 0$, and $a_0 > 0$, by the Routh-Hurwitz criterion, all roots of the equation (2.56) have negative real parts. Hence if

- $\alpha > \mu_0 \left(u_f, \mu_2^{-1}(\alpha) \right)$, then ${}_{(011)}\mathcal{E}$ is asymptotically stable,
- $\alpha < \mu_0 \left(u_f, \mu_2^{-1}(\alpha) \right)$, then ${}_{(011)}\mathcal{E}$ is a saddle point.

- For the boundary equilibrium ${}_{(110)}\mathcal{E}$, the corresponding Jacobian ${}_{(110)}J$ has the following form

$${}_{(110)}J = \begin{bmatrix} {}_{(110)}x_0 \left(-\frac{\partial \mu_0}{\partial s_0} - \omega_2 \frac{\partial \mu_0}{\partial s_2} \right) & \omega_1 \, {}_{(110)}x_0 \frac{\partial \mu_0}{\partial s_2} & - {}_{(110)}x_0 \frac{\partial \mu_0}{\partial s_2} \\ {}_{(110)}x_1 \left(\omega_0 \frac{\partial \mu_1}{\partial s_1} - \omega_2 \frac{\partial \mu_1}{\partial s_2} \right) & {}_{(110)}x_1 \left(-\frac{\partial \mu_1}{\partial s_1} + \omega_1 \frac{\partial \mu_1}{\partial s_2} \right) & - {}_{(110)}x_1 \frac{\partial \mu_1}{\partial s_2} \\ 0 & 0 & \mu_2 - \alpha \end{bmatrix}. \tag{2.59}$$

We immediately obtain one eigenvalue $\lambda_1 = \mu_2 - \alpha$. The other two eigenvalues are solutions of the following quadratic equation

$$\lambda^2 + a_1 \lambda + a_0 = 0, \tag{2.60}$$

where

$$a_1 = {}_{(110)}x_0 \left(\frac{\partial \mu_0}{\partial s_0} + \omega_2 \frac{\partial \mu_0}{\partial s_2} \right) + {}_{(110)}x_1 \left(\frac{\partial \mu_1}{\partial s_1} - \omega_1 \frac{\partial \mu_1}{\partial s_2} \right), \tag{2.61}$$

$$\begin{aligned} a_0 = {}_{(110)}x_0 \, {}_{(110)}x_1 & \left(\frac{\partial \mu_0}{\partial s_0} + \omega_2 \frac{\partial \mu_0}{\partial s_2} \right) \left(\frac{\partial \mu_1}{\partial s_1} - \omega_1 \frac{\partial \mu_1}{\partial s_2} \right) \\ & - \omega_1 \, {}_{(110)}x_0 \, {}_{(110)}x_1 \frac{\partial \mu_0}{\partial s_2} \left(\omega_0 \frac{\partial \mu_1}{\partial s_1} - \omega_2 \frac{\partial \mu_1}{\partial s_2} \right). \end{aligned} \tag{2.62}$$

We have $a_1 > 0$, and

$$a_0 > 0 \iff \frac{\partial \mu_0}{\partial s_0} \frac{\partial \mu_1}{\partial s_1} - \omega_1 \frac{\partial \mu_0}{\partial s_0} \frac{\partial \mu_1}{\partial s_2} + (\omega_2 - \omega_0 \omega_1) \frac{\partial \mu_0}{\partial s_2} \frac{\partial \mu_1}{\partial s_1} > 0. \tag{2.63}$$

Hence if

- $\alpha > \mu_2$ and $\frac{\partial \mu_0}{\partial s_0} \frac{\partial \mu_1}{\partial s_1} - \omega_1 \frac{\partial \mu_0}{\partial s_0} \frac{\partial \mu_1}{\partial s_2} + (\omega_2 - \omega_0 \omega_1) \frac{\partial \mu_0}{\partial s_2} \frac{\partial \mu_1}{\partial s_1} > 0$ (where all the functions are evaluated at the steady state), then ${}_{(110)}\mathcal{E}$ is asymptotically stable,
- $\alpha < \mu_2$ or $\frac{\partial \mu_0}{\partial s_0} \frac{\partial \mu_1}{\partial s_1} - \omega_1 \frac{\partial \mu_0}{\partial s_0} \frac{\partial \mu_1}{\partial s_2} + (\omega_2 - \omega_0 \omega_1) \frac{\partial \mu_0}{\partial s_2} \frac{\partial \mu_1}{\partial s_1} < 0$, then ${}_{(110)}\mathcal{E}$ is unstable.

- For the interior equilibrium ${}_{(111)}\mathcal{E}$, the corresponding Jacobian ${}_{(111)}J$ has the following form

$$ {}_{(111)}J = \begin{bmatrix} \overset{*}{x}_0\left(-\frac{\partial\mu_0}{\partial s_0} - \omega_2\frac{\partial\mu_0}{\partial s_2}\right) & \omega_1\overset{*}{x}_0\frac{\partial\mu_0}{\partial s_2} & -\overset{*}{x}_0\frac{\partial\mu_0}{\partial s_2} \\ \overset{*}{x}_1\left(\omega_0\frac{\partial\mu_1}{\partial s_1} - \omega_2\frac{\partial\mu_1}{\partial s_2}\right) & \overset{*}{x}_1\left(-\frac{\partial\mu_1}{\partial s_1} + \omega_1\frac{\partial\mu_1}{\partial s_2}\right) & -\overset{*}{x}_1\frac{\partial\mu_1}{\partial s_2} \\ -\omega_2\overset{*}{x}_2\mu_2' & \omega_1\overset{*}{x}_2\mu_2' & -\overset{*}{x}_2\mu_2' \end{bmatrix}, \tag{2.64} $$

and its eigenvalues are solutions of the following cubic equation

$$ \lambda^3 + a_2\lambda^2 + a_1\lambda + a_0 = 0, \tag{2.65} $$

where

$$ a_2 = -\overset{*}{x}_0\left(-\frac{\partial\mu_0}{\partial s_0} - \omega_2\frac{\partial\mu_0}{\partial s_2}\right) - \overset{*}{x}_1\left(-\frac{\partial\mu_1}{\partial s_1} + \omega_1\frac{\partial\mu_1}{\partial s_2}\right) + \overset{*}{x}_2\mu_2', \tag{2.66} $$

$$ a_1 = \overset{*}{x}_1\frac{\partial\mu_1}{\partial s_1}\left(\overset{*}{x}_0\frac{\partial\mu_0}{\partial s_0} - (\omega_0\omega_1 - \omega_2)\overset{*}{x}_0\frac{\partial\mu_0}{\partial s_2} + \overset{*}{x}_2\mu_2'\right) + \overset{*}{x}_0\frac{\partial\mu_0}{\partial s_0}\left(-\omega_1\overset{*}{x}_1\frac{\partial\mu_1}{\partial s_2} + \overset{*}{x}_2\mu_2'\right), \tag{2.67} $$

$$ a_0 = \overset{*}{x}_0\overset{*}{x}_1\overset{*}{x}_2\frac{\partial\mu_0}{\partial s_0}\frac{\partial\mu_1}{\partial s_1}\mu_2'. \tag{2.68} $$

By the Routh-Hurwitz criterion, all eigenvalues have negative real parts if and only if $a_2 > 0$, $a_0 > 0$, and $a_2a_1 > a_0$. We have $a_2 > 0$, and $a_0 > 0$ always, and

$$ \begin{aligned} a_2a_1 > a_0 \iff & \left[-\overset{*}{x}_0\left(-\frac{\partial\mu_0}{\partial s_0} - \omega_2\frac{\partial\mu_0}{\partial s_2}\right) - \overset{*}{x}_1\left(-\frac{\partial\mu_1}{\partial s_1} + \omega_1\frac{\partial\mu_1}{\partial s_2}\right) + \overset{*}{x}_2\mu_2'\right]\cdot \\ & \left[\overset{*}{x}_1\frac{\partial\mu_1}{\partial s_1}\left(\overset{*}{x}_0\frac{\partial\mu_0}{\partial s_0} - (\omega_0\omega_1 - \omega_2)\overset{*}{x}_0\frac{\partial\mu_0}{\partial s_2} + \overset{*}{x}_2\mu_2'\right) + \overset{*}{x}_0\frac{\partial\mu_0}{\partial s_0}\left(-\omega_1\overset{*}{x}_1\frac{\partial\mu_1}{\partial s_2} + \overset{*}{x}_2\mu_2'\right)\right] \\ & -\overset{*}{x}_0\overset{*}{x}_1\overset{*}{x}_2\frac{\partial\mu_0}{\partial s_0}\frac{\partial\mu_1}{\partial s_1}\mu_2' > 0. \end{aligned} \tag{2.69} $$

Thus ${}_{(111)}\mathcal{E}$ is asymptotically stable if $a_2a_1 > a_0$, and is unstable if $a_2a_1 < a_0$.

2.2 Analysis on the faces

We will now study the behaviour of system (2.13) on the faces of the positively invariant set Ω, i.e., on the regions where one of the variables x_0, x_1, or x_2 equals zero. Notice that by lemma 2.0.1 these faces are invariant. The systems obtained this way are two-dimensional, which will simplify their analysis and rule out periodic orbits coming inside the invariant set through the faces. In the following analysis, we will often use the fact that

$$ \omega_2 - \omega_0\omega_1 < 0. \tag{2.70} $$

This crucial assumption comes from biology and will be used to determine the domains of the analyzed systems. It means that yield coefficients Y_{ch} and Y_{ph} have to be less than 0.5, or solutions become negative.

We also introduce a notation to differentiate between the faces, endpoints of nullclines and the equilibrium points. Specifically, we will use the left lower subscript to differentiate between faces and to indicate to which nullcline does the point belong to. For example, $\left(1\widehat{1}0\right)$ means that we are referring to the x_0x_1 face and the x_1-nullcline. Also, the space above the variable will be used to indicate if the point is an equilibrium point (denoted by $*$), or just an endpoint of a nullcline (denoted by $\widehat{\ }$). In particular, a point

$$x_0 = \overset{*}{\underset{\left(\widehat{1}01\right)}{x}}_0, \tag{2.71}$$

denotes the value of x_0 at an equilibrium point on the x_0x_2 face.

2.2.1 Face with $x_0 = 0$

We have the following reduced system:

$$\begin{cases} x_1' = \left(-\alpha + \mu_1\left(-x_1 + u_g, \omega_1 x_1 - x_2 + u_h\right)\right) x_1, \\ x_2' = \left(-\alpha + \mu_2\left(\omega_1 x_1 - x_2 + u_h\right)\right) x_2. \end{cases} \tag{2.72}$$

Thus the entire food web is reduced to a food chain, having only the phenol degrader and methanogen present. Since the chlorophenol degrader is absent, we anticipate that phenol has to be supplied to the system in order to sustain existence of the phenol degrader.

The domain for system (2.72) is given by the following set Ω_{12}:

$$\Omega_{12} = \left\{(x_1, x_2) \in \mathbb{R}^2 : 0 \le x_1 \le u_g, 0 \le x_2 \le u_h + \omega_1 x_1\right\}. \tag{2.73}$$

This region is sketched in Figure 2.1 using the Ipe software [5].

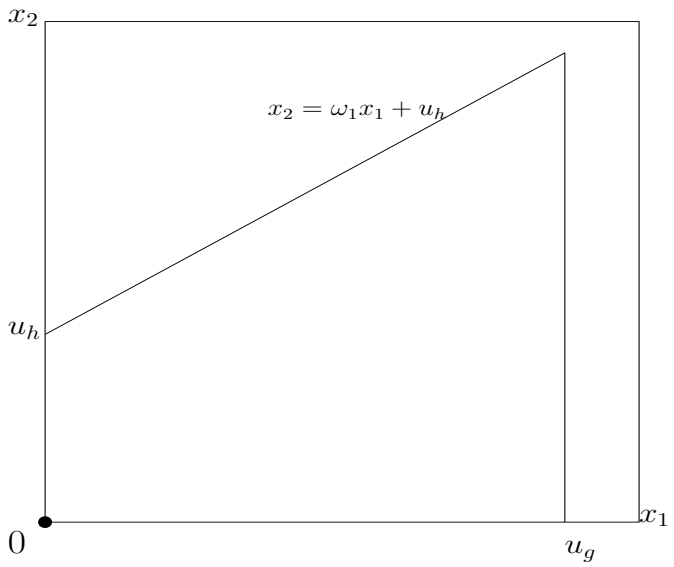

FIGURE 2.1: Domain Ω_{12} of system (2.72).

In order to determine the behaviour of the solutions, we need to consider different cases for the values of the parameter α.

- $\alpha > \mu_1(u_g, 0)$, $\alpha > \mu_2(\omega_1 u_g + u_h)$.
  In that case only the zero equilibrium exists, which is globally asymptotically stable.

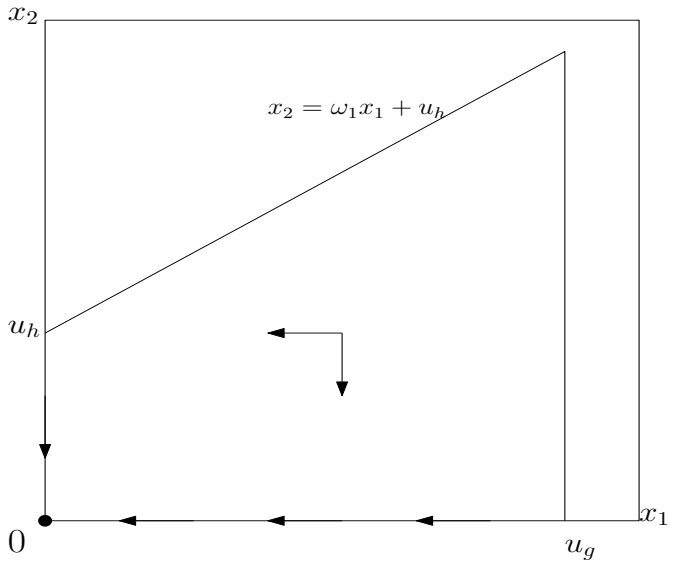

FIGURE 2.2: Sketch of the phase portrait of system (2.72) with $\alpha > \mu_1(u_g, 0)$, $\alpha > \mu_2(\omega_1 u_g + u_h)$.

- $\alpha > \mu_1(u_g, 0)$, $\mu_2(u_h) < \alpha < \mu_2(\omega_1 u_g + u_h)$.
  We have an additional x_2-nullcline, given by the equation $x_2 = \omega_1 x_1 + u_h - \mu_2^{-1}(\alpha)$, intersecting the x_1-axis. Again, the zero equilibrium is globally asymptotically stable, and it is the only equilibrium of the system.

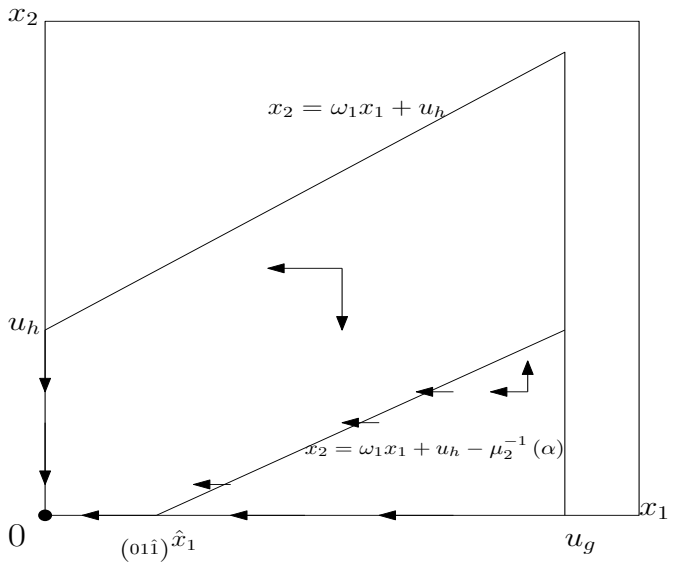

FIGURE 2.3: Sketch of the phase portrait of system (2.72) with $\alpha > \mu_1(u_g, 0)$, $\mu_2(u_h) < \alpha < \mu_2(\omega_1 u_g + u_h)$.

- $\alpha > \mu_1(u_g, 0)$, $0 < \alpha < \mu_2(u_h)$.
  Here, we still have the x_2-nullcline given by the equation $x_2 = \omega_1 x_1 + u_h - \mu_2^{-1}(\alpha)$, but this time it intersects the x_2-axis at some some point $x_2 = {}_{(01\widehat{1})}\overset{*}{x}_2$. This results in another equilibrium ${}_{(001)}\mathcal{E} = \left(0, 0, {}_{(01\widehat{1})}\overset{*}{x}_2\right)$ appearing. The zero equilibrium is unstable, and the ${}_{(001)}\mathcal{E}$ equilibrium is globally asymptotically stable with respect to the interior of the region Ω_{12}.

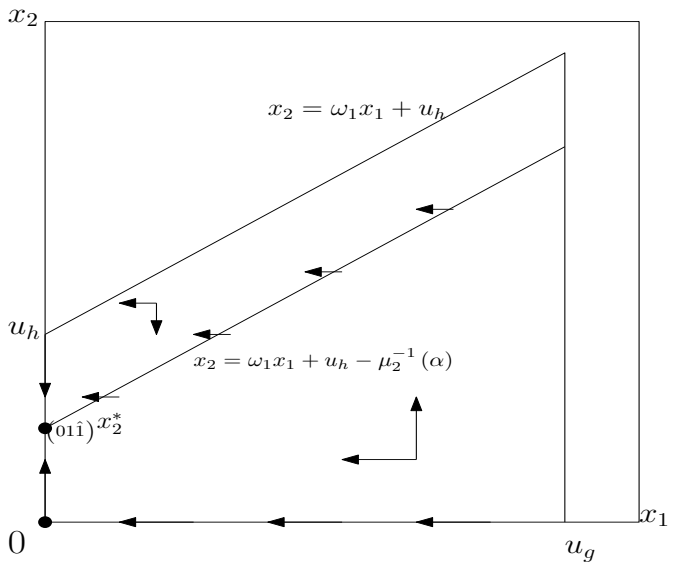

FIGURE 2.4: Sketch of the phase portrait of system (2.72) with $\alpha > \mu_1(u_g, 0)$, $0 < \alpha < \mu_2(u_h)$.

- $\mu_1(u_g, u_h) < \alpha < \mu_1(u_g, 0)$, $\alpha > \mu_2(\omega_1 u_g + u_h)$.
  We have some unique $x_2 =_{(0\hat{1}\hat{1})} \hat{x}_2$, such that $\mu_1\left(u_g, -_{(0\hat{1}\hat{1})}\hat{x}_2 + u_h\right) = \alpha$, and also since

  $$\frac{\partial}{\partial x_2}\left[\mu_1(-x_1 + u_g, \omega_1 x_1 - x_2 + u_h)\right] = -\partial_{s_2}\mu_1(-x_1 + u_g, \omega_1 x_1 - x_2 + u_h) > 0$$

  inside the admissible region Ω_{12}, we can use the Implicit Function Theorem to obtain existence of the function $x_2 =_{(0\hat{1}\hat{1})} \lambda(x_1)$, such that

  $$\mu_1\left(-x_1 + u_g, \omega_1 x_1 -_{(0\bar{1}\hat{1})} \lambda(x_1) + u_h\right) = \alpha. \tag{2.74}$$

  This function (which is the x_1-nullcline) is defined for $x_1 \in \left[0, _{(0\hat{1}\hat{1})}\hat{x}_1\right]$, where $x_1 =_{(0\hat{1}\hat{1})} \hat{x}_1 < u_g$ is the unique point of the nullcline lying on the $x_2 = \omega_1 x_1 + u_h$ line (i.e., $_{(0\hat{1}\hat{1})}\lambda(_{(0\hat{1}\hat{1})}\hat{x}_1) = \omega_1 {}_{(0\hat{1}\hat{1})}\hat{x}_1 + u_h$). We also know that the derivative of this function is given by

  $$_{(0\hat{1}\hat{1})}\lambda'(x_1) = -\frac{\partial_{s_1}\mu_1\left(-x_1 + u_g, \omega_1 x_1 -_{(0\bar{1}\hat{1})} \lambda(x_1) + u_h\right)}{\partial_{s_2}\mu_1\left(-x_1 + u_g, \omega_1 x_1 -_{(0\bar{1}\hat{1})} \lambda(x_1) + u_h\right)} + \omega_1. \tag{2.75}$$

  The only equilibrium present is the zero equilibrium, which is globally asymptotically stable.

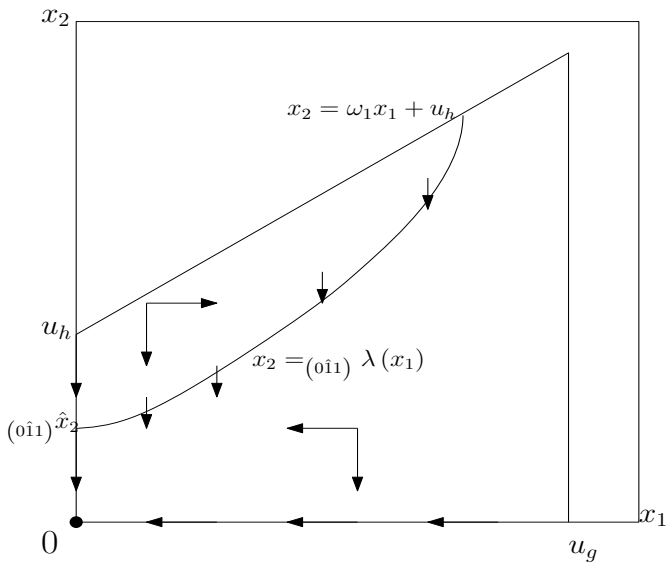

FIGURE 2.5: Sketch of the phase portrait of system (2.72) with $\mu_1(u_g, u_h) < \alpha < \mu_1(u_g, 0)$, $\alpha > \mu_2(\omega_1 u_g + u_h)$.

- $0 < \alpha < \mu_1(u_g, u_h)$, $\alpha > \mu_2(\omega_1 u_g + u_h)$.
  Analogously to the previous case, we have a x_1-nullcline given by the function $x_2 =_{(0\widehat{1}1)} \lambda(x_1)$, but this time the function starts on the x_1-axis, i.e., there is the unique $x_1 =_{(0\widehat{1}1)} \overset{*}{x}_1$ with $_{(0\widehat{1}1)}\lambda(0) =_{(0\widehat{1}1)} \overset{*}{x}_1$. This results in another equilibrium $_{(010)}\mathcal{E} = \left(0, {}_{(0\widehat{1}1)}\overset{*}{x}_1, 0\right)$. The x_1-nullcline ends on the line $x_2 = \omega_1 x_1 + u_h$ at some $x_1 =_{(0\widehat{1}1)} \hat{x}_1$. In this case, the zero equilibrium is unstable, and the $_{(010)}\mathcal{E}$ equilibrium is globally asymptotically stable with respect to the interior of Ω_{12}.

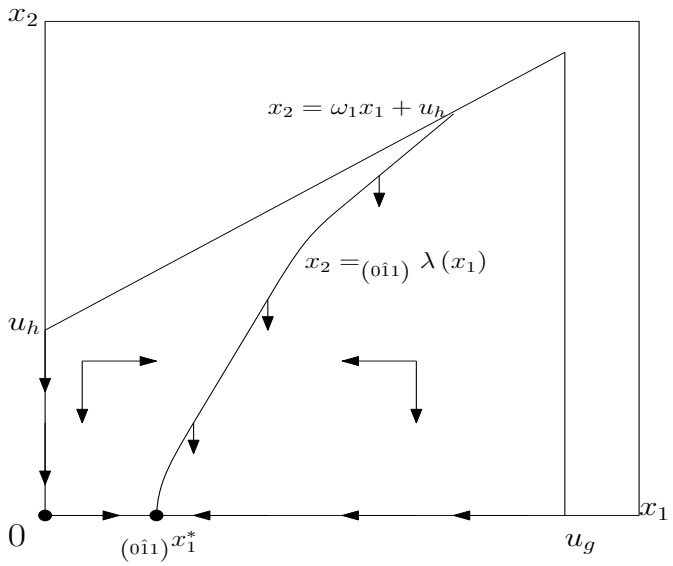

FIGURE 2.6: Sketch of the phase portrait of system (2.72) with $0 < \alpha < \mu_1(u_g, u_h)$, $\alpha > \mu_2(\omega_1 u_g + u_h)$.

- $\mu_1(u_g, u_h) < \alpha < \mu_1(u_g, 0)$, $\mu_2(u_h) < \alpha < \mu_2(\omega_1 u_g + u_h)$.
  In that case we have both x_1 and x_2 nullclines. The x_2-nullcline $x_2 = \omega_1 x_1 + u_h - \mu_2^{-1}(\alpha)$ intersects the x_1-axis, and the x_1-nullcline intersects the x_2-axis. By (2.75), the slope of the x_1-nullcline is larger than the slope of the x_2-nullcline, so they don't intersect. We have only the zero equilibrium, which is globally asymptotically stable.

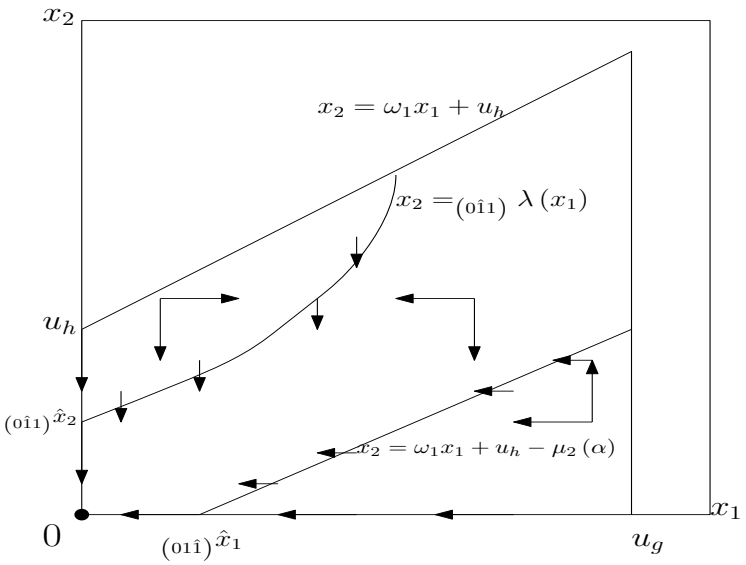

FIGURE 2.7: Sketch of the phase portrait of system (2.72) with $\mu_1(u_g, u_h) < \alpha < \mu_1(u_g, 0)$, $\mu_2(u_h) < \alpha < \mu_2(\omega_1 u_g + u_h)$.

- $\mu_1(u_g, u_h) < \alpha < \mu_1(u_g, 0)$, $0 < \alpha < \mu_2(u_h)$.
  We have the x_1-nullcline starting on the x_2-axis at some point $x_2 =_{(0\hat{1}\hat{1})} \hat{x}_2$ and we also have the x_2-nullcline $x_2 = \omega_1 x_1 + u_h$ which intersects the x_2-axis at some $x_2 =_{(01\hat{1})} \overset{*}{x}_2$. We have two cases to consider:

  - ${}_{(0\hat{1}\hat{1})}\hat{x}_2 > {}_{(01\hat{1})}\overset{*}{x}_2$. By (2.75) the slope of the x_1-nullcline is greater than the slope of the x_2-nullcline, so the x_1-nullcline lies entirely above the x_2-nullcline. Hence there is no interior equilibrium. The zero equilibrium is unstable and the ${}_{(001)}\mathcal{E}$ equilibrium is globally asymptotically stable with respect to the interior of the admissible region Ω_{12}.

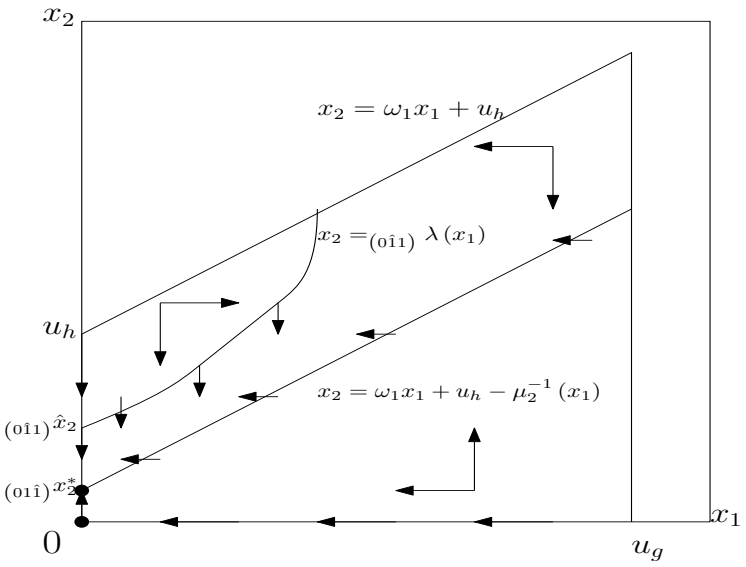

FIGURE 2.8: Sketch of the phase portrait of system (2.72) with $\mu_1(u_g, u_h) < \alpha < \mu_1(u_g, 0)$, $0 < \alpha < \mu_2(u_h)$, and ${}_{(0\hat{1}\hat{1})}\hat{x}_2 > {}_{(01\hat{1})}\overset{*}{x}_2$.

  - ${}_{(0\hat{1}\hat{1})}\hat{x}_2 < {}_{(01\hat{1})}\overset{*}{x}_2$. In that case the x_1-nullcline starts under the x_2-nullcline, so by the similar argument the nullclines intersect exactly once inside the region Ω_{12}, which results in the ${}_{(011)}\mathcal{E}$ appearing. Analysis of the phase plane shows that this equilibrium is globally asymptotically stable with respect to the interior of the admissible region Ω_{12}. The zero equilibrium and the ${}_{(001)}\mathcal{E}$ equilibrium are both unstable.

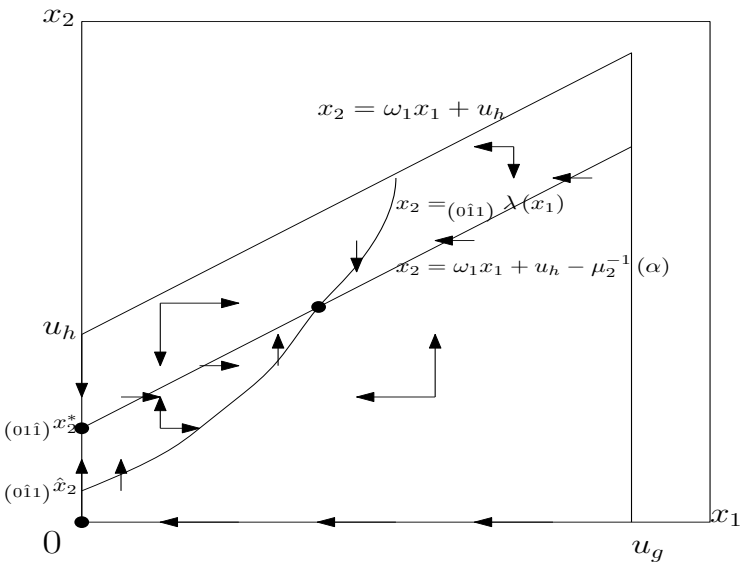

FIGURE 2.9: Sketch of the phase portrait of system (2.72) with $\mu_1(u_g, u_h) < \alpha < \mu_1(u_g, 0)$, $0 < \alpha < \mu_2(u_h)$, and ${}_{\left(0\widehat{1}1\right)}\hat{x}_2 < {}_{\left(01\widehat{1}\right)}\overset{*}{x}_2$.

- $0 < \alpha < \mu_1(u_g, u_h)$, $\mu_2(u_h) < \alpha < \mu_2(\omega_1 u_g + u_h)$.
  Both the x_1 and x_2 nullclines are present. The x_1-nullcline intersects the x_1-axis at some $x_1 = {}_{(0\widehat{1}1)}\overset{*}{x}_1$, and the x_2-nullcline intersects the x_1-axis at some $x_1 = {}_{(01\widehat{1})}\hat{x}_1$. Again, we have to consider two cases:
  - ${}_{(01\widehat{1})}\hat{x}_1 < {}_{(0\widehat{1}1)}\overset{*}{x}_1$. By a similar argument, the nullclines intersect exactly once, which results in the interior equilibrium ${}_{(011)}\mathcal{E}$ appearing. Analysis of the phase plane shows that this equilibrium is globally asymptotically stable with respect to the interior of the admissible region Ω_{12}. The zero equilibrium and the ${}_{(010)}\mathcal{E}$ equilibrium are both unstable.

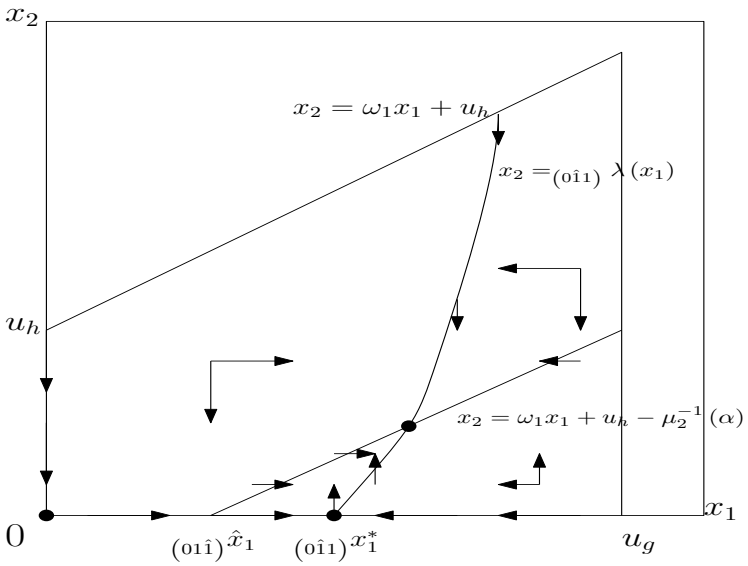

FIGURE 2.10: Sketch of the phase portrait of system (2.72) with $0 < \alpha < \mu_1(u_g, u_h)$, $\mu_2(u_h) < \alpha < \mu_2(\omega_1 u_g + u_h)$, and ${}_{(01\widehat{1})}\hat{x}_1 < {}_{(0\widehat{1}1)}\overset{*}{x}_1$.

- ${}_{(01\widehat{1})}\hat{x}_1 > {}_{(0\widehat{1}1)}\overset{*}{x}_1$. Since the slope of the x_1-nullcline is greater than the slope of the x_2-nullcline, the x_1-nullcline lies entirely above the x_2-nullcline. Hence there is no interior equilibrium. Analysis of the phase plane shows that the ${}_{(010)}\mathcal{E}$ equilibrium is globally asymptotically stable with respect to the interior of the admissible region Ω_{12}, and the zero equilibrium is unstable.

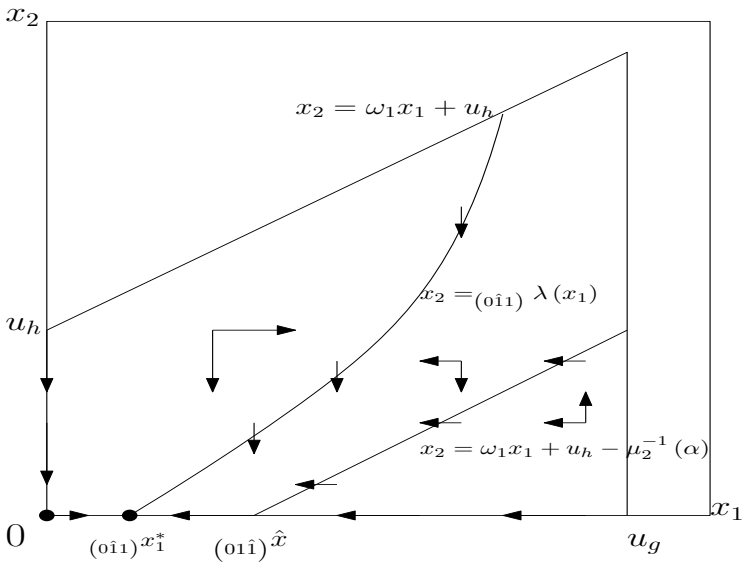

FIGURE 2.11: Sketch of the phase portrait of system (2.72) with $0 < \alpha < \mu_1(u_g, u_h)$, $\mu_2(u_h) < \alpha < \mu_2(\omega_1 u_g + u_h)$, and $_{(0\hat{1}\hat{1})}\hat{x}_1 >_{(0\hat{1}\hat{1})} \overset{*}{x}_1$.

- $0 < \alpha < \mu_1(u_g, u_h)$, $0 < \alpha < \mu_2(u_h)$.
  Here, we have both the x_1 and x_2 nullclines. The x_2-nullcline $x_2 = \omega_1 x_1 + u_h - \mu_2^{-1}(\alpha)$ intersects the x_2-axis, and the x_1-nullcline starts at the x_1-axis and ends at the $x_2 = \omega_1 x_1 + u_h$ line, hence they intersect at some interior point of the admissible region Ω_{12}, which results in the $_{(011)}\mathcal{E}$ equilibrium appearing. We also know that the nullclines intersect exactly once, since by (2.75), the slope of the x_1-nullcline is greater than the slope of the x_2-nullcline. We also have the $_{(010)}\mathcal{E}$ equilibrium at the point $x_1 =_{(0\hat{1}\hat{1})} \overset{*}{x}_1$ of intersection of the x_1-nullcline and the x_1-axis, and the $_{(001)}\mathcal{E}$ equilibrium at the point of intersection of the x_2-nullcline with x_2-axis. The interior equilibrium $_{(011)}\mathcal{E}$ is globally asymptotically stable with respect to the interior of the admissible region Ω_{12}, and the $_{(010)}\mathcal{E}$, $_{(001)}\mathcal{E}$ equilibria and the zero equilibrium are unstable.

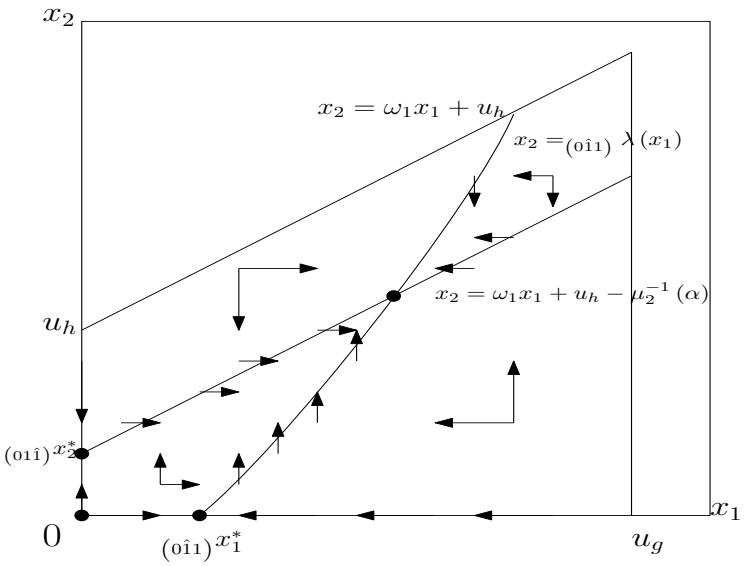

FIGURE 2.12: Sketch of the phase portrait of system (2.72) with $0 < \alpha < \mu_1(u_g, u_h)$, $0 < \alpha < \mu_2(u_h)$.

2.2.2 Face with $x_1 = 0$

We have the following reduced system:

$$\begin{cases} x_0' = (-\alpha + \mu_0(-x_0 + u_f, -\omega_2 x_0 - x_2 + u_h))\, x_0, \\ x_2' = (-\alpha + \mu_2(-\omega_2 x_0 - x_2 + u_h))\, x_2. \end{cases} \tag{2.76}$$

System (2.76) represents a food chain, with the chlorophenol degrader and methanogen present. Since the phenol degrader is absent, we anticipate that in order to both population survive, we need to suply both chlorophenol and hydrogen to the system.

We have two possible cases for our admissible region, depending on the sign of the $u_h - \omega_2 u_f$ expression. Here, we consider $u_h - \omega_2 u_f < 0$, since this is the usual case from the biological point of view. Thus, the domain for our system is given by the following set Ω_{02}:

$$\Omega_{02} = \left\{(x_0, x_2) \in \mathbb{R}^2 : 0 \le x_2 \le u_h, 0 \le x_0 \le \frac{u_h - x_2}{\omega_2}\right\}. \tag{2.77}$$

This region is sketched in Figure 2.13.

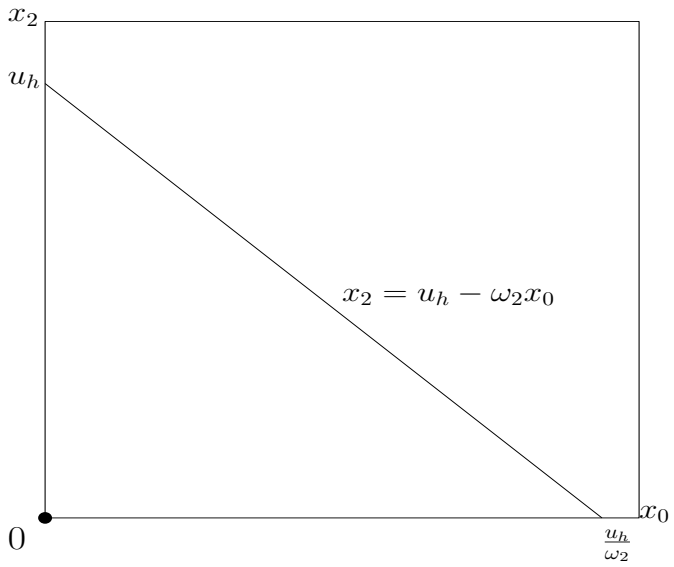

FIGURE 2.13: Domain Ω_{02} of system (2.76).

Again, the behaviour of the solutions depends on the value of the parameter α. We have the following cases to consider.

- $\alpha > \mu_0(u_f, u_h)$, $\alpha > \mu_2(u_h)$. In that case only the zero equilibrium exists, which is globally asymptotically stable.

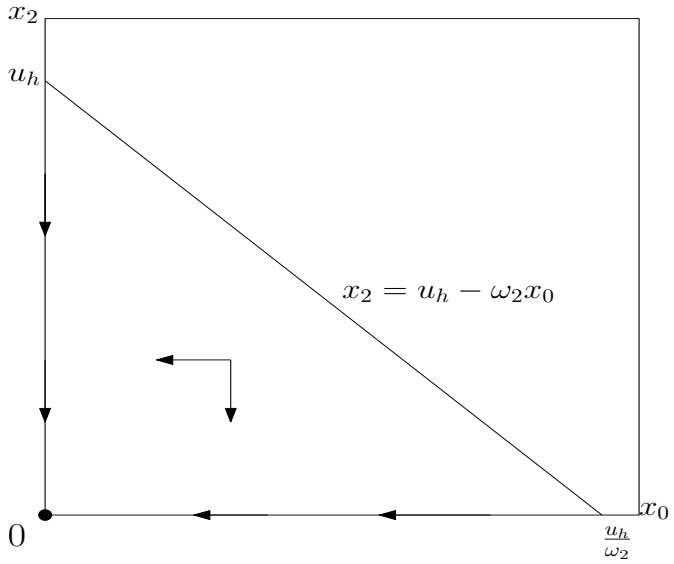

FIGURE 2.14: Sketch of the phase portrait of system (2.76) with $\alpha > \mu_0(u_f, u_h)$, $\alpha > \mu_2(u_h)$.

- $\alpha > \mu_0(u_f, u_h)$, $0 < \alpha < \mu_2(u_h)$. We have an additional x_2-nullcline given by the equation $x_2 = -\omega_2 x_0 + u_h - \mu_2^{-1}(\alpha)$. It intersects the x_2-axis at some $x_2 =_{(10\widehat{1})} \overset{*}{x}_2$ and x_0-axis at some $x_0 =_{(10\widehat{1})} \hat{x}_0$ (in fact, ${}_{(10\widehat{1})}\overset{*}{x}_2 = u_h - \mu_2^{-1}(\alpha)$ and ${}_{(10\widehat{1})}\hat{x}_0 = \frac{u_h}{\omega_2} - \frac{\mu_2^{-1}(\alpha)}{\omega_2}$). We have the boundary equilibrium ${}_{(001)}\mathcal{E}$ which is globally asymptotically stable with respect to the interior of the admissible region Ω_{02}. The zero equilibrium is unstable.

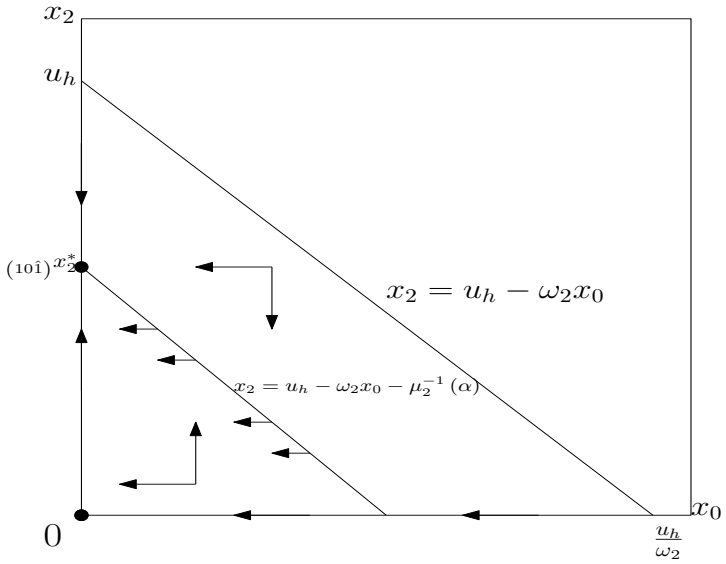

FIGURE 2.15: Sketch of the phase portrait of system (2.76) with $\alpha > \mu_0(u_f, u_h)$, $0 < \alpha < \mu_2(u_h)$.

- $0 < \alpha < \mu_0(u_f, u_h)$, $\alpha > \mu_2(u_h)$. We have some unique point $x_2 =_{(\widehat{101})} \hat{x}_2$, such that $\mu_0\left(u_f, -{}_{(\widehat{101})}\hat{x}_2 + u_h\right) = \alpha$, and some unique $x_0 =_{(\widehat{101})} \overset{*}{x}_0$, such that

$$\mu_0\left(-{}_{(\widehat{101})}\overset{*}{x}_0 + u_f, -\omega_2 {}_{(\widehat{101})}\overset{*}{x}_0 + u_h\right) = \alpha. \tag{2.78}$$

Also, since

$$\frac{\partial}{\partial x_2}\left[\mu_0(-x_0 + u_f, -\omega_2 x_0 - x_2 + u_h)\right] = -\partial s_2 \mu_0(-x_0 + u_f, -\omega_2 x_0 - x_2 + u_h) < 0 \tag{2.79}$$

inside the admissible region Ω_{02}, the Implicit Function Theorem implies existence of the function $x_2 =_{(\widehat{101})} \lambda(x_0)$, such that

$$\mu_0\left(-x_0 + u_f, -\omega_2 x_0 -_{(\widehat{101})} \lambda(x_0) + u_h\right) = \alpha. \tag{2.80}$$

This function (which is the x_0-nullcline) is defined for $x_0 \in \left[0, {}_{(\widehat{101})}\overset{*}{x}_0\right]$ and it connects the points $\left(0, {}_{(\widehat{101})}\hat{x}_2\right)$ and $\left({}_{(\widehat{101})}\overset{*}{x}_0, 0\right)$. We also know that the derivative of this function is given by

$$ {}_{(\widehat{101})}\lambda'(x_0) = -\frac{\partial_{s_0}\mu_0\left(-x_0+u_f, -\omega_2 x_0 - {}_{(\widehat{101})}\lambda(x_0)+u_h\right)}{\partial s_2\mu_0\left(-x_0+u_f, -\omega_2 x_0 - {}_{(\widehat{101})}\lambda(x_0)+u_h\right)} - \omega_2. \tag{2.81} $$

We have the ${}_{(100)}\mathcal{E} = \left({}_{(\widehat{101})}\overset{*}{x}_0, 0, 0\right)$ equilibrium and the phase portrait analysis shows that it is globally asymptotically stable with respect to the interior of the admissible region Ω_{02}. The zero equilibrium is unstable.

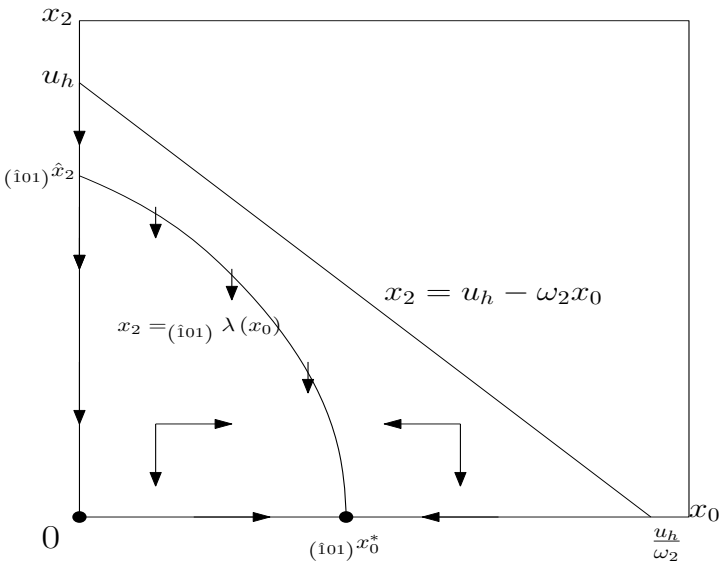

FIGURE 2.16: Sketch of the phase portrait of system (2.76) with $0 < \alpha < \mu_0(u_f, u_h)$, $\alpha > \mu_2(u_h)$.

- $0 < \alpha < \mu_0(u_f, u_h)$, $0 < \alpha < \mu_2(u_h)$. Here, both the x_0-nullcline and the x_2-nullcline are present. The x_0-nullcline $x_2 = {}_{(\widehat{100})}\lambda(x_0)$ intersects the x_2-axis at $x_2 = {}_{(\widehat{101})}\hat{x}_2$, and the x_0-axis at $x_0 = {}_{(\widehat{101})}\overset{*}{x}_0$. The x_2 nullcline $x_2 = -\omega_2 x_0 + u_h - \mu_2^{-1}(\alpha)$ intersects the x_2-axis at $x_2 = {}_{(10\widehat{1})}\overset{*}{x}_2 = u_h - \mu_2^{-1}(\alpha)$, and the x_0-axis at $x_0 = {}_{(10\widehat{1})}\hat{x}_0$. We have to consider four cases.

  - ${}_{(\widehat{101})}\overset{*}{x}_0 < {}_{(10\widehat{1})}\hat{x}_0$, ${}_{(\widehat{101})}\hat{x}_2 < {}_{(10\widehat{1})}\overset{*}{x}_2$.
    Here, since by equation (2.81), the slope of the x_0-nullcline is less than the slope of the x_2-nullcline (which equals $-\omega_2$), the two curves don't intersect.

We have three equilibria present: ${}_{(001)}\mathcal{E}$ (globally asymptotically stable with respect to the interior of the admissible region Ω_{02}), ${}_{(100)}\mathcal{E}$ (unstable), and the zero equilibrium (unstable).

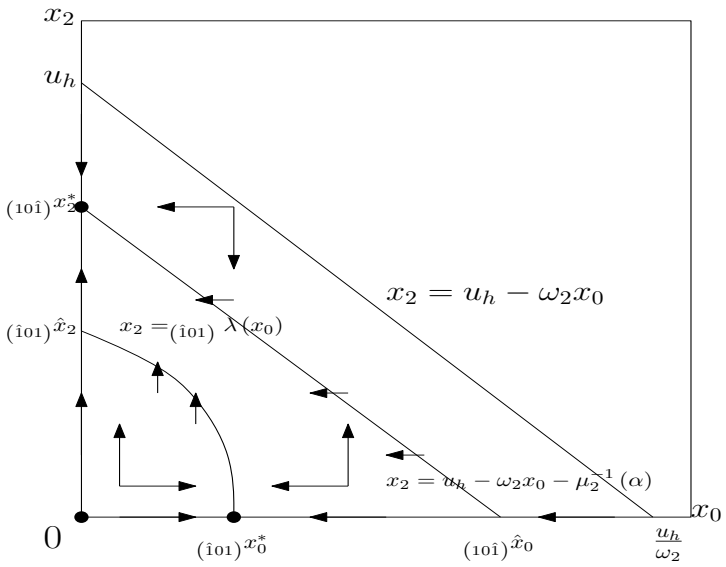

FIGURE 2.17: Sketch of the phase portrait of system (2.76) with $0 < \alpha < \mu_0(u_f, u_h)$, $0 < \alpha < \mu_2(u_h)$, and ${}_{(\widehat{1}01)}\overset{*}{x}_0 < {}_{(10\widehat{1})}\hat{x}_0$, ${}_{(\widehat{1}01)}\hat{x}_2 < {}_{(10\widehat{1})}\overset{*}{x}_2$.

- ${}_{(\widehat{1}01)}\overset{*}{x}_0 < {}_{(10\widehat{1})}\hat{x}_0$, ${}_{(\widehat{1}01)}\hat{x}_2 > {}_{(10\widehat{1})}\overset{*}{x}_2$.
  In that case the curves intersect at some interior equilibrium ${}_{(101)}\mathcal{E}$, and the intersection is unique, since the slope of the x_0-nullcline is smaller than the slope of the x_2-nullcline. The analysis of the phase plane shows that the ${}_{(101)}\mathcal{E}$ equilibrium is globally asymptotically stable with respect to the interior of the admissible region Ω_{02}, and ${}_{(001)}\mathcal{E}$, ${}_{(100)}\mathcal{E}$, and the zero equilibrium are all unstable.

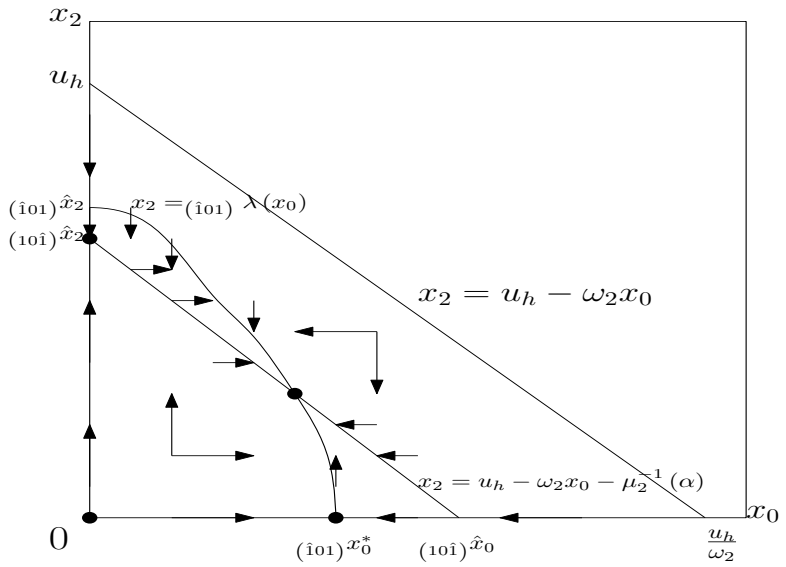

FIGURE 2.18: Sketch of the phase portrait of system (2.76) with $0 < \alpha < \mu_0(u_f, u_h)$, $0 < \alpha < \mu_2(u_h)$, and ${}_{(\hat{1}01)}\overset{*}{x}_0 <_{(10\hat{1})} \hat{x}_0$, ${}_{(\hat{1}01)}\hat{x}_2 >_{(10\hat{1})} \overset{*}{x}_2$.

- ${}_{(\hat{1}01)}\overset{*}{x}_0 >_{(10\hat{1})} \hat{x}_0$, ${}_{(\hat{1}01)}\hat{x}_2 <_{(10\hat{1})} \overset{*}{x}_2$.
  This situation is impossible, since if the x_0-nullcline starts below the x_2-nullcline, and because its slope is smaller than the slope of the x_2-nullcline, it has to lie entirely under it.

- ${}_{(\hat{1}01)}\overset{*}{x}_0 >_{(10\hat{1})} \hat{x}_0$, ${}_{(\hat{1}01)}\hat{x}_2 >_{(10\hat{1})} \overset{*}{x}_2$.
  In the last case, using a similar argument we can show that the x_0-nullcline lies entirely above the x_2-nullcline. Hence they do not intersect and we have only three equilibria present. Using the phase plane argument we can see that ${}_{(001)}\mathcal{E}$ is unstable, ${}_{(100)}\mathcal{E}$ is globally asymptotically stable with respect to the interior of the admissible region Ω_{02}, and the zero equilibrium is unstable.

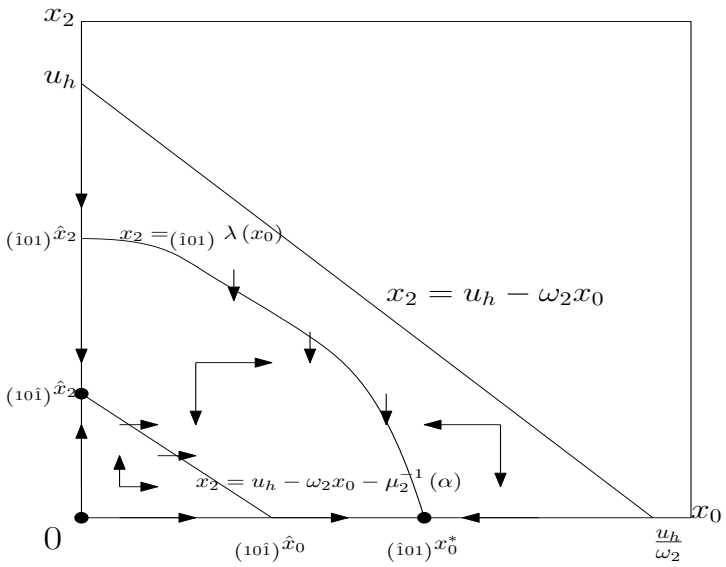

FIGURE 2.19: Sketch of the phase portrait of system (2.76) with $0 < \alpha < \mu_0(u_f, u_h)$, $0 < \alpha < \mu_2(u_h)$, and ${}_{(\hat{1}01)}\overset{*}{x}_0 > {}_{(10\hat{1})}\hat{x}_0$, ${}_{(\hat{1}01)}\hat{x}_2 > {}_{(10\hat{1})}\overset{*}{x}_2$.

2.2.3 Face with $x_2 = 0$

We have the following reduced system:

$$\begin{cases} x_0' = (-\alpha + \mu_0(-x_0 + u_f, -\omega_2 x_0 + \omega_1 x_1 + u_h))\, x_0, \\ x_1' = (-\alpha + \mu_1(\omega_0 x_0 - x_1 + u_g, -\omega_2 x_0 + \omega_1 x_1 + u_h))\, x_1. \end{cases} \tag{2.82}$$

System (2.82) represents a food chain, with the chlorophenol degrader and phenol degrader present. The relationship between the microorganisms is more complicated than in the cases of x_0x_2, and x_1x_2 faces, since now hydrogen acts not only as a substrate for the chlorophenol degrader, but it also inhibits growth of the phenol degrader. We thus might expect both populations surviving without the need of supplying hydrogen externally, i.e., with $u_h = 0$.

System (2.82) is considered on the following admissible region Ω_{01}:

$$\Omega_{01} = \left\{(x_0, x_1) \in \mathbb{R}^2 : 0 \le x_0 \le u_f, \max\left(0, \frac{\omega_2 x_0 - u_h}{\omega_1}\right) \le x_1 \le u_g + \omega_0 x_0\right\}. \tag{2.83}$$

Thus, we have two cases to consider: either $\omega_2 u_f - u_h > 0$, or $\omega_2 u_f - u_h < 0$. Here, we assume that $\omega_2 u_f - u_h > 0$, since this is the more plausible case from the biological point of view. As in the previous analysis, the behaviour of the solutions of the system depends on the value of parameter α. The admissible region Ω_{01} is represented in Figure 2.20.

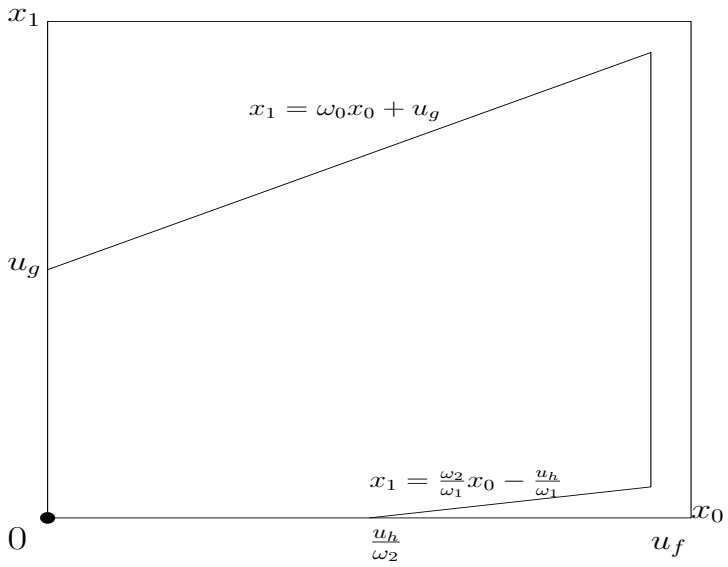

FIGURE 2.20: Domain Ω_{01} of the system (2.82) in the case $\omega_2 u_f - u_h > 0$.

- $\alpha > \mu_0 (u_f, \omega_1 u_g + u_h)$, $\alpha > \mu_1 \left(\left(\omega_0 - \frac{\omega_2}{\omega_1} \right) u_f + \frac{u_h}{\omega_1} + u_g, 0 \right)$.
  Here, only the zero equilibrium is present, and it is globally asymptotically stable.

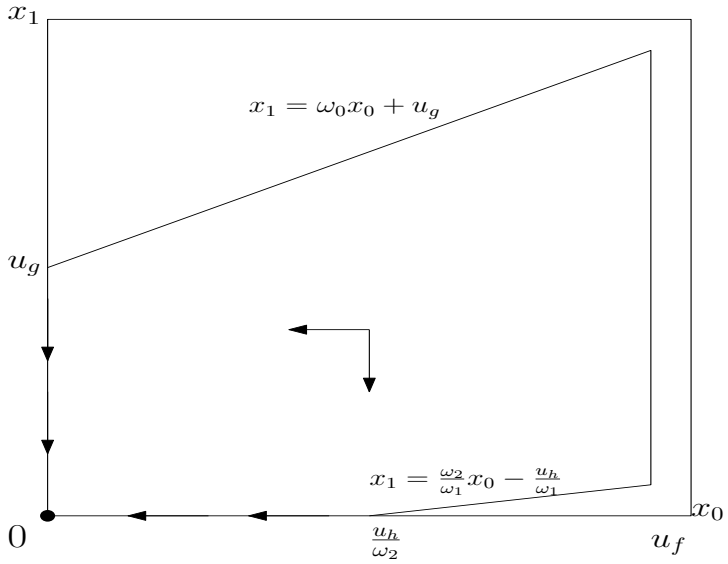

FIGURE 2.21: Sketch of the phase portrait of system (2.82) with $\alpha > \mu_0 (u_f, \omega_1 u_g + u_h)$, $\alpha > \mu_1 \left(\left(\omega_0 - \frac{\omega_2}{\omega_1} \right) u_f + \frac{u_h}{\omega_1} + u_g, 0 \right)$.

- $\mu_0 (u_f, u_h) < \alpha < \mu_0 (u_f, \omega_1 u_g + u_h)$, $\alpha > \mu_1 \left(\left(\omega_0 - \frac{\omega_2}{\omega_1} \right) u_f + \frac{u_h}{\omega_1} + u_g, 0 \right)$.
  We have only the zero equilibrium, and we have an additional x_0-nullcline. We can

find some unique $x_1 =_{(\widehat{1}10)} \hat{x}_1$, such that $\mu_0\left(u_f, \omega_{1(\widehat{1}10)}\hat{x}_1 + u_h\right) = \alpha$, and since

$$\frac{\partial}{\partial x_1}\left[\mu_0\left(-x_0 + u_f, -\omega_2 x_0 + \omega_1 x_1 + u_h\right)\right] \\ = \omega_1 \partial_{s_2}\mu_0\left(-x_0 + u_f, -\omega_2 x_0 + \omega_1 x_1 + u_h\right) \geq 0, \quad (2.84)$$

and the above expression equals 0 only for $x_0 = u_f$, for which $\mu_0 = 0$. Hence we can use the Implicit Function Theorem to obtain existence of the function $x_1 =_{(\widehat{1}10)} \lambda(x_0)$, such that

$$\mu_0\left(-x_0 + u_f, -\omega_2 x_0 + \omega_{1(\widehat{1}10)}\lambda(x_0) + u_h\right) = \alpha, \quad (2.85)$$

and which derivative is given by

$$_{(\widehat{1}10)}\lambda'(x_0) = -\frac{-\partial_{s_0}\mu_0 - \omega_2\partial_{s_2}\mu_0}{\omega_1\partial_{s_2}\mu_0} = \underbrace{\frac{1}{\omega_1}\frac{\partial_{s_0}\mu_0}{\partial_{s_2}\mu_0}}_{>0} + \frac{\omega_2}{\omega_1} > \frac{\omega_2}{\omega_1}. \quad (2.86)$$

The function intersects the line $x_1 = \omega_0 x_0 + u_g$. However, notice that on this line we have

$$\frac{\partial}{\partial x_0}\left[\mu_0\left(-x_0 + u_f, \left(\omega_0\omega_1 - \omega_2\right)x_0 + \omega_1 u_g + u_h\right)\right] = \\ = \underbrace{-\partial_{s_0}\mu_0}_{<0} + \underbrace{\left(\omega_0\omega_1 - \omega_2\right)\partial_{s_2}\mu_0}_{>0}, \quad (2.87)$$

hence (since the sign of the above expression is not determined) we don't know if the x_0-nullcline hits that line only once. In fact, it has been shown in [14] that we can have two such points, which results in two equilibria appearing when the x_1-nullcline is also present. Without the x_1-nullcline we have only the zero equilibrium, which is globally asymptotically stable with respect to the interior of the admissible region Ω_{01}. In Figure 2.22 we can see a possible phase portrait of the system.

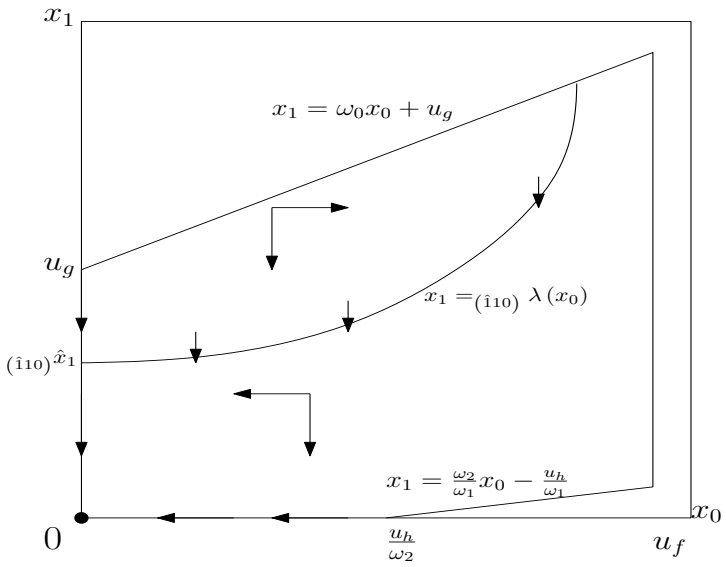

FIGURE 2.22: Sketch of the possible phase portrait of system (2.82) with $\mu_0(u_f, u_h) < \alpha < \mu_0(u_f, \omega_1 u_g + u_h)$, $\alpha > \mu_1\left(\left(\omega_0 - \frac{\omega_2}{\omega_1}\right) u_f + \frac{u_h}{\omega_1} + u_g, 0\right)$.

- $0 < \alpha < \mu_0(u_f, u_h)$, $\alpha > \mu_1\left(\left(\omega_0 - \frac{\omega_2}{\omega_1}\right) u_f + \frac{u_h}{\omega_1} + u_g, 0\right)$.
  Here, the x_0-nullcline $x_1 =_{(\hat{1}10)} \lambda(x_0)$ is present again, but this time it starts at some $x_0 =_{(\hat{1}10)} \overset{*}{x}_0$, i.e., $x_1 =_{(\hat{1}10)} \lambda\left({}_{(\hat{1}10)}\overset{*}{x}_0\right) = 0$. The nullcline hits this line $x_1 = \omega_0 x_0 + u_g$, but again, we do not know if it hits the line only once. We have another equilibrium ${}_{(100)}\mathcal{E} = \left({}_{(\hat{1}10)}\overset{*}{x}_0, 0, 0\right)$. Analysis of the phase plane shows that ${}_{(100)}\mathcal{E}$ is globally asymptotically stable with respect to the interior of the admissible region Ω_{01}, and the zero equilibrium is unstable.

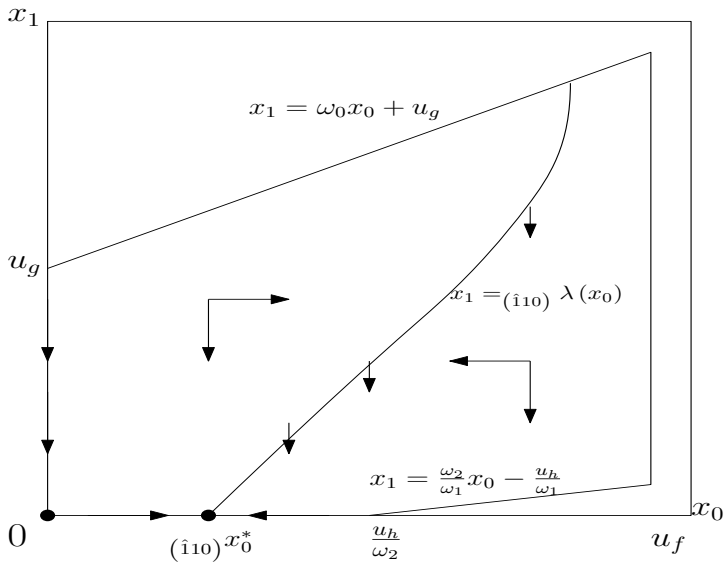

FIGURE 2.23: Sketch of the possible phase portrait of system (2.82) with $0 < \alpha < \mu_0(u_f, u_h)$, $\alpha > \mu_1\left(\left(\omega_0 - \frac{\omega_2}{\omega_1}\right)u_f + \frac{u_h}{\omega_1} + u_g, 0\right)$.

- $\alpha > \mu_0(u_f, \omega_1 u_g + u_h)$, $\mu_1(u_g, u_h,) < \alpha < \mu_1\left(\left(\omega_0 - \frac{\omega_2}{\omega_1}\right)u_f + \frac{u_h}{\omega_1} + u_g, 0\right)$.
  In this case with have an additional x_1-nullcline. There exists some unique point $\left({}_{(1\hat{1}\hat{0})}\hat{x}_0, {}_{(1\hat{1}\hat{0})}\hat{x}_1\right)$ on the line

$$\Gamma : \begin{cases} x_1 = 0, \quad x_0 \in \left(0, \dfrac{u_h}{\omega_2}\right), \\ x_1 = \dfrac{\omega_2}{\omega_1} x_0 - \dfrac{u_h}{\omega_1}, \quad x_0 \in \left[\dfrac{u_h}{\omega_2}, u_f\right), \end{cases} \tag{2.88}$$

such that $\mu_1\left(\omega_0 {}_{(1\hat{1}\hat{0})}\hat{x}_0 - {}_{(1\hat{1}\hat{0})}\hat{x}_1 + u_g, -\omega_2 {}_{(1\hat{1}\hat{0})}\hat{x}_0 + \omega_1 {}_{(1\hat{1}\hat{0})}\hat{x}_1 + u_h\right) = \alpha$. Since

$$\begin{aligned} \frac{\partial}{\partial x_1}\left[\mu_1(\omega_0 x_0 - x_1 + u_g, -\omega_2 x_0 + \omega_1 x_1 + u_h)\right] = \\ -\partial_{s_1}\mu_1(\omega_0 x_0 - x_1 + u_g, -\omega_2 x_0 + \omega_1 x_1 + u_h) + \\ \omega_1 \partial_{s_2}\mu_1(\omega_0 x_0 - x_1 + u_g, -\omega_2 x_0 + \omega_1 x_1 + u_h) < 0 \end{aligned} \tag{2.89}$$

inside the admissible region Ω_{01}, we can use the Implicit Function Theorem to obtain existence of the function ${}_{(1\hat{1}\hat{0})}\lambda(x_0)$ such that

$$\mu_1\left(\omega_0 x_0 - {}_{(1\hat{1}\hat{0})}\lambda(x_0) + u_g, -\omega_2 x_0 + \omega_1 {}_{(1\hat{1}\hat{0})}\lambda(x_0) + u_h\right) = \alpha. \tag{2.90}$$

This function is defined for $x_0 \in \left[{}_{(1\hat{1}\hat{0})}\hat{x}_0, u_f\right]$ with ${}_{1\hat{1}\hat{0}}\lambda(u_f) = {}_{(1\hat{1}\hat{0})}\hat{x}_1^{(2)}$, where

$x_1 =_{(1\hat{1}0)} \hat{x}_1^{(2)}$ is the x_1-coordinate of the unique point on the line $x_0 = u_f$ such that

$$\mu_1\left(\omega_0 u_f -_{(1\hat{1}0)} \hat{x}_1^{(2)} + u_g, -\omega_2 u_f + \omega_1{}_{(1\hat{1}0)}\hat{x}_1^{(2)} + u_h\right) = \alpha. \tag{2.91}$$

We also know that

$$(1\hat{1}0)\lambda'(x_0) = \frac{\omega_0 M_1(x_0) - \omega_2 M_2(x_0)}{M_1(x_0) - \omega_1 M_2(x_0)}, \tag{2.92}$$

where

$$M_1(x_0) = \partial_{s_1}\mu_1\left(\omega_0 x_0 -_{(1\hat{1}0)} \lambda(x_0) + u_g, -\omega_2 x_0 + \omega_1{}_{(1\hat{1}0)}\lambda(x_0) + u_h\right), \tag{2.93}$$

$$M_2(x_0) = \partial_{s_2}\mu_1\left(\omega_0 x_0 -_{(1\hat{1}0)} \lambda(x_0) + u_g, -\omega_2 x_0 + \omega_1{}_{(1\hat{1}0)}\lambda(x_0) + u_h\right). \tag{2.94}$$

We have only the zero equilibrium and analysis of the phase plane shows that it is globally asymptotically stable with respect to the interior of the admissible region Ω_{01}.

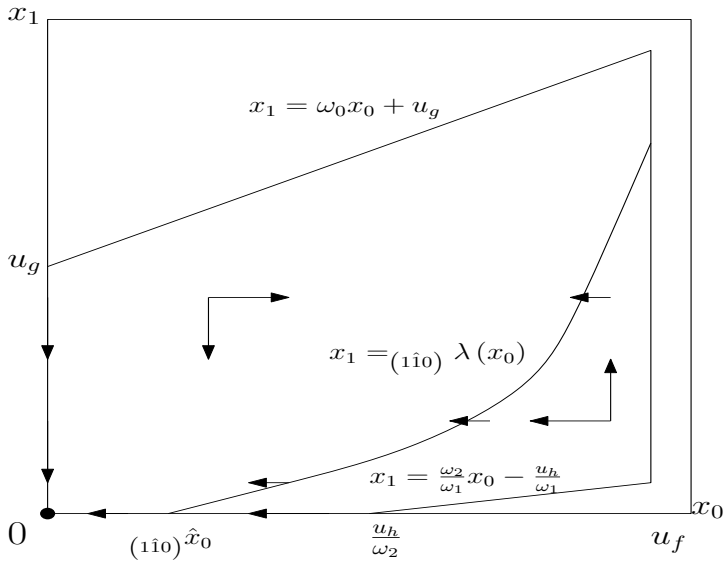

FIGURE 2.24: Sketch of the phase portrait of system (2.82) with $\alpha > \mu_0(u_f, \omega_1 u_g + u_h)$, $\mu_1(u_g, u_h,) < \alpha < \mu_1\left(\left(\omega_0 - \frac{\omega_2}{\omega_1}\right) u_f + \frac{u_h}{\omega_1} + u_g, 0\right)$.

- $\alpha > \mu_0(u_f, \omega_1 u_g + u_h)$, $0 < \alpha < \mu_1(u_g, u_h)$.
  Again, we have the x_1-nullcline given by the function $x_1 =_{(1\hat{1}0)} \lambda(x_0)$. This nullcline is defined for $x_0 \in [0, u_f]$ with $_{(1\hat{1}0)}\lambda(0) =_{(1\hat{1}0)} \overset{*}{x}_1$ (where $x_1 =_{(1\hat{1}0)} \overset{*}{x}_1$ is

the unique point on the x_1-axis, such that $\mu_1\left(-_{(1\hat{1}0)}\overset{*}{x}_1+u_g,\omega_1{}_{(1\hat{1}0)}\overset{*}{x}_1+u_h\right)=\alpha\Big)$, and $_{(1\hat{1}0)}\lambda\left(u_f\right)=_{(1\hat{1}0)}\hat{x}_1$ $\Big($where $x_1=_{(1\hat{1}0)}\hat{x}_1$ is the unique point on the line $x_1=u_f$, such that $\mu_1\left(\omega_0u_f-_{(1\hat{1}0)}\hat{x}_1+u_g,-\omega_2u_f+\omega_1{}_{(1\hat{1}0)}\hat{x}_1+u_h\right)=\alpha\Big)$. We have another equilibrium $_{(010)}\mathcal{E}=\left(0,_{(1\hat{1}0)}\overset{*}{x}_1,0\right)$ present. Analysis of the phase plane shows that $_{(010)}\mathcal{E}$ equilibrium is globally asymptotically stable with respect to the interior of the admissible region Ω_{01}, and the zero equilibrium is unstable.

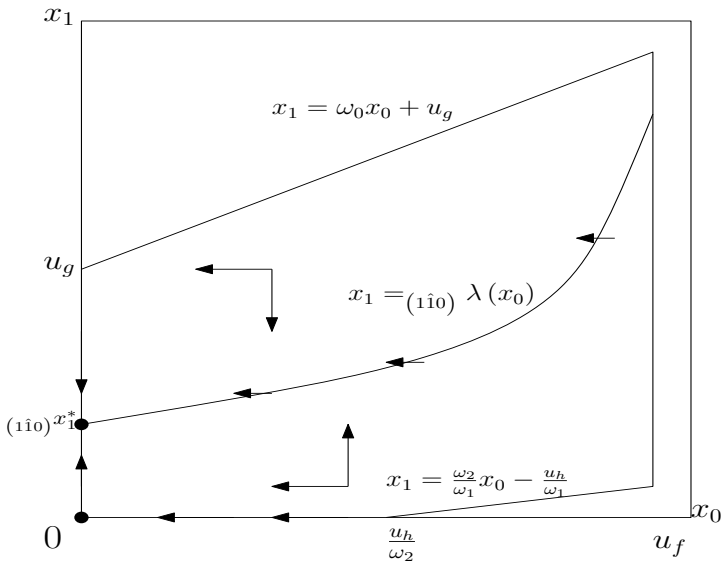

FIGURE 2.25: Sketch of the phase portrait of system (2.82) with $\alpha>\mu_0\left(u_f,\omega_1u_g+u_h\right)$, $0<\alpha<\mu_1\left(u_g,u_h\right)$.

The following four cases

- $\mu_0\left(u_f,u_h\right)<\alpha<\mu_0\left(u_f,\omega_1u_g+u_h\right)$, $\mu_1\left(u_g,u_h,\right)<\alpha<\mu_1\left(\left(\omega_0-\frac{\omega_2}{\omega_1}\right)u_f+\frac{u_h}{\omega_1}+u_g,0\right)$,
- $\mu_0\left(u_f,u_h\right)<\alpha<\mu_0\left(u_f,\omega_1u_g+u_h\right)$, $0<\alpha<\mu_1\left(u_g,u_h\right)$,
- $0<\alpha<\mu_0\left(u_f,u_h\right)$, $\mu_1\left(u_g,u_h,\right)<\alpha<\mu_1\left(\left(\omega_0-\frac{\omega_2}{\omega_1}\right)u_f+\frac{u_h}{\omega_1}+u_g,0\right)$,
- $0<\alpha<\mu_0\left(u_f,u_h\right)$, $0<\alpha<\mu_1\left(u_g,u_h\right)$,

are too complicated to be dealt with in the general class of the prototypes μ_0 and μ_1. The additional assumptions that might be considered are on the signs of the second partial derivatives of the functions μ_0 and μ_1 (which might result in the convexity or concavity of the implicitly defined nullclines $_{(\hat{1}10)}\lambda$ and $_{(1\hat{1}0)}\lambda$). We can however rule out periodic orbits on that face using the Dulac's Criterion [7]. First, notice that no periodic orbit can intersect the axes $x_0=0$ or $x_1=0$, since they are invariant. Now, let

us define an auxiliary function

$$\varphi(x_0, x_1) = \frac{1}{x_0 x_1}, \quad (x_0, x_1) \in \Omega_{01} \setminus (\{x_0 = 0\} \cup \{x_1 = 0\}). \tag{2.95}$$

Then

$$\nabla \cdot (\varphi(-\alpha + \mu_0) x_0, \varphi(-\alpha + \mu_1) x_1) = \frac{-\partial_{s_0}\mu_0 - \omega_2 \partial_{s_2}\mu_0}{x_1} + \frac{-\partial_{s_1}\mu_1 + \omega_1 \partial_{s_2}\mu_1}{x_0} < 0 \tag{2.96}$$

for all (x_0, x_1) in the domain of φ. Thus, by the Dulac's Criterion, there are no periodic orbits in the x_0x_1 face.

We gather the results concerning the existence and local stability of the equilibria of (2.13) in table 2.1. The symbol " $\star$ " refers to the conditions for existence obtained in subsection 2.1.1, and the symbol "†" refers to the conditions derived from the phase plane analysis in section 2.2. Moreover, all the functions in the "Local stability" column are evaluated at the corresponding steady states, and all the symbols are given by equations (2.97)-(2.107). The conditions for existence of the ${}_{(110)}\mathcal{E}$ equilibrium are discussed in subsection 2.1.1.

Equilibrium	Existence	Local stability
${}_{(000)}\mathcal{E}$	Always	$\alpha > \max(\mu_0, \mu_1, \mu_2)$
${}_{(100)}\mathcal{E}$	$\alpha < \mu_0(u_f, u_h)$	$\alpha > \max(\mu_1, \mu_2)$
${}_{(010)}\mathcal{E}$	$\alpha < \mu_1(u_g, u_h)$	$\alpha > \max(\mu_0, \mu_2)$
${}_{(001)}\mathcal{E}$	$\alpha < \mu_2(u_h)$	$\alpha > \max(\mu_0, \mu_1)$
${}_{(101)}\mathcal{E}$	${}_{(101)}\star$ or ${}_{(101)}\dagger$	$\alpha > \mu_1$
${}_{(011)}\mathcal{E}$	${}_{(011)}\star$ or ${}_{(011)}\dagger^{(1)}$ or ${}_{(011)}\dagger^{(2)}$ or ${}_{(011)}\dagger^{(3)}$	$\alpha > \mu_0$
${}_{(110)}\mathcal{E}$	-	$\alpha > \mu_2$ and ${}_{(110)}a_0 > 0$
${}_{(111)}\mathcal{E}$	${}_{(111)}\star$	${}_{(111)}a_2\,{}_{(111)}a_1 - {}_{(111)}a_0 > 0$,

TABLE 2.1: Equilibria of system (2.13) together with their local stability.

$$
\begin{aligned}
{}_{(101)}\star &= \alpha \in \left(\mu_0\left(u_f - \min\left(u_f, \frac{u_h - \mu_2^{-1}(\alpha)}{\omega_2}\right), \mu_2^{-1}(\alpha)\right), \mu_0\left(u_f, \mu_2^{-1}(\alpha)\right)\right), \qquad (2.97)\\
&\quad \text{and } \alpha < \mu_2(u_h),\\
{}_{(101)}\dagger &= \alpha < \min\left(\mu_0(u_f, u_h), \mu_2(u_h)\right), \text{ and } {}_{(\widehat{1}01)}\overset{*}{x}_0 <_{(10\widehat{1})} \hat{x}_0, {}_{(\widehat{1}01)}\hat{x}_2 >_{(10\widehat{1})} \overset{*}{x}_2, \qquad (2.98)\\
{}_{(011)}\star &= \alpha \in \left[0, \mu_1\left(u_g - \max\left(0, \frac{\mu_2^{-1}(\alpha) - u_h}{\omega_1}\right), \mu_2^{-1}(\alpha)\right)\right), \qquad (2.99)\\
&\quad \text{and } \alpha < \mu_2(\omega_1 u_g + u_h),\\
{}_{(011)}\dagger^{(1)} &= \mu_1(u_g, u_h) < \alpha < \mu_1(u_g, 0), 0 < \alpha < \mu_2(u_h), \text{ and } {}_{(0\widehat{1}1)}\hat{x}_2 <_{(01\widehat{1})} \overset{*}{x}_2, \qquad (2.100)\\
{}_{(011)}\dagger^{(2)} &= \alpha < \mu_1(u_g, u_h), \mu_2(u_h) < \alpha < \mu_2(\omega_1 u_g + u_h), \text{ and } {}_{(01\widehat{1})}\hat{x}_1 <_{(0\widehat{1}1)} \overset{*}{x}_1, \qquad (2.101)\\
{}_{(011)}\dagger^{(3)} &= \alpha < \mu_1(u_g, u_h), \text{ and } \alpha < \mu_2(u_h), \qquad (2.102)\\
{}_{(110)}a_0 &= \frac{\partial\mu_0}{\partial s_0}\frac{\partial\mu_1}{\partial s_1} - \omega_1\frac{\partial\mu_0}{\partial s_0}\frac{\partial\mu_1}{\partial s_2} + (\omega_2 - \omega_0\omega_1)\frac{\partial\mu_0}{\partial s_2}\frac{\partial\mu_1}{\partial s_1}, \qquad (2.103)\\
{}_{(111)}\star &= \alpha \in \left[0, \min\left(\mu_0\left(u_f, \mu_2^{-1}(\alpha)\right), \mu_1\left(\omega_0\overset{*}{x}_0 - \max\left(0, \frac{\omega_2\overset{*}{x}_0 - u_h}{\omega_1}\right)\right.\right.\right. \qquad (2.104)\\
&\quad \left.\left.\left. + u_g, \mu_2^{-1}(\alpha)\right), \mu_2\left(-\omega_2\overset{*}{x}_0 + \omega_1\overset{*}{x}_1 + u_h\right)\right)\right),\\
{}_{(111)}a_2 &= -\overset{*}{x}_0\left(-\frac{\partial\mu_0}{\partial s_0} - \omega_2\frac{\partial\mu_0}{\partial s_2}\right) - \overset{*}{x}_1\left(-\frac{\partial\mu_1}{\partial s_1} + \omega_1\frac{\partial\mu_1}{\partial s_2}\right) + \overset{*}{x}_2\mu_2', \qquad (2.105)\\
{}_{(111)}a_1 &= \overset{*}{x}_1\frac{\partial\mu_1}{\partial s_1}\left(\overset{*}{x}_0\frac{\partial\mu_0}{\partial s_0} - (\omega_0\omega_1 - \omega_2)\overset{*}{x}_0\frac{\partial\mu_0}{\partial s_2} + \overset{*}{x}_2\mu_2'\right) \qquad (2.106)\\
&\quad + \overset{*}{x}_0\frac{\partial\mu_0}{\partial s_0}\left(-\omega_1\overset{*}{x}_1\frac{\partial\mu_1}{\partial s_2} + \overset{*}{x}_2\mu_2'\right),\\
{}_{(111)}a_0 &= \overset{*}{x}_0\overset{*}{x}_1\overset{*}{x}_2\frac{\partial\mu_0}{\partial s_0}\frac{\partial\mu_1}{\partial s_1}\mu_2'. \qquad (2.107)
\end{aligned}
$$

Chapter 3

Analysis of the full system

3.1 Hopf Bifurcation

In this work we are especially interested in developing a more systematic approach to studying the Hopf bifurcation of the interior equilibrium. That Hopf bifurcation occurs in this model was previously observed numerically [14]. Occurrence of a stable periodic orbit in system (2.13) represents a situation in which all three populations of microorganisms oscillate indefinitely, and as a consequence, the concentrations of substrates fluctuates. The characteristic polynomial of the Jacobian ${}_{(111)}J$ corresponding to the interior equilibrium is given by

$$\lambda^3 + a_2\lambda^2 + a_1\lambda + a_0 = 0, \tag{3.1}$$

where

$$a_2 = -\overset{*}{x}_0\left(-\frac{\partial\mu_0}{\partial s_0} - \omega_2\frac{\partial\mu_0}{\partial s_2}\right) - \overset{*}{x}_1\left(-\frac{\partial\mu_1}{\partial s_1} + \omega_1\frac{\partial\mu_1}{\partial s_2}\right) + \overset{*}{x}_2\mu_2', \tag{3.2}$$

$$a_1 = \overset{*}{x}_1\frac{\partial\mu_1}{\partial s_1}\left(\overset{*}{x}_0\frac{\partial\mu_0}{\partial s_0} - (\omega_0\omega_1 - \omega_2)\overset{*}{x}_0\frac{\partial\mu_0}{\partial s_2} + \overset{*}{x}_2\mu_2'\right) + \overset{*}{x}_0\frac{\partial\mu_0}{\partial s_0}\left(-\omega_1\overset{*}{x}_1\frac{\partial\mu_1}{\partial s_2} + \overset{*}{x}_2\mu_2'\right), \tag{3.3}$$

$$a_0 = \overset{*}{x}_0\overset{*}{x}_1\overset{*}{x}_2\frac{\partial\mu_0}{\partial s_0}\frac{\partial\mu_1}{\partial s_1}\mu_2', \tag{3.4}$$

and the coefficients a_2, a_1, and a_0 depend on the parameters u_f, u_g, u_h, and α. The coefficients a_2 and a_0 are sign-definite (they are both positive), and a_1 might possibly change sign. Let us first notice that since the polynomial has order three, a real eigenvalue always exists. By the Routh-Hurwitz criterion, the above polynomial has a pair of purely imaginary eigenvalues if and only if

$$a_2a_1 = a_0 \quad (\text{which implies } a_1 > 0). \tag{3.5}$$

In that case we also have

$$\lambda^3 + a_2\lambda^2 + a_1\lambda + a_0 = \lambda^3 + a_2\lambda^2 + a_1\lambda + a_2a_1 = (\lambda + a_2)\left(\lambda^2 + a_1\right). \tag{3.6}$$

Hence the eigenvalues are $\lambda_1 = -a_2$ and $\lambda_{2,3} = \pm\sqrt{a_1}i$. Since eigenvalues are continuous functions of the parameters, we can see that if there is some $(u_f, u_g, u_h, \alpha) = \left(u_f^*, u_g^*, u_h^*, \alpha^*\right)$ such that $a_2 a_1 = a_0$, then if we denote by λ_1 the always present real eigenvalue, there is some $\delta > 0$ such that for $\left\|(u_f, u_g, u_h, \alpha) - \left(u_f^*, u_g^*, u_h^*, \alpha^*\right)\right\| < \delta$ we always have $\lambda_1 < 0$. By lemma 5.1, section 5.2 in [7], this implies the existence of a parameter-dependent, smooth, attracting, two dimensional, center manifold $W^c_{(u_f,u_g,u_h,\alpha)}$. In the following analysis, we consider only parameters that are in the δ-neighborhood of (u_f, u_g, u_h, α) in order to ensure that the real eigenvalue λ_1 is negative.

By the Routh-Hurwitz criterion (since we just showed that when ${}_{(111)}\mathcal{E}$ exists that a_0 and a_2 are always positive), a Hopf bifurcation occurs when the expression $a_2 a_1 - a_0$ changes sign as a parameter varies. This ensures that the real part of a pair of complex eigenvalues with nonzero imaginary part passes through 0 and hence changes sign. This is related to the transversality condition: the derivative of the real part of the eigenvalue with respect to the bifurcation parameter evaluated at the critical value when the real parts are zero is non-zero. We check this condition for specific forms of the functions μ_0, μ_1, and μ_2. For the prototypes proposed in (1.20), and with the values of parameters from table 1.1 fixed, the function

$$f\left(u_f, u_g, u_h, \alpha\right) = a_2 a_1 - a_0 \tag{3.7}$$

is an algebraic function in u_f, u_g, u_h, and α. Hence fixing all the parameters except one makes the function f a polynomial, the order of which depends on the choice of the free parameter. Specifically if we choose:

- α - free parameter $\implies$ f has order 27,
- u_f - free parameter $\implies$ f has order 3,
- u_g - free parameter $\implies$ f has order 3,
- u_h - free parameter $\implies$ f has order 2.

We do bifurcation diagrams to explore the possibility of Hopf bifurcations as α varies in section 3.3, and begin our theoretical analysis by choosing u_f as the free parameter. We have

$$f_{u_f}\left(u_f\right) = a_2 a_1 - a_0 = b_3 u_f^3 + b_2 u_f^2 + b_1 u_f + b_0, \tag{3.8}$$

and we assume that there is a value $u_f = u_f^*$ such that $f_{u_f}(u_f^*) = 0$. We want to find conditions on the coefficients of f_{u_f} that guarantee that the derivative of $a_2 a_1 - a_0$ with respect to u_f is not equal to zero when $a_2 a_1 - a_0 = 0$, i.e., that u_f^* is not a local extremum of f_{u_f}. We have

$$f'_{u_f}\left(u_f\right) = 3b_3 u_f^2 + 2b_2 u_f + b_1. \tag{3.9}$$

The necessary condition for u_f^* to be a local extremum for f_{u_f} is $f'_{u_f}(u_f^*) = 0$, that is

$$u_f^* = \frac{-b_2 \pm \sqrt{b_2^2 - 3b_1b_3}}{3b_3}. \tag{3.10}$$

We can derive sufficient conditions for u_f^* to be an extremum (for example by computing the second derivative of f_{u_f}), but the condition (3.10) is already very restrictive and will be sufficient for our work. We have thus obtained a sufficient condition for a Hopf bifurcation.

If we choose u_g as the free parameter, we have

$$f_{u_g}(u_h) = c_3u_g^3 + c_2u_g^2 + c_1u_g + c_0, \tag{3.11}$$

and with the assumption that $f_{u_g}\left(u_g^*\right) = 0$, by a similar analysis as in the previous case, we obtain an analogous sufficient condition for a Hopf bifurcation in u_g.

Finally, if we choose u_h as the free parameter, we have

$$f_{u_h}(u_h) = d_2u_h^2 + d_1u_h + d_0. \tag{3.12}$$

Once again, we assume that $f_{u_h}(u_h^*) = 0$, that is

$$u_h^* = \frac{-d_1 \pm \sqrt{d_1^2 - 4d_2d_0}}{2d_2}. \tag{3.13}$$

Here, u_h^* is the local extremum if and only if the discriminant of equation (3.12) is zero, i.e., if $d_1^2 - 4d_2d_0 = 0$.

We summarize our results in the following theorem.

Theorem 1. *Consider system (2.13) with the prototypes given by (1.20) and with the values of parameters from table 1.1 fixed. Assume that there exists a point* $(u_f, u_g, u_h, \alpha) = \left(u_f^*, u_g^*, u_h^*, \alpha^*\right)$ *such that* $f\left(u_f^*, u_g^*, u_h^*, \alpha^*\right) = 0$ *for* f *defined in (3.7). Then* $f_{u_f}(u_f) = f\left(u_f, u_g^*, u_h^*, \alpha^*\right)$, $f_{u_g}(u_g) = f\left(u_f^*, u_g, u_h^*, \alpha^*\right)$, *and* $f(u_h) = f\left(u_f^*, u_g^*, u_h, \alpha^*\right)$ *are given by the equations (3.8), (3.11), and (3.12), respectively. Also, there exists* $\delta > 0$ *such that if* $\left\|(u_f, u_g, u_h, \alpha) - \left(u_f^*, u_g^*, u_h^*, \alpha^*\right)\right\| < \delta$, *then*

I. if

$$u_f^* \neq \frac{-b_2 \pm \sqrt{b_2^2 - 3b_1b_3}}{3b_3}, \tag{3.14}$$

then there is a Hopf bifurcation in u_f *at* $u_f = u_f^*$,

II. if

$$u_g^* \neq \frac{-c_2 \pm \sqrt{c_2^2 - 3c_1c_3}}{3c_3}, \tag{3.15}$$

then there is a Hopf bifurcation in u_g *at* $u_g = u_g^*$,

III. if

$$d_1^2 - 4d_2d_0 \neq 0, \tag{3.16}$$

then there is a Hopf bifurcation in u_h *at* $u_h = u_h^*$.

We now illustrate the theoretical results with the numerical simulations. To approximate values of the equilibria we used Maple software [9], rounding all the values to 6 significant digits. For the choice of parameters given in Table 1.1 and

$$\alpha = 0.01, \quad u_g = 0, \quad u_h = 0.1, \tag{3.17}$$

it follows that the only zero of (3.8) occurs for $u_f = 0.538725$. In Figure 3.1 we plot the phase space for $u_f = 0.538$ (just before the Hopf bifurcation) using the ode15s solver from [10]. For this set of parameters, we have the following approximate values of the equilibria

$$\begin{aligned}
{}_{(000)}\mathcal{E} &= (0,0,0) \quad \text{(unstable)},\\
{}_{(100)}\mathcal{E} &= (0.000605984,0,0) \quad \text{(stable)},\\
{}_{(001)}\mathcal{E} &= (0,0,0.0973693) \quad \text{(unstable)},\\
{}_{(110)}\mathcal{E}^{(1)} &= (0.0611201,0.00595680,0) \quad \text{(unstable)},\\
{}_{(110)}\mathcal{E}^{(2)} &= (0.527493,0.0524709,0) \quad \text{(unstable)},\\
{}_{(111)}\mathcal{E} &= (0.344611,0.0584659,40.7588) \quad \text{(unstable)}.
\end{aligned} \tag{3.18}$$

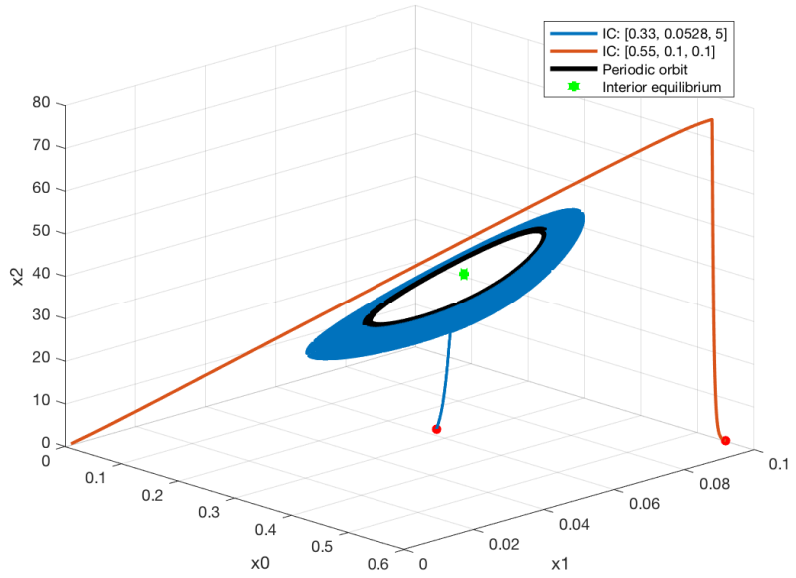

FIGURE 3.1: Phase space of system (2.13) with $\alpha = 0.01$, $u_f = 0.538$, $u_g = 0$, and $u_h = 0.1$.

We can see that there exists a stable periodic orbit in the system, but depending on the initial conditions, the solution might also converge to the boundary equilibrium ${}_{(100)}\mathcal{E}$. Thus in this case we observe bistability.

We now repeat the simulations for $u_f = 0.6$ (after the predicted Hopf bifurcation), presented in Figure 3.2. With all the other parameters set to the same values as in the previous case, we have the following equilibria

$$\begin{aligned}
{}_{(000)}\mathcal{E} &= (0,0,0) \quad \text{(unstable)},\\
{}_{(100)}\mathcal{E} &= (0.000606483,0,0) \quad \text{(stable)},\\
{}_{(001)}\mathcal{E} &= (0,0,0.0973693) \quad \text{(unstable)},\\
{}_{(110)}\mathcal{E}^{(1)} &= (0.0610742,0.00595223,0) \quad \text{(unstable)},\\
{}_{(110)}\mathcal{E}^{(2)} &= (0.589539,0.0586557,0) \quad \text{(unstable)},\\
{}_{(111)}\mathcal{E} &= (0.406611,0.0699610,49.6919) \quad \text{(stable)}.
\end{aligned} \tag{3.19}$$

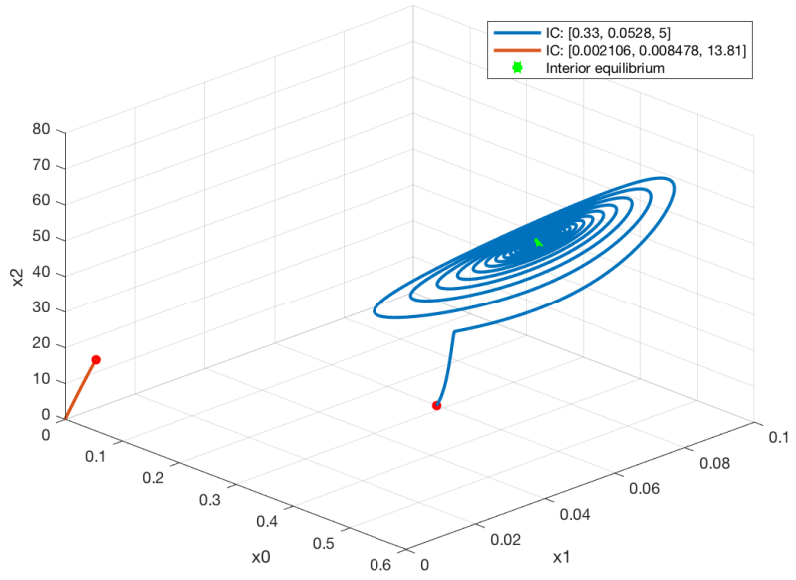

FIGURE 3.2: Phase space of system (2.13) with $\alpha = 0.01$, $u_f = 0.6$, $u_g = 0$, and $u_h = 0.1$.

We can see that the Hopf bifurcation occurs between $u_f = 0.538$ and $u_f = 0.6$. The stable periodic orbit is no longer present, and the interior equilibrium is stable. Once again, the boundary equilibrium ${}_{(100)}\mathcal{E}$ is stable, and thus we observe bistability in the system.

To illustrate a Hopf bifurcation in u_g, we fix the following parameters

$$\alpha = 0.01, \quad u_f = 0.5, \quad u_h = 0.1. \tag{3.20}$$

Then, the only zero of (3.11) occurs at $u_g = 0.000601604$. For $u_g = 0.0006$ we have the following equilibria

$$\begin{aligned}
{}_{(000)}\mathcal{E} &= (0, 0, 0) \quad \text{(unstable)}, \\
{}_{(100)}\mathcal{E} &= (0.000605615, 0, 0) \quad \text{(stable)}, \\
{}_{(001)}\mathcal{E} &= (0, 0, 0.0973693) \quad \text{(unstable)}, \\
{}_{(110)}\mathcal{E}^{(1)} &= (0.0542490, 0.00528049, 0) \quad \text{(unstable)}, \\
{}_{(110)}\mathcal{E}^{(2)} &= (0.489465, 0.0486886, 0) \quad \text{(unstable)}, \\
{}_{(111)}\mathcal{E} &= (0.306611, 0.0520205, 36.2777) \quad \text{(unstable)}.
\end{aligned} \tag{3.21}$$

The phase space of the system is presented in Figure 3.3.

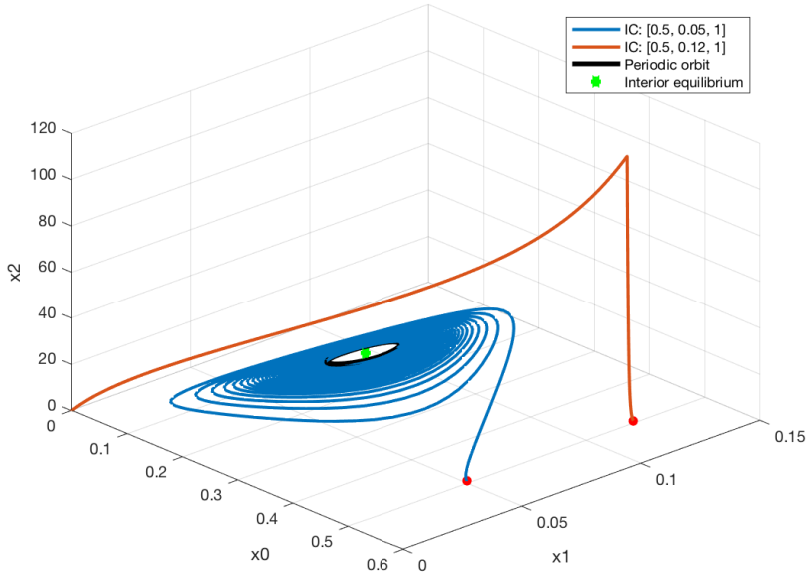

FIGURE 3.3: Phase space of system (2.13) with $\alpha = 0.01$, $u_f = 0.5$, $u_g = 0.0006$, and $u_h = 0.1$.

Similar to the previous case, there is a stable periodic orbit surrounding an unstable equilibrium point. The ${}_{(100)}\mathcal{E}$ equilibrium is also stable.

For $u_g = 0.0008$ (after the predicted Hopf bifurcation) we have the following equilibria

$$\begin{aligned}
{}_{(000)}\mathcal{E} &= (0,0,0) \quad \text{(unstable)},\\
{}_{(100)}\mathcal{E} &= (0.000605615,0,0) \quad \text{(stable)},\\
{}_{(001)}\mathcal{E} &= (0,0,0.0973693) \quad \text{(unstable)},\\
{}_{(110)}\mathcal{E}^{(1)} &= (0.0519472,0.00505390,0) \quad \text{(unstable)},\\
{}_{(110)}\mathcal{E}^{(2)} &= (0.489467,0.0486917,0) \quad \text{(unstable)},\\
{}_{(111)}\mathcal{E} &= (0.306611,0.0522205,36.6091) \quad \text{(stable)},
\end{aligned} \tag{3.22}$$

and the corresponding phase space is presented in Figure 3.4.

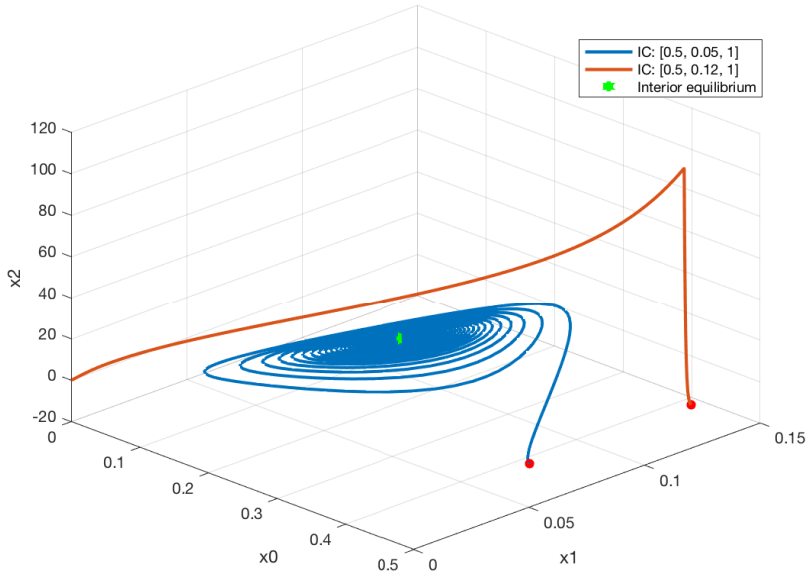

FIGURE 3.4: Phase space of system (2.13) with $\alpha = 0.01$, $u_f = 0.5$, $u_g = 0.0008$, and $u_h = 0.1$.

As expected, the periodic orbit disappears through a Hopf bifurcation, and the interior equilibrium becomes stable. The ${}_{(100)}\mathcal{E}$ equilibrium is also stable.

Finally, to illustrate the last result of theorem 1, we fix the following parameters

$$\alpha = 0.01, \quad u_f = 0.5, \quad u_g = 0.0006. \tag{3.23}$$

The predicted Hopf bifurcation occurs for $u_h = 0.102520$. For $u_h = 0.05$ we have the following equilibria

$$\begin{aligned}
{}_{(000)}\mathcal{E} &= (0,0,0) \quad \text{(unstable)},\\
{}_{(100)}\mathcal{E} &= (0.000299015,0,0) \quad \text{(stable)},\\
{}_{(001)}\mathcal{E} &= (0,0,0.0473693) \quad \text{(unstable)},\\
{}_{(110)}\mathcal{E}^{(1)} &= (0.0545964,0.00534486,0) \quad \text{(unstable)},\\
{}_{(110)}\mathcal{E}^{(2)} &= (0.489465,0.0487183,0) \quad \text{(unstable)},\\
{}_{(111)}\mathcal{E} &= (0.306611,0.0520205,36.2277) \quad \text{(unstable)},
\end{aligned} \tag{3.24}$$

and the corresponding phase space is presented in Figure 3.5.

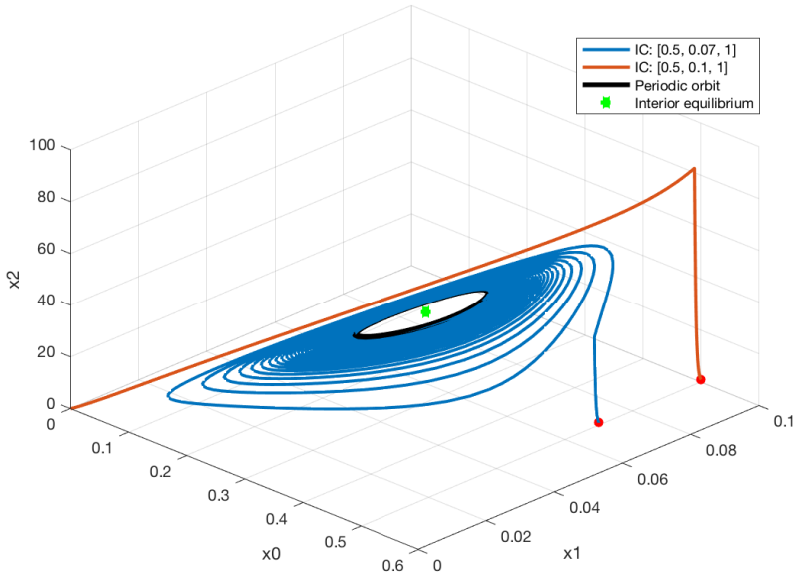

FIGURE 3.5: Phase space of system (2.13) with $\alpha = 0.01$, $u_f = 0.5$, $u_g = 0.0006$, and $u_h = 0.05$.

For $u_h = 0.3$ (after the predicted Hopf bifurcation) we have

$$\begin{aligned}
{}_{(000)}\mathcal{E} &= (0,0,0) \quad \text{(unstable)},\\
{}_{(100)}\mathcal{E} &= (0.00183202,0,0) \quad \text{(stable)},\\
{}_{(001)}\mathcal{E} &= (0,0,0.297369) \quad \text{(unstable)},\\
{}_{(110)}\mathcal{E}^{(1)} &= (0.0528596,0.00502299,0) \quad \text{(unstable)},\\
{}_{(110)}\mathcal{E}^{(2)} &= (0.489467,0.0485697,0) \quad \text{(unstable)},\\
{}_{(111)}\mathcal{E} &= (0.306611,0.0520205,36.4777) \quad \text{(stable)}.
\end{aligned} \tag{3.25}$$

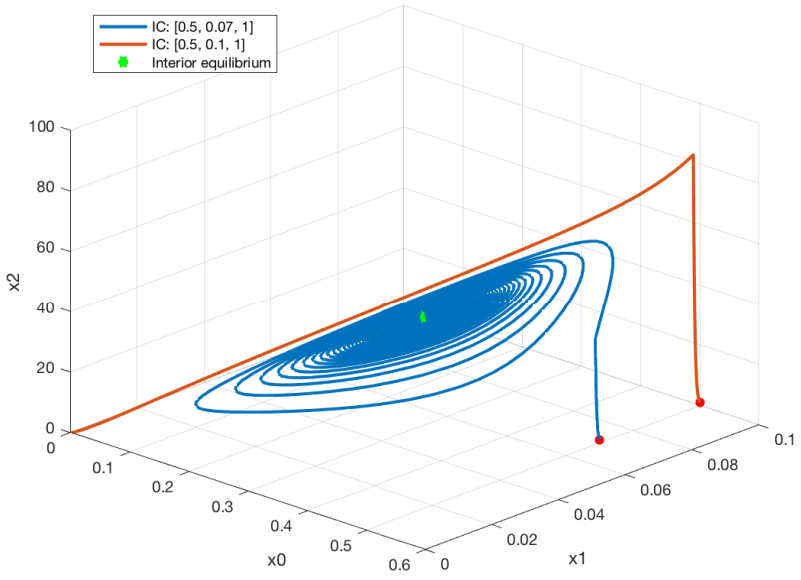

FIGURE 3.6: Phase space of system (2.13) with $\alpha = 0.01$, $u_f = 0.5$, $u_g = 0.0006$, and $u_h = 0.3$.

As expected, the dynamics of the system follows the same pattern as in the previous cases. The stable periodic orbit surrounding the unstable interior equilibrium disappears, and the interior equilibrium becomes unstable.

It is worth to notice, that in all three cases, the increase of the bifurcation parameter had a stabilizing effect on the system. This result is especially important in the context of the modeled phenomenon, since the most desirable situation happens when the production of methane is not fluctuating. Variable rates of gas production can result in decreased productivity of the biogas plant.

3.2 Persistence

The notion of persistence is particularly important in modeling biological phenomena. Roughly speaking, we say that a system is persistent if all the species with positive initial populations survive. The formal definition is as follows.

Definition 3.2.1. The system

$$\begin{aligned} x_i' &= x_i f_i\left(x_1, x_2, \ldots, x_n\right), \\ x_i\left(0\right) &= x_{i0} \geq 0, \quad i = 1, 2, \ldots, n, \end{aligned} \tag{3.26}$$

is said to be weakly persistent if

$$\limsup_{t\to\infty} x_i(t) > 0, \quad i = 1, 2, \ldots, n \tag{3.27}$$

for every trajectory with positive initial conditions, and is said to be persistent if

$$\liminf_{t\to\infty} x_i(t) > 0, \quad i = 1, 2, \ldots, n \tag{3.28}$$

for every trajectory with positive initial conditions. This system is said to be uniformly persistent if there exists a positive number ϵ such that

$$\liminf_{t\to\infty} x_i(t) \geq \epsilon, \quad i = 1, 2, \ldots, n \tag{3.29}$$

for every trajectory with positive initial conditions.

To prove that system (2.13) is persistent, we will use the Butler-McGehee lemma [15] repeatedly.

Lemma 3.2.1. *Suppose that x^* is a hyperbolic equilibrium point of the system*

$$\begin{aligned} x' &= f(x), \\ x(0) &= x_0, \end{aligned} \tag{3.30}$$

with $x \in \mathbb{R}^n$ and $f : \mathbb{R}^n \to \mathbb{R}^n$, where f is continuously differentiable. Suppose also that x^* is in $\omega(x_0)$, the omega limit set of $\gamma^+(x_0)$ (the positive semi-orbit through x_0), but is not the entire omega limit set. Then $\omega(x_0)$ has nontrivial (i.e., different from x^*) intersection with the stable and unstable manifolds of x^*.

As we already noticed in section 3.1, there are values of the parameters where one of the boundary equilibria and the interior equilibrium are both asymptotically stable, and hence system (2.13) is not persistent, even though an interior equilibrium point exists. We will thus focus on the cases for which no boundary equilibrium point of system (2.13) is stable.

Theorem 2. *Let system (2.13) have the following equilibria configuration (as represented schematically in Figure 3.7):*

Equilibrium	*Number of eigenvalues with positive real part*	*Number of eigenvalues with negative real part*
$_{(000)}\mathcal{E}$	*2*	*1*
$_{(100)}\mathcal{E}$	*1*	*2*
$_{(001)}\mathcal{E}$	*1*	*2*
$_{(110)}\mathcal{E}$	*1*	*2*

Then system (2.13) is persistent.

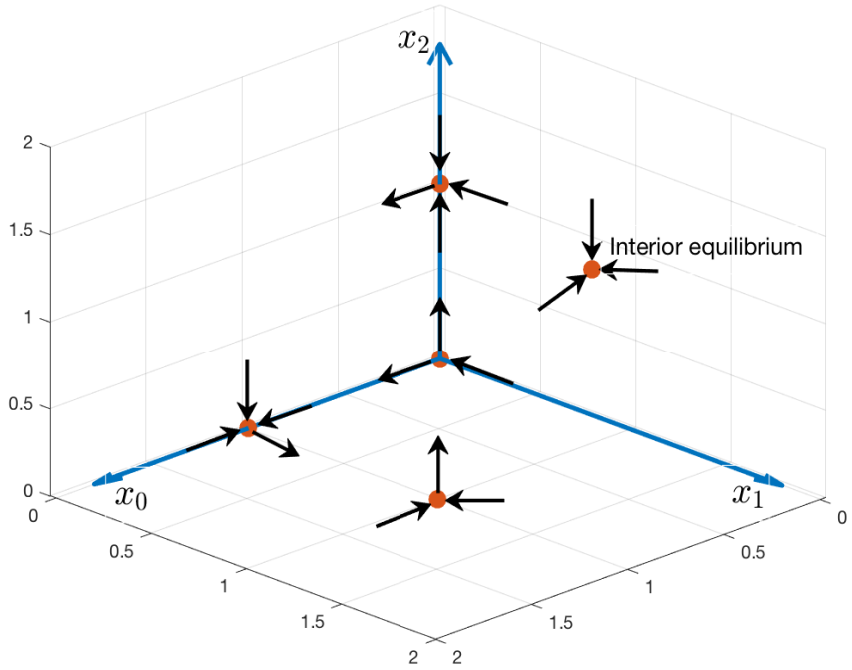

FIGURE 3.7: Schematic representation of the equilibria configuration occurring in the hypothesis of theorem 2. Black arrows represent stable and unstable manifolds of each of the equilibrium (marked by the orange dots). In the example for the parameters we select in model (2.13) to illustrate this theorem (see (3.31)), there is an asymptotically stable interior equilibrium (as shown). However, this is not necessary for the proof of theorem 2.

Proof. By the phase plane analysis in section 2.2 we know where the stable and unstable manifolds of the boundary equilibria lie. This is represented in a schematic way in Figure 3.7. Keeping this picture in mind should make the following argument much more transparent. Assume that a solution $\vec{x}(t) = (x_0(t), x_1(t), x_2(t))$ with an initial condition $\vec{x}^{(0)} = \left(x_0^{(0)}, x_1^{(0)}, x_2^{(0)}\right)$, where $x_i^{(0)} > 0$, $i = 1, 2, 3$, is given. First, suppose that ${}_{(000)}\mathcal{E}$ belongs to $\omega\left(\gamma^+\left(\vec{x}^{(0)}\right)\right)$, the omega limit set of $\gamma^+\left(\vec{x}^{(0)}\right)$. Since ${}_{(000)}\mathcal{E}$ is a saddle point with one-dimensional stable manifold restricted to the x_1-axis, it is not the entire omega limit set $\omega\left(\gamma^+\left(\vec{x}^{(0)}\right)\right)$. Hence, by lemma 3.2.1, there is a point $x^* \neq {}_{(000)}\mathcal{E}$ in both $\omega\left(\gamma^+\left(\vec{x}^{(0)}\right)\right)$ and $W^s\left({}_{(000)}\mathcal{E}\right)$, the stable manifold of ${}_{(000)}\mathcal{E}$. The entire orbit through any point in an omega limit set is also in the omega limit set. The stable manifold of ${}_{(000)}\mathcal{E}$ is the x_1-axis, and the x_1-axis is unbounded. We have already proven in chapter 2 that all orbits of system (2.13) are bounded, and hence the omega limit set

of any orbit of (2.13) is bounded. This contradicts the existence of such an x^* and thus ${}_{(000)}\mathcal{E} \notin \omega\left(\gamma^+\left(\vec{x}^{(0)}\right)\right)$.

Now, suppose that ${}_{(001)}\mathcal{E} \in \omega\left(\gamma^+\left(\vec{x}^{(0)}\right)\right)$. Since ${}_{(001)}\mathcal{E}$ is a saddle point with two-dimensional stable manifold restricted to the x_0x_1-plane, $\left\{{}_{(001)}\mathcal{E}\right\}$ is not the entire omega limit set $\omega\left(\gamma^+\left(\vec{x}^{(0)}\right)\right)$. Thus, using lemma 3.2.1, there is a point $x^* \in \omega\left(\gamma^+\left(\vec{x}^{(0)}\right)\right) \cap W^s\left({}_{(001)}\mathcal{E}\right) \setminus \left\{{}_{(001)}\mathcal{E}\right\}$. Since the stable manifold $W^s\left({}_{(001)}\mathcal{E}\right)$ lies entirely in the x_1x_2-plane, and the entire orbit through x^* is in $\omega\left(\gamma^+\left(\vec{x}^{(0)}\right)\right)$, by the analysis in subsection 2.2.1, this orbit becomes unbounded in backward time. This contradiction shows that ${}_{(001)}\mathcal{E} \notin \omega\left(\gamma^+\left(\vec{x}^{(0)}\right)\right)$.

Now, suppose that ${}_{(100)}\mathcal{E} \in \omega\left(\gamma^+\left(\vec{x}^{(0)}\right)\right)$. Similarly as in the previous cases, this implies that there exists a point $x^* \in \omega\left(\gamma^+\left(\vec{x}^{(0)}\right)\right) \cap W^s\left({}_{(100)}\mathcal{E}\right) \setminus \left\{{}_{(100)}\mathcal{E}\right\}$. This time the stable manifold $W^s\left({}_{(100)}\mathcal{E}\right)$ is two-dimensional and lies entirely in the x_0x_2-plane. By the analysis in subsection 2.2.2, the entire orbit through x^* $\Big($which belongs to $\omega\left(\gamma^+\left(\vec{x}^{(0)}\right)\right)\Big)$ becomes unbounded in backward time or its closure contains ${}_{(001)}\mathcal{E}$. This contradiction proves that ${}_{(100)}\mathcal{E} \notin \omega\left(\gamma^+\left(\vec{x}^{(0)}\right)\right)$.

Now, suppose that ${}_{(110)}\mathcal{E} \in \omega\left(\gamma^+\left(\vec{x}^{(0)}\right)\right)$. Again, $\left\{{}_{(110)}\mathcal{E}\right\}$ is not the entire omega limit set $\omega\left(\gamma^+\left(\vec{x}^{(0)}\right)\right)$, so there exists a point $x^* \in \omega\left(\gamma^+\left(\vec{x}^{(0)}\right)\right) \cap W^s\left({}_{(110)}\mathcal{E}\right) \setminus \left\{{}_{(110)}\mathcal{E}\right\}$. This point lies in the x_0x_1-plane, since $W^s\left({}_{(110)}\mathcal{E}\right)$ is two-dimensional and is entirely contained in this plane. As in the previous cases, the entire orbit through x^* is in $\omega\left(\gamma^+\left(\vec{x}^{(0)}\right)\right)$. Since there are no periodic orbits in the x_0x_1 face, and since $\left\{{}_{(100)}\mathcal{E}\right\} \notin \omega\left(\gamma^+\left(\vec{x}^{(0)}\right)\right)$, the orbit becomes unbounded in backward time. This contradiction proves that ${}_{(110)}\mathcal{E} \notin \omega\left(\gamma^+\left(\vec{x}^{(0)}\right)\right)$.

Finally, consider any $\widehat{x} = (\widehat{x}_0, \widehat{x}_1, \widehat{x}_2)$, such that $\widehat{x}_i = 0$ for at least one $i = 1, 2, 3$, and suppose that $\widehat{x} \in \omega\left(\gamma^+\left(\vec{x}^{(0)}\right)\right)$. Then, the entire orbit through $\widehat{x}$ is in $\omega\left(\gamma^+\left(\vec{x}^{(0)}\right)\right)$. But since this orbit lies entirely in either x_0x_1, x_1x_2, or x_0x_2 face, it converges to one of the boundary equilibria. This implies that this boundary equilibrium is in $\omega\left(\gamma^+\left(\vec{x}^{(0)}\right)\right)$, and this possibility has been eliminated in the previous part of the proof.

We have therefore proven that

$$\liminf_{t\to\infty} x_i(t) > 0, \quad i = 1, 2, 3,$$

i.e., that system (2.13) is persistent. □

An example satisfying the assumptions of theorem 2 occurs for

$$\alpha = 0.0002, \quad u_f = 0.6, \quad u_g = 0, \quad u_h = 0.1. \tag{3.31}$$

Persistence can also be observed with the addition of phenol, i.e., with $u_g > 0$.

Theorem 3. *Let system (2.13) have the following equilibria configuration (as represented schematically in Figure 3.8):*

Equilibrium	*Number of eigenvalues with positive real part*	*Number of eigenvalues with negative real part*
$_{(000)}\mathcal{E}$	*2*	*1*
$_{(100)}\mathcal{E}$	*1*	*2*
$_{(001)}\mathcal{E}$	*1*	*2*
$_{(011)}\mathcal{E}$	*1*	*2*
$_{(110)}\mathcal{E}$	*1*	*2*

Then system (2.13) is persistent.

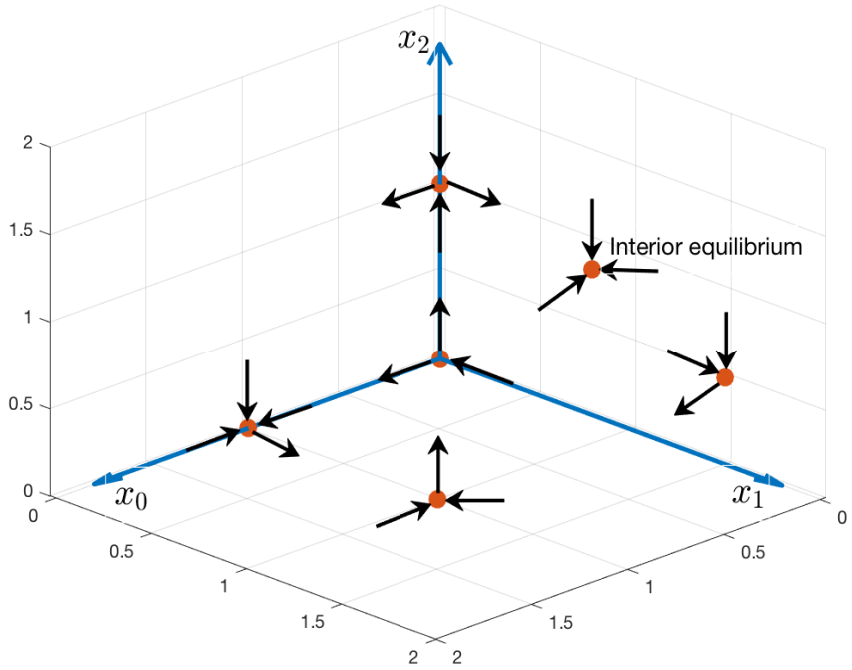

FIGURE 3.8: Schematic representation of the equilibria configuration occurring in the hypothesis of theorem 3. Black arrows represent stable and unstable manifolds of each of the equilibrium (marked by the orange dots). In the example for the parameters we select in model (2.13) to illustrate this theorem (see (3.32)), there is an asymptotically stable interior equilibrium (as shown). However, this is not necessary for the proof of theorem 3.

Proof. The idea behind this proof is very similar to the method presented in the proof of theorem 2. Let $\vec{x}(t) = (x_0(t), x_1(t), x_2(t))$ be a solution of (2.13) with an initial condition $\vec{x}^{(0)} = \left(x_0^{(0)}, x_1^{(0)}, x_2^{(0)}\right)$, where $x_i^{(0)} > 0$, $i = 1, 2, 3$. Since the stable and unstable manifolds of the all of the equilibria, except ${}_{(001)}\mathcal{E}$ and ${}_{(011)}\mathcal{E}$, have the same configuration as in the hypothesis of theorem 2, the argument eliminating them from the omega limit set of $\gamma^+\left(\vec{x}^{(0)}\right)$ is exactly the same and we only need to focus on ${}_{(001)}\mathcal{E}$ and ${}_{(011)}\mathcal{E}$ equilibria.

Suppose that ${}_{(001)}\mathcal{E} \in \omega\left(\gamma^+\left(\vec{x}^{(0)}\right)\right)$. Since ${}_{(001)}\mathcal{E}$ is a saddle point with one-dimensional stable manifold restricted to the x_2-axis, we have $\omega\left(\gamma^+\left(\vec{x}^{(0)}\right)\right) \setminus \left\{{}_{(001)}\mathcal{E}\right\} \neq \emptyset$. Hence, by lemma 3.2.1, there is a point $x^* \in \omega\left(\gamma^+\left(\vec{x}^{(0)}\right)\right) \cap W^s\left({}_{(001)}\mathcal{E}\right) \setminus \left\{{}_{(001)}\mathcal{E}\right\}$. The entire orbit through x^*, which also belongs to $\omega\left(\gamma^+\left(\vec{x}^{(0)}\right)\right)$, either becomes unbounded in backward

time, or converges to the ${}_{(000)}\mathcal{E}$ equilibrium. Since all orbits of system (2.13) are bounded, and ${}_{(000)}\mathcal{E} \notin \omega\left(\gamma^+\left(\vec{x}^{(0)}\right)\right)$, we obtain a contradiction. Hence ${}_{(001)}\mathcal{E} \notin \omega\left(\gamma^+\left(\vec{x}^{(0)}\right)\right)$.

Now, suppose that ${}_{(011)}\mathcal{E} \in \omega\left(\gamma^+\left(\vec{x}^{(0)}\right)\right)$. Since ${}_{(011)}\mathcal{E}$ is a saddle point with two-dimensional stable manifold restricted to the x_1x_2-plane (it is repelling into the interior), we have $\omega\left(\gamma^+\left(\vec{x}^{(0)}\right)\right) \setminus \left\{{}_{(011)}\mathcal{E}\right\} \neq \emptyset$. By using lemma 3.2.1, there exists a point $x^* \in \omega\left(\gamma^+\left(\vec{x}^{(0)}\right)\right) \cap W^s\left({}_{(011)}\mathcal{E}\right) \setminus \left\{{}_{(011)}\mathcal{E}\right\}$. The entire orbit through x^*, which also belongs to $\omega\left(\gamma^+\left(\vec{x}^{(0)}\right)\right)$, either becomes unbounded in backward time, or converges to ${}_{(000)}\mathcal{E}$, or ${}_{(001)}\mathcal{E}$ (we have previously shown in subsection 2.2.1 that there are no periodic orbits in the x_1x_2 face). Since we have already proven that ${}_{(000)}\mathcal{E} \notin \omega\left(\gamma^+\left(\vec{x}^{(0)}\right)\right)$, and ${}_{(001)}\mathcal{E} \notin \omega\left(\gamma^+\left(\vec{x}^{(0)}\right)\right)$, we obtain a contradiction, which proves that ${}_{(011)}\mathcal{E} \notin \omega\left(\gamma^+\left(\vec{x}^{(0)}\right)\right)$.

Finally, consider any $\widehat{x} = (\widehat{x}_0, \widehat{x}_1, \widehat{x}_2)$, such that $\widehat{x}_i = 0$ for at least one $i = 1, 2, 3$, and suppose that $\widehat{x} \in \omega\left(\gamma^+\left(\vec{x}^{(0)}\right)\right)$. Then, the entire orbit through $\widehat{x}$ is in $\omega\left(\gamma^+\left(\vec{x}^{(0)}\right)\right)$. But since this orbit lies entirely in either x_0x_1, x_1x_2, or x_0x_2 face, it converges to one of the boundary equilibria. This implies that this boundary equilibrium is in $\omega\left(\gamma^+\left(\vec{x}^{(0)}\right)\right)$, and this possibility has been eliminated in the previous part of the proof. □

An example satisfying the assumptions of theorem 3 occurs for

$$\alpha = 0.0002, \quad u_f = 0.6, \quad u_g = 0.00015, \quad u_h = 0.1. \tag{3.32}$$

Remark 1. Interestingly enough, in many cases of models describing biological phenomena, persistence already implies uniform persistence. The rigorous results were obtained in [3]. In our context, the key theorem from [3] states that if $\mathcal{F}$ is a dynamical system for which $\mathbb{R}^n_+$ and $\partial\mathbb{R}^n_+$ are invariant, then $\mathcal{F}$ is uniformly persistent provided that

1. $\mathcal{F}$ is dissipative (meaning that $\forall x \in \mathbb{R}^n_+ \ \omega(x) \neq \emptyset$ and $\bigcup_{x\in\mathbb{R}^n_+} \omega(x)$ has compact closure),
2. $\mathcal{F}$ is weakly persistent,
3. $\partial\mathcal{F}$ (the restriction of $\mathcal{F}$ to the boundary $\partial\mathbb{R}^n_+$) is "isolated",
4. $\partial\mathcal{F}$ is "acyclic".

These results can be easily modified so that we consider the flow $\mathcal{F}$ on Ω defined in (2.11). Although $\partial\Omega$ is not invariant, the theorem from [3], as explained in [4], can be modified so that it applies in the case when $\partial\Omega$ is the union of two sets Ω_1 and Ω_2, for which $\mathcal{F}$ is invariant on Ω_1 and Ω_2 is repelling into the interior of Ω, provided that conditions 3. and 4. are satisfied for the restriction of $\mathcal{F}$ to Ω_1. In our case, the positively invariant set Ω, on which we analyze system (2.13) is bounded, hence condition 1. is satisfied. Condition 2. holds by theorem 2 (persistence implies weak persistence). In our context condition 3. is satisfied, because all the boundary equilibria are hyperbolic, and hence each one is the

maximal invariant set in a neighbourhood of itself. Also, their union forms a covering of the omega limit sets of Ω_1. Condition 4. is satisfied because the boundary equilibria are not cyclically linked, i.e., there is no cyclic chain of heteroclinic orbits joining them. Thus, we have shown not only persistence, but also uniform persistence of system (2.13) in the case of theorem 2 and theorem 3.

We have thus proven the following theorem:
Theorem 4. *Under the hypotheses of theorems 2 and 3, system* (2.13) *is uniformly persistent.*

3.3 Bifurcation diagrams

As previously stated in section 3.1, we now study numerically effects on the qualitative behaviour of system (2.13) when considering α as the bifurcation parameter. Throughout this section, we assume that parameters ω_0, ω_1, ω_2, ϕ_1, ϕ_2, K_P, and K_I are fixed at the values given in table 1.1.

We now fix the following parameters

$$u_f = 2, \quad u_g = 0, \quad u_h = 0, \tag{3.33}$$

and plot a one-parameter bifurcation diagram in α, with x_0 on the y-axis. All simulations were performed using [17].

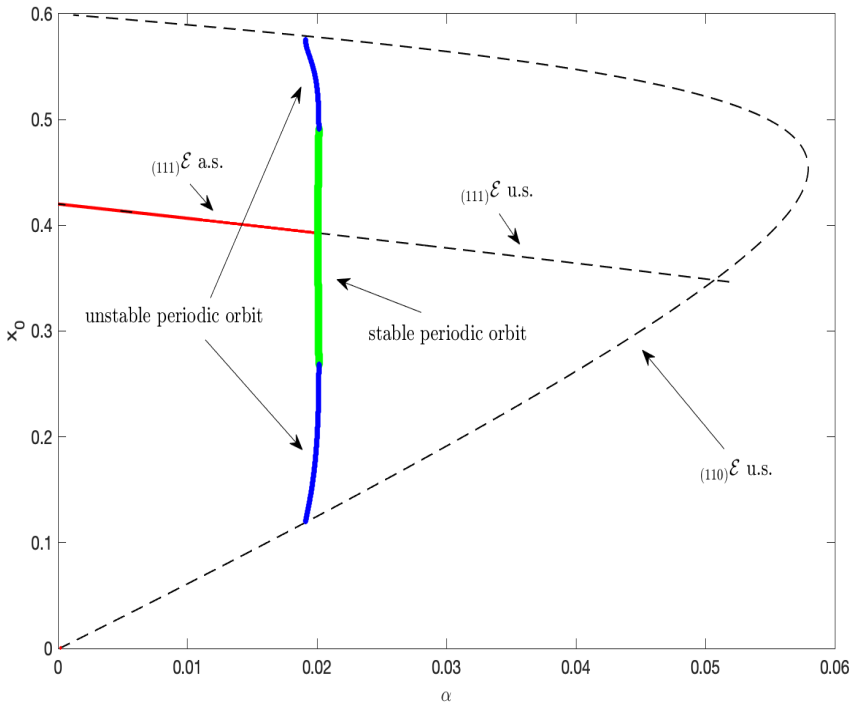

FIGURE 3.9: One-parameter bifurcation diagram of system (2.13) with α as the bifurcation parameter and $u_f = 2$, $u_g = 0$, $u_h = 0$.

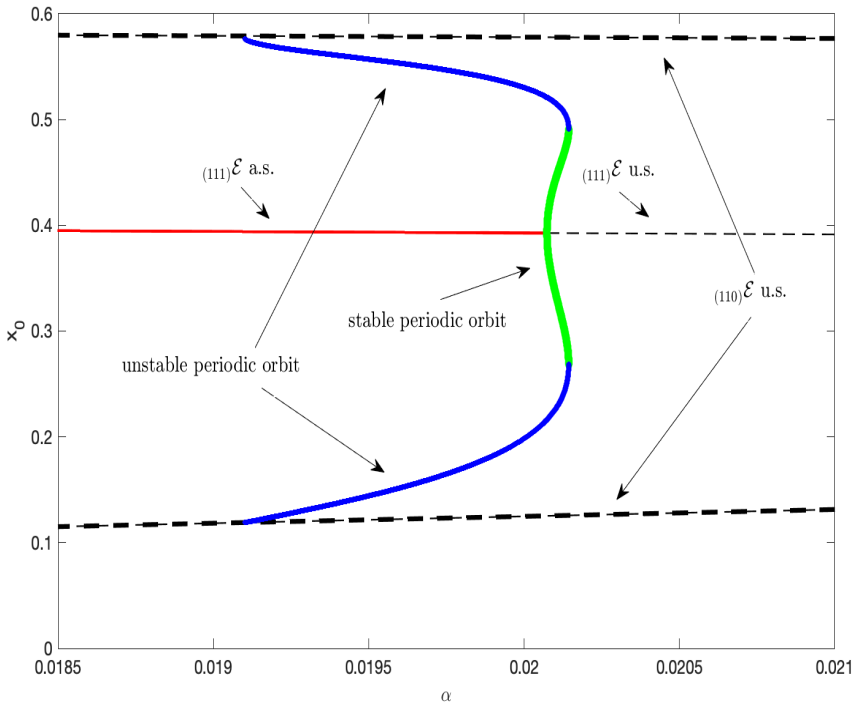

FIGURE 3.10: Close-up of on the one-parameter bifurcation diagram represented in Figure 3.9.

We can see that as α decreases, there is a saddle-node bifurcation, resulting in two equilibria $_{(110)}\mathcal{E}^{(1)}$ and $_{(110)}\mathcal{E}^{(2)}$ appearing (both unstable). Next, there is a transcritical bifurcation with the $_{(110)}\mathcal{E}^{(1)}$ equilibrium, which results in the positive equilibrium coming into the interior of the admissible region Ω. After that, a saddle-node of limit cycles bifurcation occurs, which gives birth to a stable and unstable periodic orbits. The $_{(111)}\mathcal{E}$ equilibrium (unstable), undergoes a Hopf bifurcation, and as a consequence it becomes asymptotically stable, and the stable periodic orbits disappears. Since these bifurcations occur for a narrow range of α, a close-up is presented in Figure 3.10. Stable periodic orbit represents a case in which all three populations oscillate indefinitely, and hence the production of methane fluctuates. As already mentioned in section 3.1, this situation is not a desirable one, because it might result it decreased productivity of the biogas plant. The unstable periodic orbits acts as a separatrix, giving the border of the basin of attraction of two asymptotically stable equilibria in the case of bistability.

Since by the conservation principles (2.12), $s_0 = u_f - x_0$, the bifurcation diagram in α with s_0 on the y-axis is similar to the one presented in Figure 3.9. The amount of chlorophenol in the system is inversely proportional to the concentration of the phenol degrader. As the dilution rate α decreases, concentration of the chlorophenol degrader in the interior equilibrium increases, and as a consequence, the amount of chlorophenol

decreases. It thus suggests, that operating on lower dilution rates results in the most desirable dynamics, i.e., an asymptotically stable interior equilibrium and fast chlorophenol removal.

To extend the previous analysis, we now fix the following parameters

$$u_g = 0, \quad u_h = 0.1, \tag{3.34}$$

and plot a two-parameter bifurcation diagram of system (2.13), choosing α and u_f as the bifurcation parameters. Each region of the diagram is labeled and the corresponding dynamics are represented in Figures 3.14-3.25. Red curve corresponds to saddle-node of equilibria bifurcation (LP), black curve represents saddle-node of limit cycles bifurcation (SNLC), blue curve denotes Hopf bifurcation (HB), and cyan curves represent transcritical bifurcations (BP).

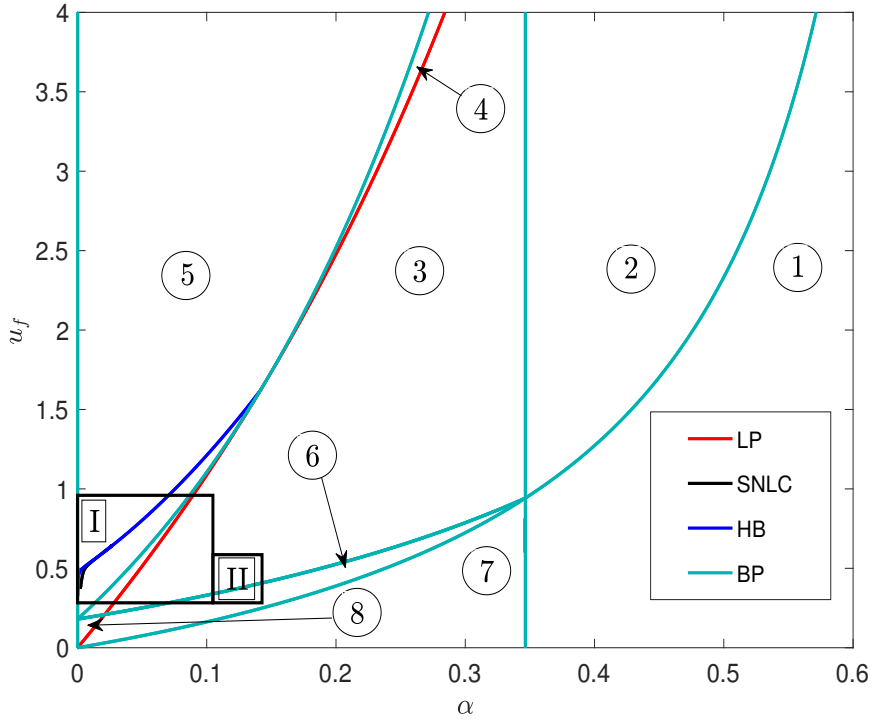

FIGURE 3.11: Two-parameter bifurcation diagram of system (2.13) with $u_g = 0$ and $u_h = 0.1$.

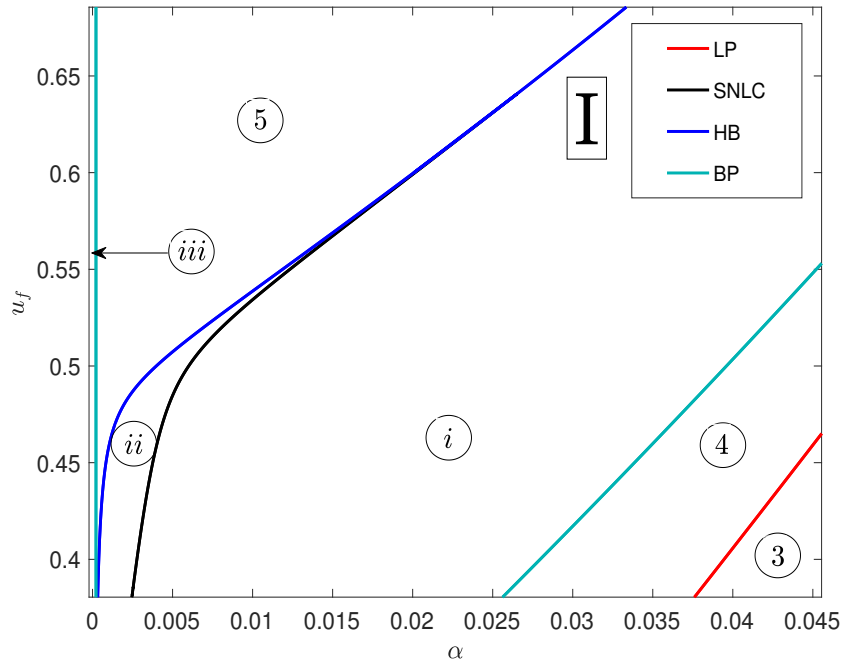

FIGURE 3.12: Close-up on region I of Figure 3.11. The SNLC curve intersects the HB curve at Bautin bifurcation. This results in the change of criticality of the Hopf bifurcation from supercritical (on the left) to subcritical (on the right).

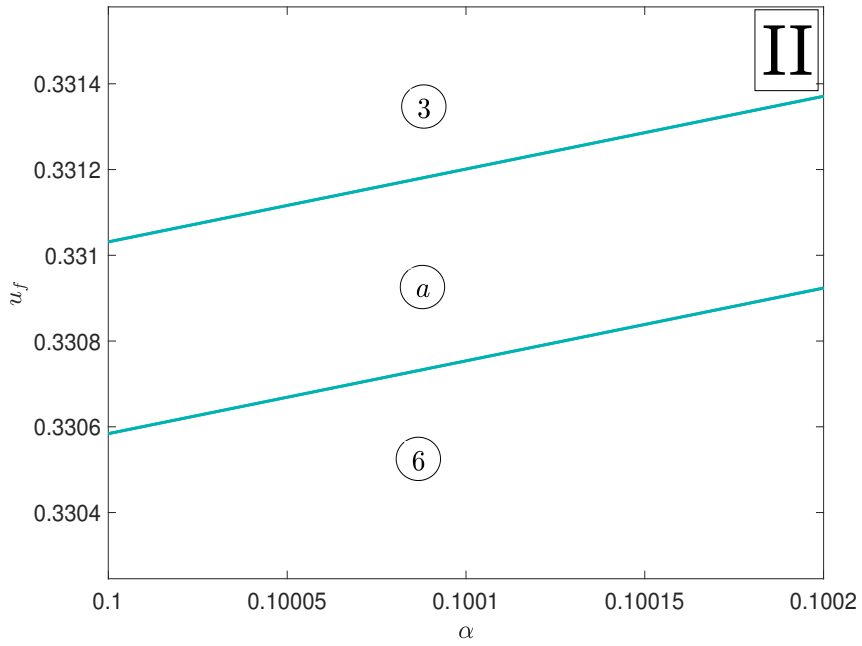

FIGURE 3.13: Close-up on region II of Figure 3.11.

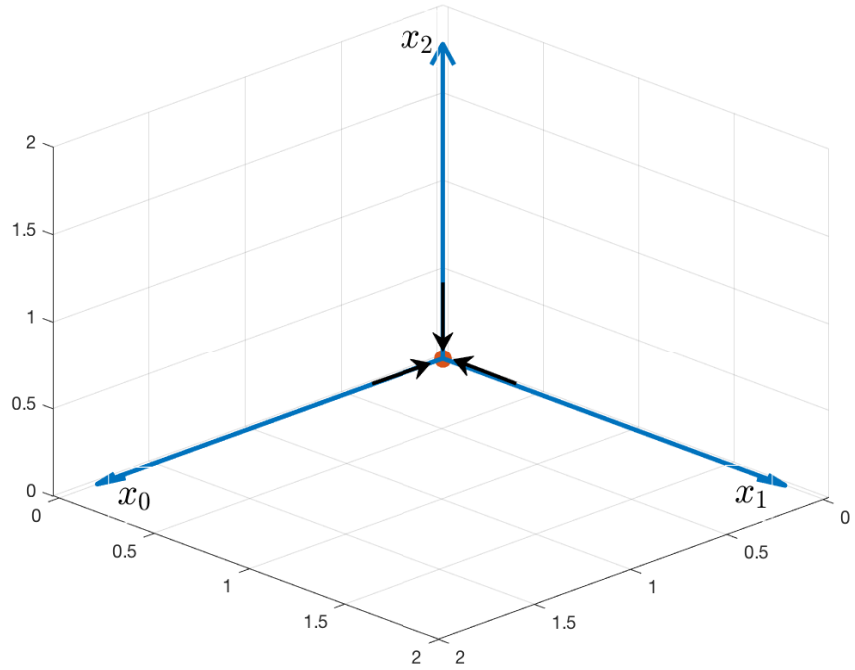

FIGURE 3.14: Schematic representation of the dynamics of system (2.13) in region 1 of Figure (3.11).

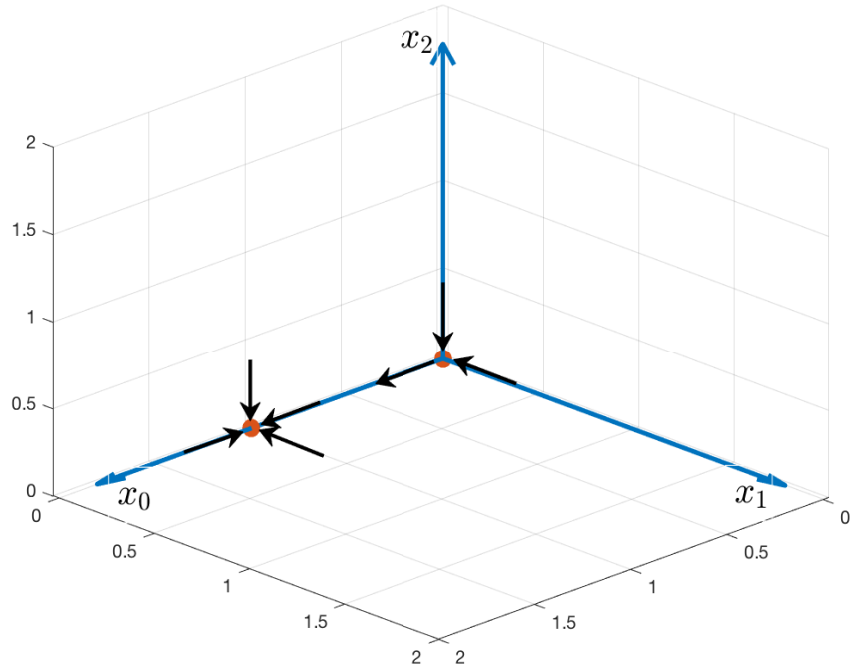

FIGURE 3.15: Schematic representation of the dynamics of system (2.13) in region 2 of Figure (3.11).

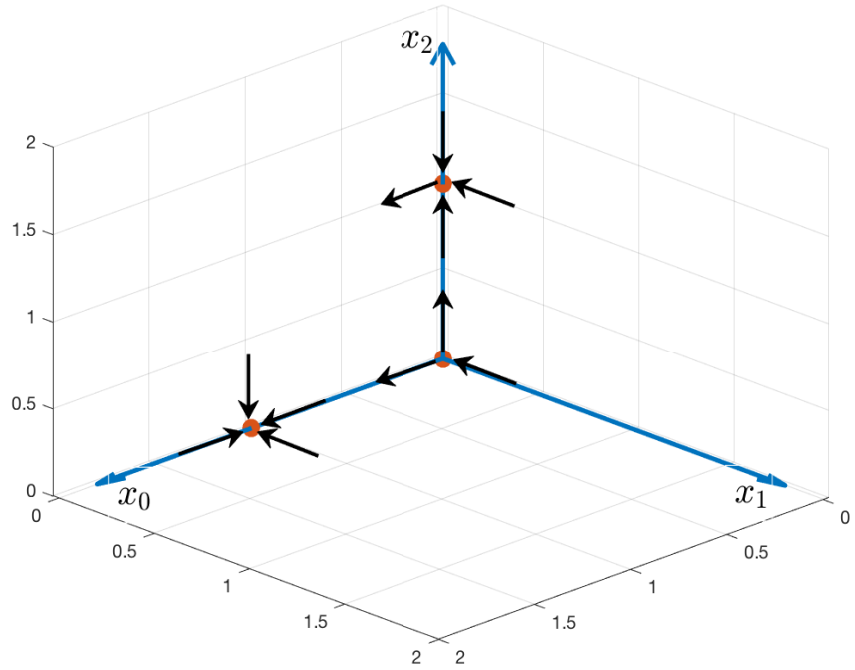

FIGURE 3.16: Schematic representation of the dynamics of system (2.13) in region 3 of Figure (3.11).

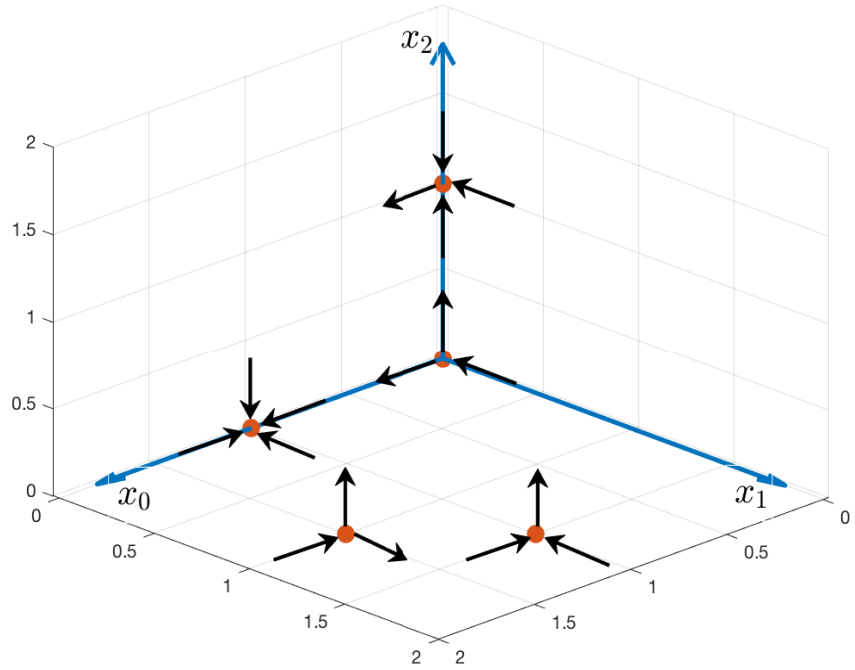

FIGURE 3.17: Schematic representation of the dynamics of system (2.13) in region 4 of Figure (3.11).

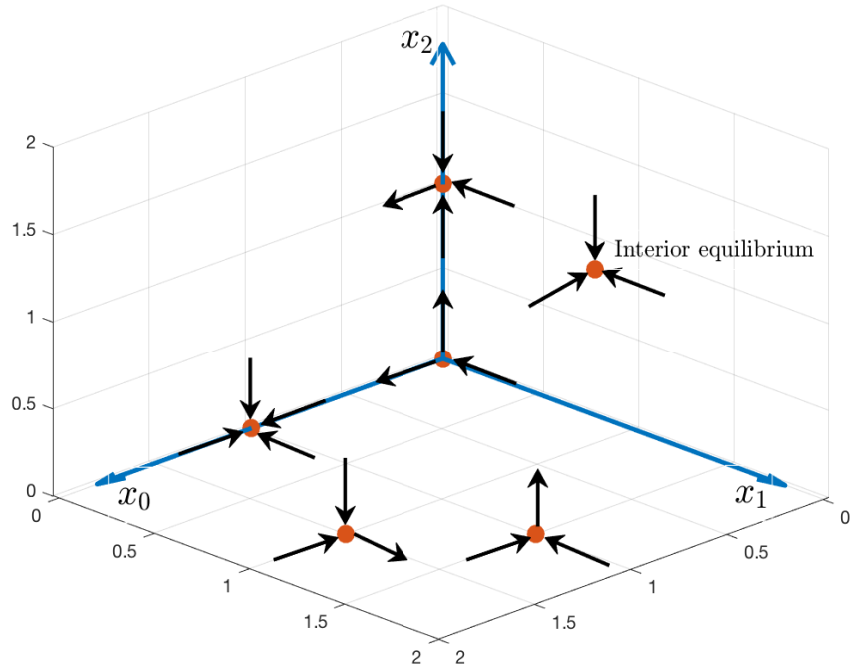

FIGURE 3.18: Schematic representation of the dynamics of system (2.13) in region 5 of Figure (3.11).

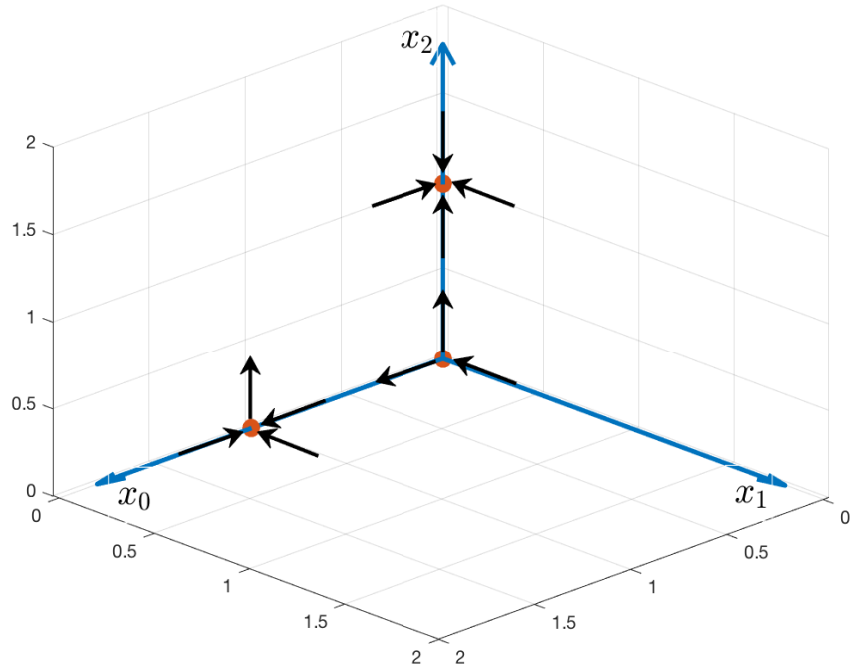

FIGURE 3.19: Schematic representation of the dynamics of system (2.13) in region 6 of Figure (3.11).

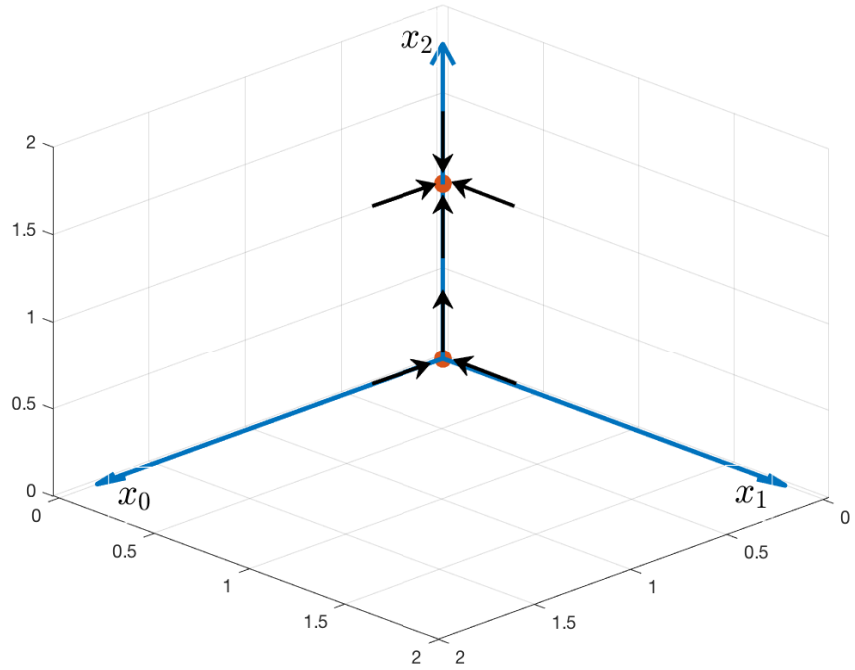

FIGURE 3.20: Schematic representation of the dynamics of system (2.13) in region 7 of Figure (3.11).

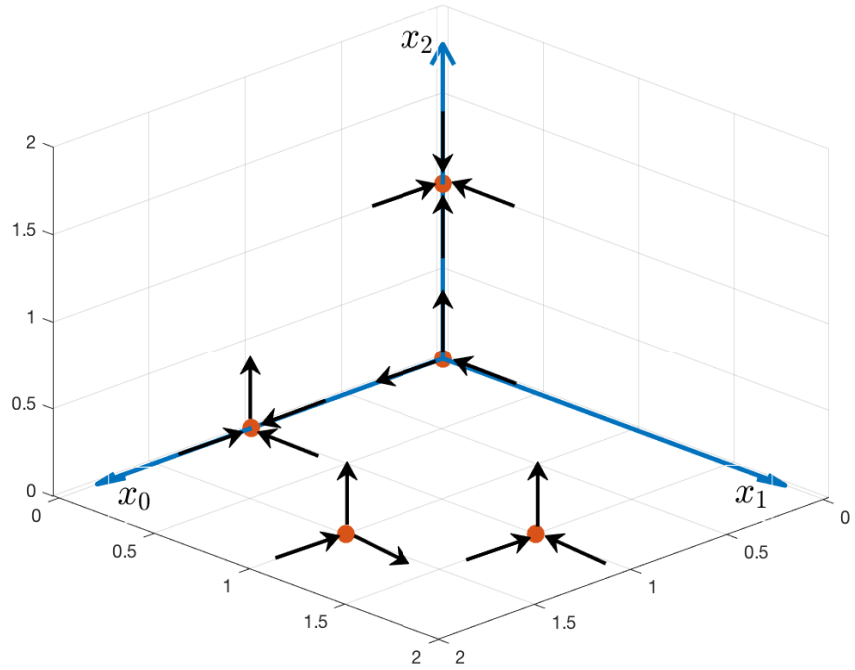

FIGURE 3.21: Schematic representation of the dynamics of system (2.13) in region 8 of Figure (3.11).

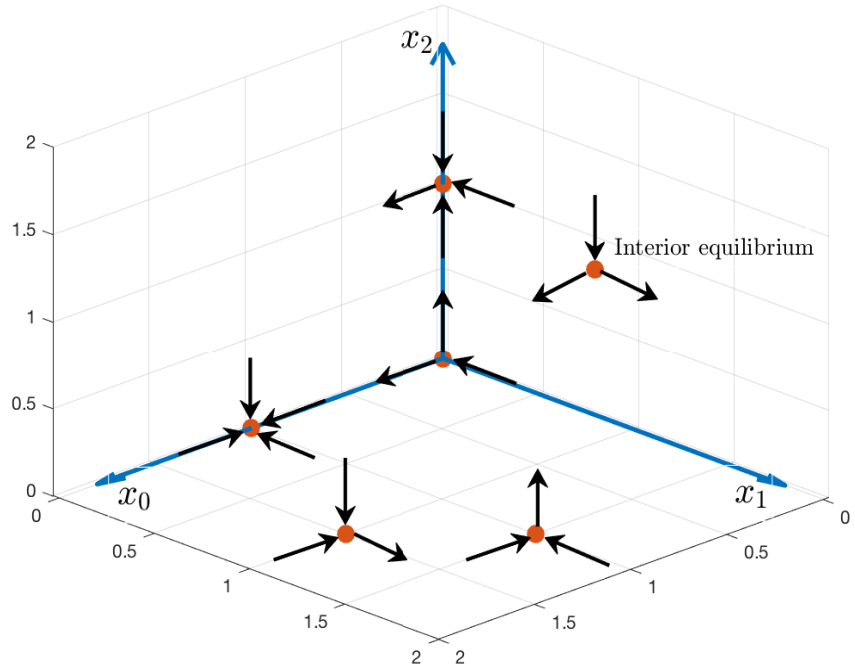

FIGURE 3.22: Schematic representation of the dynamics of system (2.13) in region i of Figure (3.12).

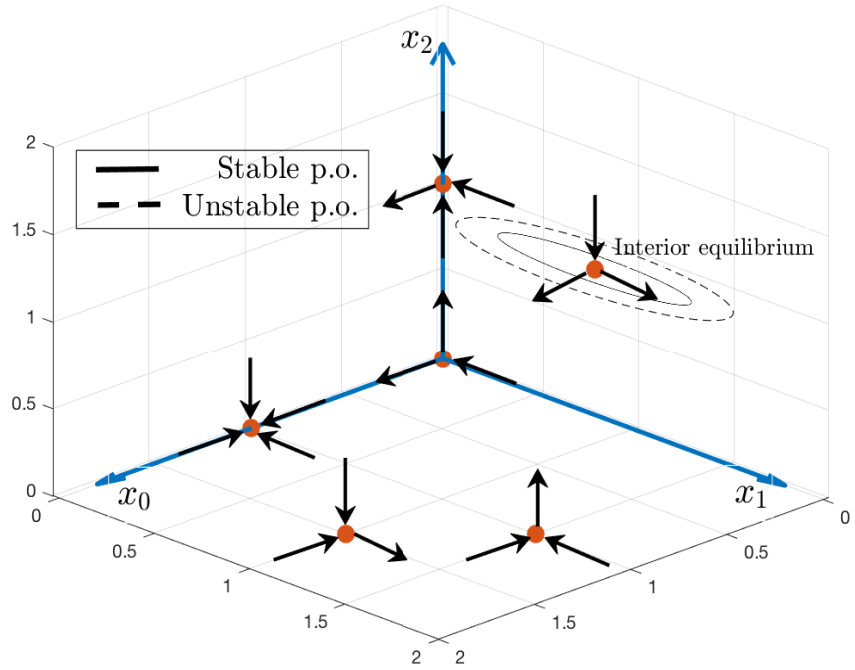

FIGURE 3.23: Schematic representation of the dynamics of system (2.13) in region ii of Figure (3.12).

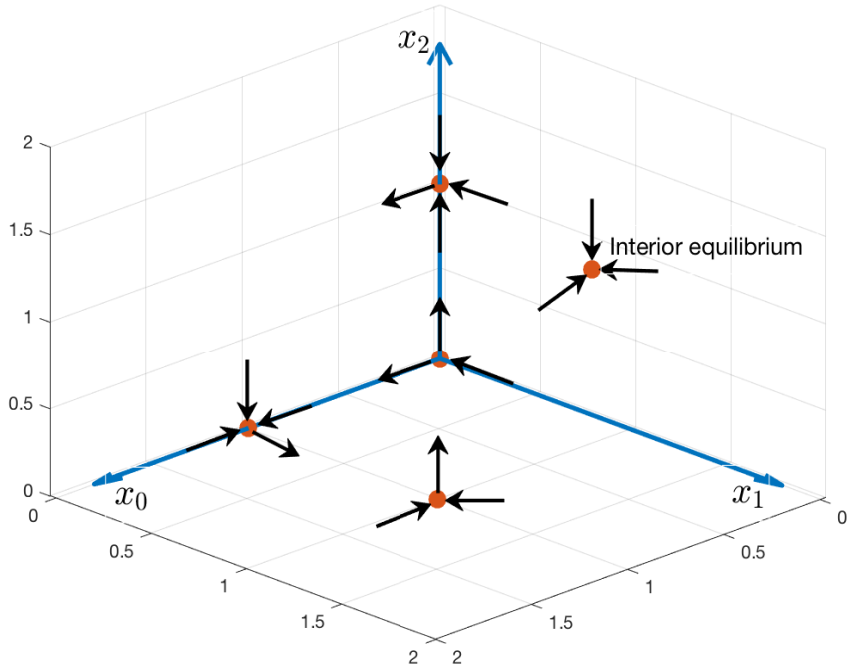

Figure 3.24: Schematic representation of the dynamics of system (2.13) in region *iii* of Figure (3.12).

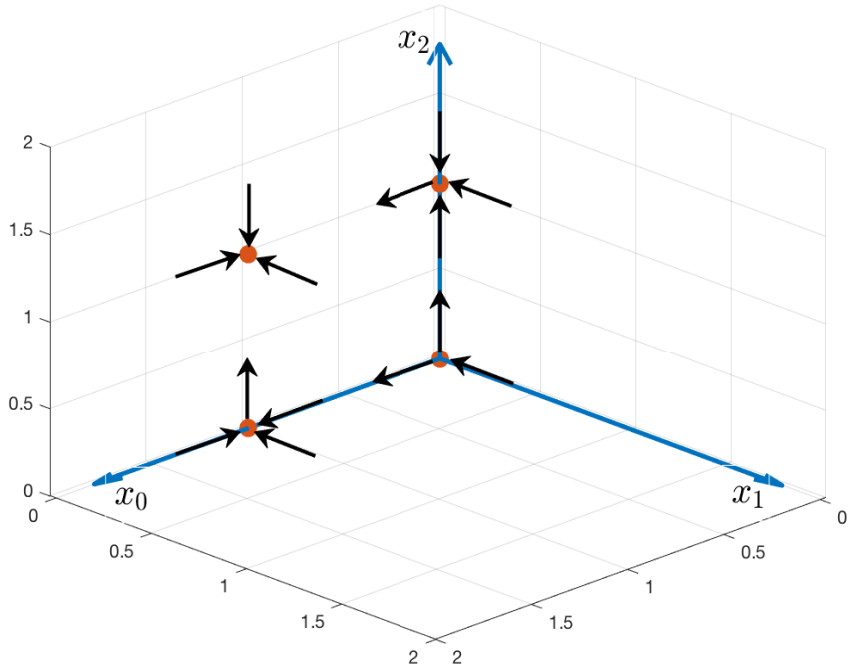

FIGURE 3.25: Schematic representation of the dynamics of system (2.13) in region a of Figure (3.13).

We can see that varying two parameters at the same time can lead to a much more complicated dynamics than in the case of one-parameter bifurcations. There is a generalized Hopf bifurcation, at the point at which the Hopf curve intersects the saddle-node of limit cycles curve. This is the point where the criticality of the Hopf bifurcation changes from supercritical to subcritical, looking from left to right. The unstable periodic orbit disappears through a heteroclinic bifurcation, however the correspoing curve lies so close to the Hopf curve (above it), that it is not included in the diagram. There are two heteroclinic orbits that form a cycle that joins the two equilibria in the x_0x_1 face, then passes into the interior, and then goes back to the boundary in the x_0x_1 face. The point at which the Hopf, homoclinic, and saddle-node of limits cycles curves intersect, represents the Bogdanov-Takens bifurcation.

From the biological viewpoint, the most interesting dynamics is occurs in regions 5 and *iii*. There, the interior equilibrium is asymptotically stable. In the case of region 5 we also observe bistability with the ${}_{(100)}\mathcal{E}$ equilibrium. In region *iii*, there is uniform persistence, and thus an interior compact attractor is present. As was previously anticipated by the analysis of the one-parameter bifurcation diagram, operating at low dilution rates is the most desirable approach. If α is small enough, it is possible to remain in region *iii*, even for high inflow rate u_f.

Chapter 4

Conclusions

In this work we have generalised the approach presented in [14] by including multiple substrate inflow into the chemostat, while maintaining generality (in most cases) with respect to the exact form of the growth functions. We observed that allowing the inflow of multiple substrates resulted in much more complex dynamics of the system. For example, eight steady states are possible. Previously, the theoretical results were limited to existence and uniqueness of up to three equilibria (when chlorophenol was the only input substrate), and to numerical evidence suggesting that the model should be subjected to a more detailed analysis. We also observed that external addition of substrates can result in bistability - two equilibria can simultaneously be asymptotically stable. As well, there can be an orbitally asymptotically stable periodic orbit with all of the populations surviving and an asymptotically stable equilibrium with only chlorophenol degrader population surviving.

We derived explicit conditions with respect to the parameters for the existence and the number of equilibria of each possible form. The original conditions, presented in subsection 2.1.1, had the disadvantage that they were given in implicit form. Since we ignored the decay terms, this allowed us to reduce the original six dimensional system to an equivalent three dimensional system. This made it possible to obtain alternative conditions for the existence of equilibria by studying the system on parts of the invariant set on which one of the variables x_0, x_1, or x_2 is zero. This made the use of phase analysis possible, together with many powerful theorems, like the Poincaré-Bendixson theorem, or the Bendixson-Dulac theorem. These theorems were also used to obtain results on the qualitative dynamics of the system on the x_0x_1 face with general forms of the growth functions. However, we did have to resort to specific forms to determine the existence and uniqueness of the equilibria on this face.

We have also confirmed the findings of the previous numerical analysis in [14], where numerical evidence of the occurrence of a supercritical Hopf bifurcation was given. Theoretical conditions for the existence of a Hopf bifurcation were provided in the case of specific forms of the growth functions. Varying any one of the three parameters: chlorophenol, phenol, and hydrogen inflow rates, was shown to result in a Hopf bifurcation. Theoretical results for varying the dilution rate as the bifurcation parameter has been left for future work. However, we have observed numerically, that varying this

parameter can result in a Hopf bifrucation and a saddle-node of limit cycles bifurcation. Our numerical investigations also showed that increasing the inflow rate of the substrates has a stabilizing effect on the entire system. This is usually the most desirable situation from the application point of view, since fluctuating substrates can be troublesome.

Another result, particularly important from the applications point of view, concerns the persistence of the system for various sets of parameters. Knowing that the microorganism populations survive is crucial information and it is one of the main theoretical results of this work. We have proven that in two configurations of equilibria (in both cases all the boundary equilibria are saddle points) we observe not only persistence, but also uniform persistence, a much stronger result. These situations occur not only when there is an inflow of all the three substrates, but also when we do not consider phenol addition (i.e., when $u_g = 0$).

Although we now know much more about the dynamics of the system, it is not fully understood. The evidence of that might be found in [16], where the authors present two-parameter bifurcation diagrams. Their analysis reveals that varying the dilution rate, and the chlorophenol inflow simultaneously, can lead to a Bogdanov-Takens, or Bautin (generalized Hopf) bifurcation. Also, for the cases of bistability, where both a boundary and the interior equilibrium are asymptotically stable, it is of great importance to biologists to have an estimation of the basins of attraction of these equilibria. This result is usually difficult to obtain theoretically, however numerical estimations are possible. Another factor that might be worth considering is including stochasticity in the model. In real-life situations, it might happen that even if the interior equilibrium is globally asymptotically stable, one of the microorganisms goes extinct. This might occur when a population is very small, and the stochastic noise effects result in the solution curve reaching one of the invariant faces of the admissible region.

Finally, it is worth noticing that although many results were obtained for a general class of growth functions, some of the results depend on a specific (Monod) form. These results include for example, existence and uniqueness of the equilibria on the x_0x_1 face, and conditions for a Hopf bifurcation.

Appendix A

Maple codes

Code for finding equilibria of system (2.1), together with their eigenvalues in the three-dimensional system (2.13).

```
mu0 := (s0,s2) -> s0*s2/((1+s0)*(Kp+s2));
mu1 := (s1,s2) -> phi1*s1/((1+s1)*(1+KI*s2));
mu2 := (s2) -> phi2*s2/(1+s2);

Y0 := 0.19e-1;
Y1 := 0.4e-1;
Y2 := 0.6e-1;
km0 := 29;
km1 := 26;
km2 := 35;
KS0 := 0.53e-1;
KS1 := .302;
KS2 := 0.25e-4;
L0 := 0.1e-5;
KI := 0.35e-5;
om0 := KS0*(224*(1/208))*(1-Y0)/KS1;
om1 := KS1*(32*(1/224))*(1-Y1)/KS2;
om2 := (16*(1/208))*KS0/KS2;
phi1 := km1*Y1/(km0*Y0);
phi2 := km2*Y2/(km0*Y0);
Kp := L0/KS2;
KI := KS2/KI;
uf := .538;
ug := 0;
uh := .1;
alpha := 0.1e-1;

# The zero equilibrium E0
x0_E0 := 0;
x1_E0 := 0;
```

```
x2_E0 := 0;
s0_E0 := -x0_E0+uf;
s1_E0 := om0*x0_E0+ug-x1_E0;
s2_E0 := om1*x1_E0-om2*x0_E0+uh-x2_E0;
print(The*zero*equilibrium*E0);
print([x0_E0, x1_E0, x2_E0, s0_E0, s1_E0, s2_E0]);
print(Eigenvalues);
print([mu0(uf, uh)-alpha, mu1(ug, uh)-alpha, mu2(uh)-alpha])

# The E100 equilibrium (x0,0,0);
if alpha > mu0(uf, uh) then
print(E_100*does*`not`*exist)
else
x0_E100 := solve((mu0(uf-x0, -om2*x0+uh) = alpha and
x0 < min(uf, uh/om2)) and x0 > 0, x0);
x1_E100 := 0;
x2_E100 := 0;
s0_E100 := -x0_E100+uf;
s1_E100 := om0*x0_E100+ug-x1_E100;
s2_E100 := om1*x1_E100-om2*x0_E100+uh-x2_E100;
lam1_E100 := x0_E100*(-(eval(diff(mu0(s0, s2), s0),
{s0 = s0_E100, s2 = s2_E100}))-om2*(eval(diff(mu0(s0, s2), s2),
{s0 = s0_E100, s2 = s2_E100})));
lam2_E100 := mu1(s1_E100, s2_E100)-alpha;
lam3_E100 := mu2(s2_E100)-alpha;
print(The*boundary*equilibrium*E100);
print([x0_E100, x1_E100, x2_E100, s0_E100, s1_E100, s2_E100]);
print(Eigenvalues);
print([lam1_E100, lam2_E100, lam3_E100])
end if

# The E010 equilibrium (0,x1,0)
if alpha>mu1(ug,uh) then
print(E_010 does `not` exist);
else
x0_E010:=0:
x1_E010:=solve(mu1(ug-x1,om1*x1+uh)=alpha
and x1>0 and x1<ug,x1):
x2_E010:=0:
s0_E010:=-x0_E010+uf:
s1_E010:=om0*x0_E010-x1_E010+ug:
s2_E010:=-om2*x0_E010+om1*x1_E010-x2_E010+uh:
lam1_E010:=mu0(s0_E010,s2_E010)-alpha:
lam2_E010:=x1_E010*(-eval(diff(mu1(s1,s2),s1),
```

```
{s1=s1_E010,s2=s2_E010})+om1*eval(diff(mu1(s1,s2),s2),
{s1=s1_E010,s2=s2_E010})):
lam3_E010:=mu2(s2_E010)-alpha:
print(The boundary equilibrium E010);
print([x0_E010, x1_E010, x2_E010, s0_E010, s1_E010, s2_E010]);
print(Eigenvalues);
print([lam1_E010,lam2_E010,lam3_E010]);
end if:

# The E001 equilibrium (0,0,x2)
if alpha>mu2(uh) then
print(E_001 does `not` exist);
else
x0_E001:=0;
x1_E001:=0;
x2_E001:=uh-alpha/(phi2-alpha);
s0_E001:=-x0_E001+uf:
s1_E001:=om0*x0_E001-x1_E001+ug:
s2_E001:=-om2*x0_E001+om1*x1_E001-x2_E001+uh:
lam1_E001:=mu0(s0_E001,s2_E001)-alpha:
lam2_E001:=mu1(s1_E001,s2_E001)-alpha:
lam3_E001:=-x2_E001*eval(diff(mu2(s2),s2),{s2=s2_E001}):
print(The boundary equilibrium E001);
print([x0_E001, x1_E001, x2_E001, s0_E001, s1_E001, s2_E001]);
print(Eigenvalues);
print([lam1_E001,lam2_E001,lam3_E001]);
end if:

# The E101 equilibrium (x0,0,x2)
if alpha>mu0(uf-min(uf,(uh-alpha/(phi2-alpha))/(om2)),
alpha/(phi2-alpha)) and alpha<mu0(uf,alpha/(phi2-alpha))
and alpha<mu2(uh) then
x0_E101:=solve(mu0(-x0+uf,alpha/(phi2-alpha))=alpha and x0>0
and x0<min(uf,(uh-alpha/(phi2-alpha))/(om2)),x0);
x1_E101:=0;
x2_E101:=-om2*x0_E101+uh-alpha/(phi2-alpha);
s0_E101:=-x0_E101+uf:
s1_E101:=om0*x0_E101-x1_E101+ug:
s2_E101:=-om2*x0_E101+om1*x1_E101-x2_E101+uh:
lam1_E101:=mu1(s1_E101,s2_E101)-alpha;
# Quadratic equation for the other eigenvalues
a1_E101:=x0_E101*(eval(diff(mu0(s0,s2),s0),
{s0=s0_E101,s2=s2_E101})+om2*eval(diff(mu0(s0,s2),s2),
{s0=s0_E101,s2=s2_E101}))+x2_E101*eval(diff(mu2(s2),s2),
```

```
{s2=s2_E101}):
a0_E101:=x0_E101*(eval(diff(mu0(s0,s2),s0),
{s0=s0_E101,s2=s2_E101})+om2*eval(diff(mu0(s0,s2),s2),
{s0=s0_E101,s2=s2_E101}))*x2_E101*eval(diff(mu2(s2),s2),
{s2=s2_E101})-om2*x0_E101*x2_E101*eval(diff(mu0(s0,s2),s0),
{s0=s0_E101,s2=s2_E101})*eval(diff(mu2(s2),s2),{s2=s2_E101}):
lam23_E101:=solve(lambda^(2)+a1_E101*lambda+a0_E101=0,lambda);
print(The boundary equilibrium E101);
print([x0_E101, x1_E101, x2_E101, s0_E101, s1_E101, s2_E101]);
print(Eigenvalues);
print([lam1_E101,lam23_E101]);
else
print(E_101 does `not` exist);
end if:

# The E011 equilibrium
if alpha<mu1(ug-max(0,(alpha/(phi2-alpha)-uh)/(om1)),
alpha/(phi2-alpha)) and alpha<mu2(om1*ug+uh) then
x0_E011:=0:
x1_E011:=solve(mu1(-x1+ug,alpha/(phi2-alpha))=alpha and
x1>max(0,(alpha/(phi2-alpha)-uh)/(om1)) and x1<ug,x1):
x2_E011:=om1*x1_E011+uh-alpha/(phi2-alpha):
s0_E011:=-x0_E011+uf:
s1_E011:=om0*x0_E011-x1_E011+ug:
s2_E011:=-om2*x0_E011+om1*x1_E011-x2_E011+uh:
lam1_E011:=mu0(uf,alpha/(phi2-alpha))-alpha:
# Quadratic equation for the other eigenvalues
a1_E011:=x1_E011*(eval(diff(mu1(s1,s2),s1),
{s1=s1_E011,s2=s2_E011})-om1*eval(diff(mu1(s1,s2),s2),
{s1=s1_E011,s2=s2_E011}))+x2_E011*eval(diff(mu2(s2),s2),
{s2=s2_E011}):
a0_E011:=x1_E011*(eval(diff(mu1(s1,s2),s1),
{s1=s1_E011,s2=s2_E011})-om1*eval(diff(mu1(s1,s2),s2),
{s1=s1_E011,s2=s2_E011}))*x2_E011*eval(diff(mu2(s2),s2),
{s2=s2_E011})+x1_E011*om1*x2_E011*eval(diff(mu1(s1,s2),s2),
{s1=s1_E011,s2=s2_E011})*eval(diff(mu2(s2),s2),{s2=s2_E011}):
lam23_E011:=solve(lambda^(2)+a1_E011*lambda+a0_E011=0,lambda);
print(The boundary equilibrium E011);
print([x0_E011, x1_E011, x2_E011, s0_E011, s1_E011, s2_E011]);
print(Eigenvalues);
print([lam1_E011,lam23_E011]);
else
print(E_011 does `not` exist);
end if:
```

```
# The E110 equilibria
unassign('x0_tmp');
unassign('x1_tmp');
unassign('E_110');
E_110 := solve({mu0(-x00+uf, om1*x11-om2*x00+uh) = alpha and
mu1(om0*x00+ug-x11 and om1*x11-om2*x00+uh) = alpha and
x00 > 0 and x11 > 0 and x00 < uf and
x11 >= max(0, (om2*x00-uh)/om1), x11 <= om0*x00+ug},
[x00, x11]);
x0_E110 := [];
x1_E110 := [];
x2_E110 := [];
s0_E110 := [];
s1_E110 := [];
s2_E110 := [];
lam1_E110 := [];
lam23_E110 := [];
for i to nops(E_110) do
x0_tmp := eval(x00, E_110[i, 1]);
x1_tmp := eval(x11, E_110[i, 2]);
x2_tmp := 0;
s0_tmp := -x0_tmp+uf;
s1_tmp := om0*x0_tmp+ug-x1_tmp;
s2_tmp := om1*x1_tmp-om2*x0_tmp+uh;
x0_E110 := [op(x0_E110), x0_tmp];
x1_E110 := [op(x1_E110), x1_tmp];
x2_E110 := [op(x2_E110), 0];
s0_E110 := [op(s0_E110), s0_tmp];
s1_E110 := [op(s1_E110), s1_tmp];
s2_E110 := [op(s2_E110), s2_tmp];
lam1_tmp := mu2(s2_tmp)-alpha;
lam1_E110 := [op(lam1_E110), lam1_tmp];
a1_E110 := x0_tmp*(eval(diff(mu0(s0, s2), s0),
{s0 = s0_tmp, s2 = s2_tmp})+om2*(eval(diff(mu0(s0, s2), s2),
{s0 = s0_tmp, s2 = s2_tmp})))+
x1_tmp*(eval(diff(mu1(s1, s2),s1), {s1 = s1_tmp, s2 = s2_tmp})
-om1*(eval(diff(mu1(s1, s2),s2),{s1 = s1_tmp, s2 = s2_tmp})));
a0_E110 := x0_tmp*x1_tmp*(eval(diff(mu0(s0, s2), s0),
{s0 = s0_tmp, s2 = s2_tmp})+om2*(eval(diff(mu0(s0, s2), s2),
{s0 = s0_tmp, s2 = s2_tmp})))*(eval(diff(mu1(s1, s2), s1),
{s1 = s1_tmp, s2 = s2_tmp})-om1*(eval(diff(mu1(s1, s2), s2),
{s1 = s1_tmp, s2 = s2_tmp})))
-om1*x0_tmp*x1_tmp*(eval(diff(mu0(s0, s2), s2),
```

```
{s0 = s0_tmp, s2 = s2_tmp}))*(om0*(eval(diff(mu1(s1, s2), s1),
{s1 = s1_tmp, s2 = s2_tmp}))-om2*(eval(diff(mu1(s1, s2), s2),
{s1 = s1_tmp, s2 = s2_tmp})));
lam23_tmp := solve(a1_E110*lambda+lambda^2+a0_E110 = 0,
lambda);
lam23_E110 := [op(lam23_E110), lam23_tmp];
print(Equilibrium*E110);
print([x0_tmp, x1_tmp, x2_tmp, s0_tmp, s1_tmp, s2_tmp]);
print(Eigenvalues);
print([lam1_tmp, lam23_tmp])
end do

# The E111 equilibrium
x0_E111 := 1+uf+1/(Kp*(phi2-alpha)+alpha-1);
x1_E111 := om0*x0_E111+ug+1+
phi1/(alpha*(1+KI*alpha/(phi2-alpha))-phi1);
x2_E111 := -om2*x0_E111+om1*x1_E111+uh-alpha/(phi2-alpha);
s0_E111 := -x0_E111+uf;
s1_E111 := om0*x0_E111+ug-x1_E111;
s2_E111 := om1*x1_E111-om2*x0_E111+uh-x2_E111;
a2_E111 := -x0_E111*(-(eval(diff(mu0(s0, s2), s0),
{s0 = s0_E111, s2 = s2_E111}))
-om2*(eval(diff(mu0(s0, s2), s2),
{s0 = s0_E111, s2 = s2_E111})))
-x1_E111*(-(eval(diff(mu1(s1, s2), s1),
{s1 = s1_E111, s2 = s2_E111}))
+om1*(eval(diff(mu1(s1, s2), s2),
{s1 = s1_E111, s2 = s2_E111})))
+x2_E111*(eval(diff(mu2(s2), s2), {s2 = s2_E111}));
a1_E111 := x1_E111*(eval(diff(mu1(s1, s2), s1),
{s1 = s1_E111, s2 = s2_E111}))
*(x0_E111*(eval(diff(mu0(s0,s2),s0), {s0=s0_E111, s2=s2_E111}))
-(om0*om1-om2)*x0_E111*(eval(diff(mu0(s0,s2),s2),
{s0=s0_E111, s2=s2_E111}))+x2_E111*(eval(diff(mu2(s2),s2),
{s2 = s2_E111})))+x0_E111*(eval(diff(mu0(s0, s2), s0),
{s0=s0_E111,s2=s2_E111}))*(-om1*x1_E111
*(eval(diff(mu1(s1,s2),s2),{s1 = s1_E111, s2 = s2_E111}))
+x2_E111*(eval(diff(mu2(s2), s2), {s2 = s2_E111})));
a0_E111 := x0_E111*x1_E111*x2_E111*(eval(diff(mu0(s0, s2), s0),
{s0 = s0_E111, s2 = s2_E111}))*(eval(diff(mu1(s1, s2), s1),
{s1 = s1_E111, s2 = s2_E111}))*(eval(diff(mu2(s2), s2),
{s2 = s2_E111}));
lam123_E111 := solve(a2_E111*lambda^2+lambda^3
+a1_E111*lambda+a0_E111 = 0, lambda);
```

```
if min(x0_E111, x1_E111, x2_E111, s0_E111, s1_E111,
s2_E111) > 0 then
if om2*uf-uh > 0 then
if alpha < min(mu0(uf, alpha/(phi2-alpha)),
mu1(om0*x0_E111-max(0, (om2*x0_E111-uh)/om1)+ug,
alpha/(phi2-alpha)), mu2(om1*x1_E111-om2*x0_E111+uh)) then
print(The*interior*equilibrium*E111);
print([x0_E111, x1_E111, x2_E111, s0_E111, s1_E111, s2_E111]);
print(Eigenvalues);
print([lam123_E111])
else
print(E_111*does*'not'*exist)
end if
else
if alpha < min(mu0(uf, alpha/(phi2-alpha)), mu1(om0*x0_E111+ug,
alpha/(phi2-alpha)), mu2(om1*x1_E111-om2*x0_E111+uh)) then
print(The*interior*equilibrium*E111);
print([x0_E111, x1_E111, x2_E111, s0_E111, s1_E111, s2_E111]);
print(Eigenvalues);
print([lam123_E111])
else
print(E_111*does*'not'*exist)
end if
end if
else print(E_111*does*'not'*exist)
end if
```

Code for finding polynomial (3.7) when all expect one of the parameters are fixed.

```
mu0 := (s0,s2) -> s0*s2/((1+s0)*(Kp+s2));
mu1 := (s1,s2) -> phi1*s1/((1+s1)*(1+KI*s2));
mu2 := (s2) -> phi2*s2/(1+s2);

Y0 := 0.19e-1;
Y1 := 0.4e-1;
Y2 := 0.6e-1;
km0 := 29;
km1 := 26;
km2 := 35;
KS0 := 0.53e-1;
KS1 := .302;
KS2 := 0.25e-4;
L0 := 0.1e-5;
KI := 0.35e-5;
om0 := KS0*(224*(1/208))*(1-Y0)/KS1;
```

```
om1 := KS1*(32*(1/224))*(1-Y1)/KS2;
om2 := (16*(1/208))*KS0/KS2;
phi1 := km1*Y1/(km0*Y0);
phi2 := km2*Y2/(km0*Y0);
Kp := L0/KS2;
KI := KS2/KI;

# Interior equilibrium (x0,x1,x2)
x0 := 1+uf+1/(Kp*(phi2-alpha)+alpha-1);
x1 := om0*x0+ug+1+phi1/(alpha*(1+KI*alpha/(phi2-alpha))-phi1);
x2 := -om2*x0+om1*x1+uh-alpha/(phi2-alpha);
s0_eq := -x0+uf;
s1_eq := om0*x0+ug-x1;
s2_eq := om1*x1-om2*x0+uh-x2;

a11 := x0*(-(eval(diff(mu0(s0, s2), s0),
{s0 = -x0+uf, s2 = om1*x1-om2*x0+uh-x2}))
-om2*(eval(diff(mu0(s0, s2), s2),
{s0 = -x0+uf, s2 = om1*x1-om2*x0+uh-x2})));
a12 := om1*x0*(eval(diff(mu0(s0, s2), s2),
{s0 = -x0+uf, s2 = om1*x1-om2*x0+uh-x2}));
a13 := -x0*(eval(diff(mu0(s0, s2), s2),
{s0 = -x0+uf, s2 = om1*x1-om2*x0+uh-x2}));
a21 := x1*(om0*(eval(diff(mu1(s1, s2), s1),
{s1 = om0*x0+ug-x1, s2 = om1*x1-om2*x0+uh-x2}))
-om2*(eval(diff(mu1(s1, s2), s2),
{s1 = om0*x0+ug-x1, s2 = om1*x1-om2*x0+uh-x2})));
a22 := x1*(-(eval(diff(mu1(s1, s2), s1),
{s1 = om0*x0+ug-x1, s2 = om1*x1-om2*x0+uh-x2}))
+om1*(eval(diff(mu1(s1, s2), s2),
{s1 = om0*x0+ug-x1, s2 = om1*x1-om2*x0+uh-x2})));
a23 := -x1*(eval(diff(mu1(s1, s2), s2),
{s1 = om0*x0+ug-x1, s2 = om1*x1-om2*x0+uh-x2}));
a31 := -om2*x2*(eval(diff(mu2(s2), s2),
s2 = om1*x1-om2*x0+uh-x2));
a32 := om1*x2*(eval(diff(mu2(s2), s2),
s2 = om1*x1-om2*x0+uh-x2));
a33 := -x2*(eval(diff(mu2(s2), s2),
s2 = om1*x1-om2*x0+uh-x2));

a2 := -a11-a22-a33;
a1 := x1*(eval(diff(mu1(s1, s2), s1),
{s1 = om0*x0+ug-x1, s2 = om1*x1-om2*x0+uh-x2}))
*(x0*(eval(diff(mu0(s0, s2), s0), {s0 = -x0+uf,
```

```
s2 = om1*x1-om2*x0+uh-x2}))-(om0*om1-om2)*x0
*(eval(diff(mu0(s0, s2), s2), {s0 = -x0+uf,
s2 = om1*x1-om2*x0+uh-x2}))+x2*(eval(diff(mu2(s2), s2),
s2 = om1*x1-om2*x0+uh-x2)))+x0*(eval(diff(mu0(s0, s2), s0),
{s0 = -x0+uf, s2 = om1*x1-om2*x0+uh-x2}))
*(-om1*x1*(eval(diff(mu1(s1, s2), s2),
{s1 = om0*x0+ug-x1, s2 = om1*x1-om2*x0+uh-x2}))
+x2*(eval(diff(mu2(s2), s2), s2 = om1*x1-om2*x0+uh-x2)));
a0 := x0*x1*x2*(eval(diff(mu0(s0, s2), s0),
{s0 = -x0+uf, s2 = om1*x1-om2*x0+uh-x2}))
*(eval(diff(mu1(s1, s2), s1), {s1 = om0*x0+ug-x1,
s2 = om1*x1-om2*x0+uh-x2}))*(eval(diff(mu2(s2), s2),
s2 = om1*x1-om2*x0+uh-x2))

# Hopf in alpha
unassign('alpha');
uf := .6;
ug := 0;
uh := .1;
solve(a2*a1=a0 and alpha < mu0(uf, alpha/(phi2-alpha)) and
alpha < mu1(om0*x0-max(0, (om2*x0-uh)/om1)+ug,
alpha/(phi2-alpha)) and
alpha < mu2(om1*x1-om2*x0+uh) and alpha > 0, alpha)

# Hopf in uf
unassign('uf');
ug := 0;
uh := .1;
alpha := 0.1e-1;
solve(a2*a1 = a0 and alpha < mu0(uf, alpha/(phi2-alpha)) and
alpha < mu1(om0*x0-max(0, (om2*x0-uh)/om1)+ug,
alpha/(phi2-alpha)) and alpha < mu2(om1*x1-om2*x0+uh) and
uf > 0, uf)

# Hopf in ug
unassign('ug');
uf := .6;
uh := .1;
alpha := 0.1e-1;
solve(a2*a1 = a0 and alpha < mu0(uf, alpha/(phi2-alpha)) and
alpha < mu1(om0*x0-max(0, (om2*x0-uh)/om1)+ug,
alpha/(phi2-alpha)) and alpha < mu2(om1*x1-om2*x0+uh) and
ug > 0, ug)
```

```
# Hopf in uh
unassign('uh');
uf := .6;
ug := 0;
alpha := 0.1e-1;
solve(a2*a1 = a0 and alpha < mu0(uf, alpha/(phi2-alpha)) and
alpha < mu1(om0*x0-max(0, (om2*x0-uh)/om1)+ug,
alpha/(phi2-alpha)) and alpha < mu2(om1*x1-om2*x0+uh) and
uh > 0, uh)
```

Bibliography

[1] D. Batstone, J. Keller, I. Angelidaki, S. Kalyuzhnyi, S. Pavlostathis, A. Rozzi, W. Sanders, H. Siegrist, and V. Vavilin. The IWA Anaerobic Digestion Model No 1 (ADM1). Water Science and Technology, 45(10):65–73, 05 2002.

[2] A. Bornhöft, R. Hanke-Rauschenbach, and K. Sundmacher. Steady-state analysis of the anaerobic digestion model no. 1 (adm1). Nonlinear Dynamics, 73, 07 2013.

[3] G. J. Butler, H. I. Freedman, and P. Waltman. Uniformly persistent systems. Proceedings of the American Mathematical Society, 96(3):425–430, 1986.

[4] G. J. Butler and G. S. K. Wolkowicz. Predator — mediated coexistence in a chemostat: Coexistence and competition reversal. Mathematical Modelling, 8:781 – 785, 1987.

[5] Ipe. version 7.2.9. Otfried Cheong, Korea Advanced Institute of Science and Technology, Daedeok Innopolis, Daejeon, 2019.

[6] X. Jiang, Y. Chen, C. Hou, X. Liu, C. Ou, W. Han, X. Sun, J. Li, L. Wang, and J. Shen. Promotion of para-chlorophenol reduction and extracellular electron transfer in an anaerobic system at the presence of iron-oxides. Frontiers in Microbiology, 9:2052, 2018.

[7] Y. Kuznestov. Elements of Applied Bifurcation Theory, volume 112. Springer-Verlag, New York, 2004.

[8] F. E. Löffler, J. Yan, K. M. Ritalahti, L. Adrian, E. A. Edwards, K. T. Konstantinidis, J. A. Müller, H. Fullerton, S. H. Zinder, and A. M. Spormann. Dehalococcoides mccartyi gen. nov., sp. nov., obligately organohalide-respiring anaerobic bacteria relevant to halogen cycling and bioremediation, belong to a novel bacterial class, dehalococcoidia classis nov., order dehalococcoidales ord. nov. and family dehalococcoidaceae fam. nov., within the phylum chloroflexi. International Journal of Systematic and Evolutionary Microbiology, 63(2):625–635, 2013.

[9] Maple. version 18.02. Waterloo Maple Inc., Waterloo, Ontario, 2018.

[10] MATLAB. version 9.5.0.944444 (R2018b). The MathWorks Inc., Natick, Massachusetts, 2018.

[11] J. Monod. The growth of bacterial cultures. Annual Review of Microbiology, 3(1):371–394, 1949.

[12] N. V. Pradeep, S. Anupama, K. Navya, H. N. Shalini, M. Idris, and U. S. Hampannavar. Biological removal of phenol from wastewaters: a mini review. Applied Water Science, 5(2):105–112, Jun 2015.

[13] D. Puyol, J. Sanz, J. Rodriguez, and A. Mohedano. Inhibition of methanogenesis by chlorophenols: a kinetic approach. New Biotechnology, 30(1):51 – 61, 2012. Frontiers and Challenges in the Bioremediation of Contaminated Sites.

[14] T. Sari and M. Wade. Generalised approach to modelling a three-tiered microbial food-web. J. Math. Biosci., 291:21–37, 2017.

[15] H. L. Smith and P. Waltman. The Theory of the Chemostat: Dynamics of Microbial Competition. Cambridge Studies in Mathematical Biology. Cambridge University Press, 1995.

[16] M. Wade, R. Pattinson, N. Parker, and J. Dolfing. Emergent behaviour in a chlorophenol-mineralising three-tiered microbial 'food web'. J. Theor. Biol., 389:171–186, 2016.

[17] XPPAUT. version 8.0. Dr. Bard Ermentrout, Dept of Mathematics, University of Pittsburgh, Pittsburgh PA, 2016.